Y 3.At 7:
36/11.4

See the announcement on page ii

REACTOR AND FUEL-PROCESSING TECHNOLOGY

Prepared for DIVISION OF TECHNICAL INFORMATION, U. S. ATOMIC ENERGY COMMISSION,
by ARGONNE NATIONAL LABORATORY

ILLINOIS STATE LIBRARY
MAY 9 - 1969
U.S. Depository Copy

Fall 1968

● VOLUME 11

● NUMBER 4

TECHNICAL PROGRESS REVIEWS

The United States Atomic Energy Commission publishes the Technical Progress Reviews to meet the needs of industry and government for concise summaries of current nuclear developments. Each journal digests and evaluates the latest findings in a specific area of nuclear technology and science. *Nuclear Safety* is a bimonthly journal; the other three are quarterly journals.

Isotopes and Radiation Technology
P. S. Baker, A. F. Rupp, and associates
Isotopes Information Center, Oak Ridge National Laboratory

Nuclear Safety
Wm. B. Cottrell, W. H. Jordan, J. P. Blakely, and associates
Nuclear Safety Information Center, Oak Ridge National Laboratory

Reactor and Fuel-Processing Technology
Argonne National Laboratory

Reactor Materials
E. M. Simons and associates
Battelle Memorial Institute, Columbus Laboratories

All are available from the U. S. Government Printing Office. See the back cover for ordering instructions.

The views expressed in this publication do not necessarily represent those of the United States Atomic Energy Commission, its divisions or offices, or of any Commission advisory committee or contractor.

Availability of Reports Cited in This Review

United States Atomic Energy Commission (USAEC) reports are available at USAEC depository libraries and are sold by the Clearinghouse for Federal Scientific and Technical Information (CFSTI), National Bureau of Standards, U. S. Department of Commerce, Springfield, Va. 22151. All reports sold by CFSTI are $3.00 for printed copy and $0.65 for microfiche. Each separately bound part of a report is priced as a separate report. Some reports may not be available because of their preliminary nature; however, the information contained in them will generally be found in later progress or topical reports on the subject.

Other U. S. Government agency reports identified in this journal generally are available from CFSTI.

Private-organization reports should be requested from the originator.

United Kingdom Atomic Energy Authority (UKAEA) and Atomic Energy of Canada Limited (AECL) reports are available at USAEC depository libraries. UKAEA reports are sold by Her Majesty's Stationery Office, London; AECL reports are sold by the Scientific Document Distribution Office, Atomic Energy of Canada Limited, Chalk River, Ontario, Canada. UKAEA and AECL reports issued after March 1, 1967, are sold by CFSTI to purchasers in the United States and its territories.

Y3.At7:
36/11-4

Contents

Reactor and Fuel-Processing Technology
Vol. 11, No. 4, Fall 1968

CONTROL AND DYNAMICS
Noise in Power Reactors—A Review of Experiment, Analysis, and Theory
Joseph A. Thie 167

Methods for Studying Space-Dependent Reactor Dynamics
Chun Hsu and Thomas P. Mulcahey 172

REACTOR SAFETY
Coolant Ejection Mechanisms for Use in Analyzing Fast Reactor Safety
Hans K. Fauske 180

NEW CONCEPTS
Compact Power Concept Features a Fast Reactor, Heat Pipes, and Direct Converters
John J. Roberts and Edward J. Croke 187

AQUEOUS PROCESSING
Research and Development on Aqueous Processing
C. E. Stevenson and D. M. Paige 201

NONAQUEOUS PROCESSING
Volatility Processes
G. J. Vogel and J. W. Simmons 209

Compact Pyrochemical Processes
W. E. Miller and R. K. Steunenberg 219

WASTE DISPOSAL
Progress in Research and Development on Waste Disposal
Phillip Fineman 227

INDEX
Volume 11 233

Superintendent of Documents, U. S. Government Printing Office, Washington, D. C. 20402, $2.50 per year

To the Readers of *Reactor and Fuel-Processing Technology*

Regretfully we must announce that this is the last issue of this journal which will be prepared by Argonne National Laboratory.

We want to express, to the editors and Argonne staff members who have contributed to *Reactor Fuel Processing* and this combined journal over the last 11 years, the appreciation of the AEC for a job well done!

AEC's Division of Technical Information will assemble articles from several sources for the next two issues pending a decision on the future status of the journal.

Edward J. Brunenkant

Edward J. Brunenkant, Director
Division of Technical Information
U. S. Atomic Energy Commission

Issued quarterly by the U. S. Atomic Energy Commission. Use of funds for printing this publication approved by the Director of the Bureau of the Budget on July 8, 1966.

Noise in Power Reactors—A Review of Experiment, Analysis, and Theory

By Joseph A. Thie, Consultant*

The dynamic behavior of reactors has been studied extensively for more than a decade utilizing the data of their randomly fluctuating variables. The term "reactor noise" is the accepted jargon for these time-varying random fluctuations in reactor variables, especially the ion-chamber current. Testimony to the widespread use of noise analysis has been given in numerous individual publications, from which collections and reviews have been made.[1–4] This review is based on a paper presented at the Japan–United States Seminar on Nuclear Reactor Noise Analysis held in Tokyo and Kyoto, September 1968.

Characteristics of Noise Experiments

Of the methods of obtaining dynamic information from reactors, stochastic techniques are among the more popular. Their attractiveness stems from the following features:

- There is essentially no disturbance to the reactor, and this is quite favorable to operating policies.
- Existing instrumentation and equipment are normally used (although special data-recording equipment might be added).
- Complex phenomena sometimes might require noise analysis as one of the modes of investigation.
- An experimental simplicity in noise tests has appeal.
- Considerable precedent exists in monitoring for reactor stability by noise studies.

Noise experiments have been performed in both zero-power reactors and power reactors. Table 1 generalizes about these experiments. The multiplicity of available variables and the system complexity in power reactors are perhaps two underlying reasons for the research differences of Table 1. The future research potential is rated as substantial; a few specific suggestions are given below.

Table 1 GENERAL COMPARISONS OF NOISE EXPERIMENTS ON POWER AND ZERO-POWER REACTORS

	Zero-power reactors	Power reactors
Motives	Research	Engineering
Variables for analysis	Few	Many
Environmental suitability	Good	Poor
Relative number of experiments	Extensive	Average
Data interpretation	Easy	Difficult
Future research potential	Average	Substantial

In contrast to zero-power reactor noise experiments in which only the neutron (or gamma) flux and control-rod fluctuations have been used, power-reactor experiments offer many more possibilities for variables to be studied. Table 2 lists those which have been used in noise experiments, along with suggestions for others. Investigations can have many facets when more than just neutron-flux noise is measured. Also, as one might expect, the amount of information obtained from a study is somewhat in proportion to the number of variables recorded besides the usual neutron flux.

Table 2 VARIABLES FOR NOISE ANALYSIS

Already used	Other possibilities
Neutron flux	Mechanical displacement, velocity or acceleration
Temperature	Local density
Flow	Force and stress
Control-rod position	
Pressure	
Valve position	
Pump speed	
Core gamma flux	
Coolant radioactivity	
Sound	

*Address: P. O. Box 17, Barrington, Ill. 60010.

Experimental Techniques

To see the place of noise analysis among methods of investigating reactor dynamics, the latter are broadly classified in Table 3. Noise methods are the last two listed. It might also be mentioned that further subdivisions within this table are possible — such as categorizing according to data-gathering techniques or according to types of experimental equipment.

The last method in Table 3 is found more frequently in the current literature than are the others because of its simplicity and other reasons for popularity cited above. Often it consists of a Fourier analysis of the ion-chamber fluctuations, the result being the relative distribution of frequencies in the random signal. Recently, the trend among experiments is to analyze two or more signals simultaneously, obtaining mutual interactions as well as individual frequency structures.

An example of the simultaneous analysis of two ion-chamber signals is given in Fig. 1. Individual noise spectra are given — one for the lower nonboiling part of the core, and one for the upper boiling zone of the same fuel channel. (The ordinate's units are such that the integral of the curve over all frequencies is the square of the well-known root-mean-square value of the power fluctuation.) At higher frequencies the upper ion chamber is seen to have more noise than the lower because of local steam-void fluctuations in its environment. A technique for expressing the extent of correlation at various frequencies is used here: the coherence is 0.94 at low frequencies but reduces to 0.7 at 2 cps. (Coherence[6] is a function of frequency defined such that it is unity for two signals having exactly the same fluctuations in a given frequency band but is zero if they are random with respect to each other.)

An extensive listing of the power-reactor experiments to date is given in Table 4. Evidently the most popular (in number of reactors) has been the spectral

Table 3 EXPERIMENTAL METHODS OF OBTAINING DYNAMIC INFORMATION FROM POWER REACTORS

Name	External excitation	Description
Event analysis	Any cause	Data analysis from a reactor transient, sometimes unexpected but usually planned
Rod (or other device) oscillation	Control rod (or other device)	Measurement of reactor response to oscillations
Pseudorandom excitation	Control rod (or other device)	Measurement of reactor response to almost random excitation
Noise analysis	None	Analysis of randomly fluctuating variables due to intrinsic causes

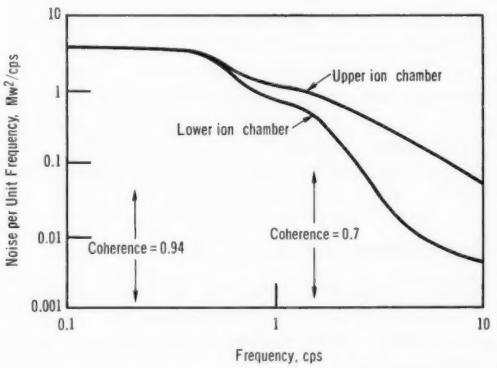

Fig. 1 Results of a computer analysis of digitized ion-chamber recordings of the Pathfinder reactor[5] at 190 Mw.

Table 4 RESULTS ACHIEVED IN AT-POWER DYNAMICS STUDIES

Method and excitation	Reactors used	Results
Fluctuating control rod (pseudorandom)	Kiwi-A3,[7] MSRE,[8] Saxton[4]	Stability study, control-system study
Noise analysis (no excitation)	BORAX-I, -II, -IV, and -V,[9,10,11] Calder Hall,[12] Chapelcross,[13] Dresden,[14] EBR-II,[15] EBWR,[16,17] Elk River,[2] GTR,[18] HBWR,[2] HFIR and ORR,[4,19] HFBR,[20] HRE-2,[21,22] HTR, JRR-1, JRR-2,[2,4,23] Indian Point, *Savannah*, and Yankee,[2] Kyoto U.,[24] ML-1,[25] Pluto,[2] SPERT-IV,[26] SRE,[27] Senn,[28] THOR,[29] Trino,[30] VBWR and Big Rock Point,[2,31] LACBWR[32]	Stability study, control-system study, boiling detection, noise-source determinations
Pseudorandom plant control	Nerva,[4] Phoebus-1A,[4] SNAP[4]	Intervariable transfer functions
Intervariable cross-correlation and spectral analysis	DFR,[2] DMTR,[33] Enrico Fermi,[34] Pathfinder,[5] Saxton,[2] SNAP[2]	Stability study, intervariable transfer functions, noise-source determinations

analysis of just the neutron flux—presumably because of its being somewhat simpler than other categories of experiments listed. The results tabulated indicate experiment incentives and utilization potentials.

Noise experiments depend on the reactor power and other variables being affected by a randomly fluctuating excitation source. This can be an external device (such as a control-rod mechanism) or something intrinsic in the reactor (such as water-temperature fluctuations stemming from inlet flow conditions). Whether external excitation or self-excitation is used to obtain information in a given frequency band depends first on the excitation energy available in that band and then on other factors, such as those in Table 5.

Table 5 A GENERAL QUALITATIVE COMPARISON OF EXCITATION EXPERIMENTS WITH INTRINSIC-NOISE-ANALYSIS EXPERIMENTS

	Excitation	Intrinsic noise
Experimental complexity and cost	More	Less
Interpretation of data	Easy	Difficult
Disturbance to reactor system	Some	None
Measures transfer function	Always	Sometimes
Measures spectra	No	Yes
Typical precision	High	Medium

Among the external-excitation experiments, the pseudorandom has in recent times been preferred over the sinusoidal where it is not necessary to have a high concentration of spectral energy at discrete frequencies. Random excitation supplies a wide band of frequencies, all at once, throughout the duration of the experiment. Kerlin[35] has discussed this energy content for various types of excitation.

Theoretical Analysis Techniques

It is usual to generate a number of statistical functions from the noise data to assist in its analysis. These range from the simplest—the mean value of variables—to rather sophisticated concepts such as the coherence in Fig. 1. Some noise experiments are engineered so as to obtain transfer functions (i.e., variation of system output amplitude with frequency for a fixed input amplitude to the system at all frequencies). In any event, from the magnitude and behavior of these quantities, it is possible to deduce information about the reactor's dynamic characteristics. Categories of this information in order of increasing sophistication are:

- Summary statements or qualities characterizing the reactor's stability.
- Values of significant parameters (frequencies, time constants, coefficients).
- Qualitative and quantitative relations among the variables observed.

Approaches for inferring this physically meaningful information are about as numerous as the experiments in Table 4. The success of a noise test often lies in the interpretation of the data, which is especially difficult in the self-excited experiments. In these, investigators have found the following approaches to have merit (in the order of increasing analytical effort required): (*a*) absolute magnitudes of variances of the variables, along with their changes with experimental conditions (power, flow, control-rod configuration, etc.); (*b*) examination of obvious characteristics of spectra and correlation functions (such as characteristics of maxima); (*c*) function behavior (such as the frequency, power, and flow dependence of spectra) compared to that of postulated theoretical models; and (*d*) simulations (such as combining a computer and a mock-up apparatus) of the reactor's noise output for the purpose of matching measures of performance.

One feature of noise tests of exceptional value to data interpretation should be singled out, for it is a rare experiment that has this feature: variety in the reactor conditions used. For example, taking data under two significantly different control-rod patterns is a simple matter for most reactors and can give the control-rod contribution (if the rods happen to be shaking randomly) to the intrinsic noise source, but very few of the experiments in Table 4 have done this.

Intrinsic Noise Sources

In Table 4, types of experimental results obtained from noise tests are listed. These were inferred by the methods just described, with stability information being the most popular. However, experiments that determine the source of the intrinsic reactivity excitation noise are important to the fundamentals of nonexcited noise analysis as an experimental tool. Where this was an experimental result, it is given in Table 6.

Although identification of a noise source is a first step, a quantitative understanding of its characteristics would eventually be desirable. To date, however, in virtually all the cases of noise-source identification, there is little quantitative information. One should ultimately expect at least empirical characterizations (much less difficult than *a priori* understandings) that would be useful in noise-analyzing reactors of a similar size and type.

The status of understanding noise sources to date is nevertheless sufficient to allow five general statements to be made:

1. The total reactivity-noise amplitude increases only in proportion to $\sqrt{N}$ for N effectively equal and independent multiple sources (example: N randomly shaking control rods or separate inlet temperature zones).[2] More generally, however, the

Table 6 IDENTIFIED INTRINSIC REACTIVITY-NOISE SOURCES IN POWER REACTORS

Type	Reactors	Noise source
BWR	Dresden[14]	Flow fluctuations outside the vessel
	Elk River[2]	Subcore temperature whose heterogeneity is caused by feedwater mixing in the vessel
	Pathfinder[5]	Thermalization noise of high steam voids near in-core detector
	VBWR[31]	Flow affecting moderator density
D_2O research	DMTR[33]	Inlet coolant temperature
	JRR-2[2]	Coolant flow shaking core
Fast	DFR[2]	Inlet sodium temperature
	Enrico Fermi[34]	Inlet sodium temperature and flow
Gas cooled	ML-1[25]	Temperature of slowly moving water moderator
Graphite CO_2	Calder Hall[12]	Control rod and fuel movements
H_2O pool and research	HFBR,[20] HFIR and ORR,[19] HTR[4]	Control rods and fuel shaken by coolant flow
Homogeneous	HRE-2 (normal flow)[21]	Fuel heterogeneity in solution
	HRE-2 (reversed flow)[22]	Fluctuating flow paths of solution going through the core
Liquid-metal compact	SNAP-2[2]	Coolant flow in turn affected by pump's line-voltage fluctuations
PWR	*Savannah*[2]	Control rods shaken by sea
	Saxton[2]	Nucleate boiling and also coolant flow
Water boiler	JRR-1[2]	Radiolytic gas bubbles

square root of the sum of the squares of the importance-weighted reactivities applies.

2. The amplitudes of fuel and control-rod motion in relation to each other, when random, are dependent on mechanical dynamic relations and incident excitation forces' frequency spectra. The resulting reactivity noise then depends on fluxes and geometrical relations in addition to these amplitudes.

3. Imperfect thermal mixing in inlet coolant fluids results in temperature heterogeneities that depend directly on system temperature differences and inversely on the mixing volume and turbulence. The spectral content of the resulting reactivity excitation, for frequencies above the reciprocals of mixing times and core transit times, is attenuated markedly.

4. Inlet flow fluctuations become converted to temperature and reactivity fluctuations[31] by virtue of coolant transit dynamics through the core, and the noise is proportional to the temperature and steam-void coefficients.

5. In-core detectors have a local thermalization noise of neutrons slowing down in a boiling-water reactor's (BWR) fluctuating moderator density in the volume near the detector.[5]

Useful Experiments

To enhance the utility of noise applications in power reactors, some variety in the types of experiments and their accompanying theoretical interpretation is desirable—especially including types rarely or never performed to date. A few possibilities for experiments are suggested here, somewhat without regard to their relative merit:

• Commonly one uses binary pseudorandom sequences as excitation functions, the excited variable spending random amounts of time in only two positions or values. In ternary sequences,[4] three values are used. Also, binary and/or ternary excitation of two or more different variables simultaneously can be done.

• Spatial correlations can be made for one variable or among several variables. The BWR's show diminishing in-core correlations with increasing detector separation and increasing local turbulences. Flow and temperature spatial correlations at the core entrance would describe the noise-excitation spectrum in many reactors.

• The use of coherence in measuring the amount of correlation between two random signals at various frequencies has been illustrated in Fig. 1. If two or more variables (such as flow and temperature) are influencing a third (such as the reactor power noise), one might take sufficient data to use partial coherences[6] to isolate the individual correlations.

• By analogy to triple-coincidence counting in zero-power reactors,[36] one might consider merits of experimental techniques using it in power reactors, i.e., on-line probability determinations, where, during time intervals Δt_i for three variables x, y, and z:

$$P_i = 1 \quad \text{if } X_a < x(t_i) < X_b, \quad Y_a < y(t_i + \tau_y) < Y_b,$$

$$\text{and } Z_a < z(t_i + \tau_z) < Z_b$$

$$P_i = 0 \quad \text{otherwise}$$

Here τ_y and τ_z are delay times for coincidences of these variables with x. Along similar lines, multiple-order correlation functions have been defined[2] and may be measured.

• On-line measurement and display for the operators[2,3] of noise parameters or functions that would be most useful in power-plant monitoring are little-used applications at present. For example, one might monitor for control-rod difficulties if rod shaking is responsible for reactor noise.

• Out-of-pile simulations,[22] scaled down for economy, can be informative, such as in investigations of temperature and flow noise phenomena.

• Monte Carlo "experiments" on computers might be valid for some test purposes. Here the computer would generate the random input for a dynamically simulated system.

• One might consider applications of random-fluctuation analysis in dimensions other than time. For example, spatial fluctuations in a fuel rod's gamma activity could be due to random material distributions.

These suggestions by no means exhaust the possibilities of future noise investigations. One concludes that the research potential and benefits therefrom are significant.

References

1. J. A. Thie, *Reactor Noise*, Rowman and Littlefield, Inc., New York, 1963.
2. R. E. Uhrig (Coordinator), *Noise Analysis in Nuclear Systems*, Gainesville, Fla., Nov. 4–6, 1963, AEC Symposium Series, No. 4 (TID-7679), 1964.
3. J. A. Thie, Noise Analysis in Reactor Safety, *Nucl. Safety*, 7(3): 271 (Spring 1966).
4. R. E. Uhrig (Coordinator), *Neutron Noise Waves and Pulse Propagation*, Gainesville, Fla., Feb. 14–16, 1966, AEC Symposium Series, No. 9 (CONF-660206), 1967.
5. Northern States Power Co., Pathfinder Atomic Power Plant Six Month Report No. 2, Minneapolis, 1967.
6. J. S. Bendat and A. G. Piersol, *Measurement and Analysis of Random Data*, John Wiley & Sons, Inc., New York, 1966.
7. J. D. Balcomb et al., A Crosscorrelation Method for Measuring the Impulse Response of Reactor Systems, *Nucl. Sci. Eng.*, 11(2): 159 (October 1961).
8. T. W. Kerlin and S. J. Ball, Power-Dependent Frequency Response Measurements on the Molten-Salt Reactor Experiment, *Trans. Amer. Nucl. Soc.*, 10(1): 219 (June 1967).
9. B. S. Maxon et al., Reactivity Transients and Steady-State Operation of a Thoria–Urania-Fueled Direct-Cycle Light-Water Boiling Reactor (BORAX-IV), USAEC Report ANL-5733, Argonne National Laboratory, February 1959.
10. J. A. Thie, Elementary Methods of Reactor Noise Analysis, *Nucl. Sci. Eng.*, 15(2): 109 (February 1963).
11. R. A. Cushman, D. Mohr, R. N. Curran, and D. H. Brown, Stability Measurements on BORAX-V Boiling Core B-2, pp. 150-168 in *Reactor Kinetics and Control*, University of Arizona, Mar. 25–27, 1963, Lynn E. Weaver (Coordinator), AEC Symposium Series, No. 2 (TID-7662), 1964.
12. J. D. Cummins, Frequency Spectrum of Calder Hall Reactor Noise, British Report AEEW-M-19, 1960.
13. P. Bentley and E. Burton, The Measurement and Analysis of Can Temperature Fluctuations in Chapelcross Reactors, *J. Nucl. Energy: Pt. A & B*, 19(5): 313 (1965).
14. E. S. Beckjord, Dresden Reactor Stability Tests, *Trans. Amer. Nucl. Soc.*, 3(2): 433 (November 1960).
15. R. Hyndman, F. S. Kirn, R. R. Smith, and H. Kuroi, EBR-II Self-Excited Oscillations, *Trans. Amer. Nucl. Soc.*, 8(2): 590 (November 1965).
16. J. A. Thie, Statistical Analysis of Power-Reactor Noise, *Nucleonics*, 17(10): 102 (October 1959).
17. H. Iskenderian, E. A. Wimunc, M. Petrick, and W. C. Lipinski, Performance Characteristics of the EBWR from 0 to 100 Mwt, *Operating Experience with Power Reactors*, Vol. I, p. 355, Conference Proceedings, Vienna, June 4–8, 1963, IAEA, Vienna, 1963 (STI/PUB/76).
18. E. Jordan, Detection of In-Core Void Formation by Noise Analysis, *Trans. Amer. Nucl. Soc.*, 9(1): 317 (June 1966).
19. J. C. Robinson and D. N. Fry, Application of a Theoretical Model for Interpreting Observed Spectral Density of Power Fluctuations in Water Reactors, *Trans. Amer. Nucl. Soc.*, 10(2): 590 (November 1967).
20. C. Sastre, Noise Measurements in a Reactor Start-Up, *Trans. Amer. Nucl. Soc.*, 10(1): 216 (June 1967).
21. J. Hirota, Statistical Analysis of Small Power Oscillations in the HRT, USAEC Report ORNL-CF-60-1-107, Oak Ridge National Laboratory, 1960.
22. C. G. Lawson et al., Effect on Neutron Level of Hydraulic Fluctuations During Reverse-Flow Core Operation of the Homogeneous Reactor Experiment-2, *Trans. Amer. Nucl. Soc.*, 4(2): 315 (November 1961).
23. J. Miida, Kinetic Studies and Control of Nuclear Reactors by Statistical Methods, in *Proceedings of the Third International Conference on the Peaceful Uses of Atomic Energy, Geneva, 1964*, Vol. 4, pp. 151-161, United Nations, New York, 1965.
24. M. Utsuro and T. Shibata, Power Noise Spectra of a Water Reactor in Low Frequency Region, *J. Nucl. Sci. Technol. (Tokyo)*, 4(6): 267 (June 1967).
25. D. H. Crimmins and H. J. Snyder, ML-1 Reactor Stability Tests, USAEC Report AGN-TM-403, Aerojet-General Nucleonics, 1963.
26. J. Crocker et al., Reactor Stability in the SPERT-IV Facility, USAEC Report IDO-17088, Phillips Petroleum Company, 1965.
27. C. W. Griffin and R. L. Randall, At-Power Low-Frequency Reactor-Power-Spectrum Measurements and Comparison with Oscillation Measurements, *Nucl. Sci. Eng.*, 15(2): 131 (1963).
28. Ente Nazionale per l'Energia Elettrica, Garigliano Nuclear Power Station Research Program Quarterly Report No. 9, Rome, 1966.
29. Y. Ko, P. Y. Ma, and J. P. Chien, The Measurement of Reactor Noise by Means of a Multiscaler Analyzer, *Trans. Amer. Nucl. Soc.*, 9(2): 507 (November 1966).
30. V. Rajagopal, Dynamic Measurements in PWR Power Plants, *Trans. Amer. Nucl. Soc.*, 10(1): 217 (June 1967).
31. General Electric Company, Atomic Power Equipment Department, VBWR Stability Test Report, USAEC Report GEAP-3971, 1963.
32. Allis-Chalmers Mfg. Co., Eleventh Monthly Operational Report on the La Crosse Boiling Water Reactor Covering the Month of May 1968, USAEC Report ACNP-68507, 1968.
33. F. D. Boardman, A Theory of Noise in DMTR, British Report TRG-Memo-1128, June 1962.
34. M. L. Batch and A. E. Klickman, Evaluation of Noise Analysis for the Enrico Fermi Reactor, APDA-NTS-13, Atomic Power Development Associates, Inc., January 1968.
35. T. W. Kerlin, Frequency-Response Testing, *Nucl. Safety*, 8(4): 339-345 (Summer 1967).
36. J. B. Dragt, Threefold Correlations and Third Order Moments in Reactor Noise, *Nukleonik*, 10(1): 7 (June 1967).

Methods for Studying Space-Dependent Reactor Dynamics

By Chun Hsu and Thomas P. Mulcahey

To ensure the safety of the public, operating personnel, and reactor power plant components, reactor dynamics (i.e., kinetics, stability, and control) has been the subject of considerable study in efforts to understand and control power reactors. Throughout the development process, the most recent tools and methods of modern physics and engineering have been adopted to analyze and explain observed phenomena and to design reactor and plant systems, control systems, and safety systems that have maintained safe and satisfactory reactor operation.

In the earlier stages of reactor development, when reactor size and power densities were more modest than they are today, it was satisfactory to analyze reactor dynamics with simpler calculations which involved only a few delayed-neutron groups and which assumed that neutron dynamics were independent of location within the reactor core. Although fuel burnup, breeding, and the presence and movement of control rods were known to introduce space-dependent effects on reactor dynamics, for reactors of modest size and power their spatial effects usually could be calculated sufficiently accurately by methods that ignore the spatial effects. Occasionally, an important unexplained phenomenon, such as xenon oscillation in medium-size thermal reactors, would provide motivation for considering the spatial effects. Still, the inability to compute spatial effects so that they could be compared with calculations that neglect spatial effects limited progress toward developing space-dependent models and methods.

However, with plans being made for the development and construction of larger and more powerful advanced reactors, it is becoming increasingly important that methods for calculating space-dependent effects be devised. Impetus for studying spatial effects has been gained from the development of methods for calculating the existence of potentially hazardous conditions in space-dependent reactors. For instance, large discrepancies have been reported in reactor power transients calculated with and without considering spatial effects.[1] In the cases studied, the magnitude of the power transient calculated by using space-dependent considerations can range from three or four times greater (in a 60-cm-diameter core) to more than several orders of magnitude greater (in a 240-cm-diameter core) than that calculated using standard nonspatial methods. From this we conclude that, for large reactors, the standard nonspatial methods for calculating reactor kinetics are inadequate to predict some situations. To ensure the safe operation of an advanced power reactor throughout its life, it is necessary to consider spatial dynamics in the design of reactor and plant control and safety systems.

Although most effort to date has been devoted to the development and use of methods that exclude the space-dependent effects on reactor dynamics, more modern space-dependent models and methods are being developed to answer design and operational questions that arise. When completed, the methods will be capable of calculating heat transfer, fluid flow, and multiple-energy-group kinetics considerations.

To give the reader a general understanding of the various methods and some insight into the current state of the art, this article discusses briefly the formulation of mathematical models and methods that are used to analyze reactor dynamics, then outlines and evaluates the concepts from the standpoints of their bases and application. For completeness, the basic mathematical theory of space-dependent reactor dynamics and the various approximation methods for obtaining solutions will be included, even though some of these concepts and methods were discussed in two earlier survey papers.[2,3] Also, because research in other engineering disciplines is related to the study of space-dependent reactor systems, some of the more important examples are mentioned.

Formulating Mathematical Models

The formulation of a mathematical model of a reactor system begins by describing the dynamic behavior of the neutron distribution in the reactor. For power-reactor systems, it usually is acceptable to use the multienergy-group diffusion model[4] that has been used in many reactor designs and is generally considered quite accurate for power reactors.

In a power reactor the large amount of heat energy released by fission in the reactor core is usually removed by coolant flowing through the core. The heat-transfer processes can be formulated separately by considering that the fission energy is the internal heat source and by constructing the equations of heat transfer and hydrodynamics.

Besides the neutron distribution and the heat-transfer processes, other dynamic processes in power reactors affect the behavior of the reactor system. An example is the xenon process in a thermal reactor. Other processes, such as plutonium production in a fast breeder reactor, can be important in various reactor systems and can have a similar effect on a longer time scale (but may not be as important) as the xenon process in a thermal reactor. However, the mathematical description can be constructed easily from the radioactive-decay equations.[5]

These seemingly independent processes are implicitly coupled because the parameters in the various processes usually depend on the states of all processes in the system. For example, the nuclear parameters are functions of the fuel and coolant temperatures due to the density change, Doppler effect, etc. This coupling is inherently within the reactor system; therefore control engineers usually refer to it as the "internal feedback."

The mathematical models thus derived are usually adequate for analyzing space–time reactor dynamics under normal operating conditions, and so they have been used to study space–time reactor systems.[6] However, when adverse conditions are considered (e.g., accident analyses, loss of coolant, or stoppage of coolant flow), the model will be different and should be treated accordingly.

Description of Methods

Although an accurate mathematical description of a reactor system can be formulated, the model consists of one or more partial differential equations in space and time variables. Because these equations defy direct solution, other methods of obtaining information about the dynamic behavior of the model are used. The six principal methods described are:

1. Point-reactor kinetics method.
2. Adiabatic method.
3. Modal method.
4. Nodal method.
5. Spatial transfer-function method.
6. Direct method.

Five of them reduce the system description to a set of ordinary differential equations by various approximation, linearizing, or averaging techniques. One retains the original equations and employs comparison techniques.

POINT-MODEL REACTOR KINETICS

The concept of point-model reactor kinetics can be stated simply as the study of reactor dynamic behavior by means of spatially averaged or weighted-average quantities of the system variables. In this method, as its name implies, the reactor is considered as a point rather than as a distributed system in space. It also can be interpreted by saying that the spatial distribution of the system variables does not change from some estimated shape. Whichever interpretation is used, the spatial variations of these variables are no longer considered in the analysis, and the only concern is the time variation of the averaged quantities.

For deriving point-model reactor equations, the various approaches proposed are based on either physical or mathematical viewpoints. The basic assumption common to all these approaches is that the space–time solution of the system variables can be separated into a single product of a space-dependent function and a time-dependent function. A space-independent equation is obtained by performing spatial integration over the reactor region. The differences among the various approaches involve the choices of the space-dependent weighting functions. The most general discussion on the derivation of the point-model kinetics equations is given by Henry,[7] who assumes the weighting function arbitrarily. The method reduces the system model to a set of ordinary differential equations.

The most often used weighting function for the point model is the steady-state adjoint solution of the system equations.[8] This choice is based on the fact that it causes the first-order part of the error in the computation of "reactivity" to vanish.[9,10] The physical interpretation is well understood as a result of the work by Hurwitz[11] and Ussachoff[12] in the critical case, and Selengut[13] and Kadomtsev[14] in the subcritical case. Other choices of weighting functions are compared by Gozani[15] and Lewins.[16]

Pros and Cons. The development of the point model was very useful in the study of reactor dynamics in the early stages of reactor development. Its advantages were:

- The introduction of a concept of reactivity that enables reactor dynamics to be studied without knowing details of the physical processes in the reactor.
- The simplification of the much more complex space–time reactor-system equations so that well-

developed methods for studying system stability and control can be applied directly to reactor systems.

However, the basic assumption used in deriving the point model means that no knowledge of the spatial variation is obtainable with this model, so it is not suitable for studying large-size power reactors, fast or thermal. Thus the consequences of using this model are:

- The stability analysis for the reactor might not be reliable because the parameters in the point-model equation are not reliable; furthermore, there is no way to account for the local peaking of the system responses (e.g., temperature) that might jeopardize the safe operation of the reactor.
- The control-system design based on the point model might not be adequate; in particular, if control is to be optimal (e.g., to produce uniform burnup), the point model might not even be near true optimal without taking into account the spatial effect of the control method.

Numerous analyses of reactor stability and control have used the point-model approximation; the major references are cited in Ref. 17.

ADIABATIC METHOD

The adiabatic method introduced by Henry and Curlee[18,19] is essentially based on the same principle as the point model. The difference is that the adiabatic method modifies the solution of the system variables as well as the spatial weighting function at various time intervals while retaining the point-model formulation. Lewins[20] and Marchuk and Orlov[21] have discussed using the time-dependent adjoint solution as weighting function; that approach, which also can be categorized as the adiabatic method, usually reduces the system either to a set of time-variant equations or to time-invariant equations between successive time intervals.

This modified version of the point model implies that the flux shape responds instantaneously to the change of reactor properties. However, its inapplicability for large power reactors means that it has the same drawbacks as the point model, although to a lesser extent.

MODAL METHOD

In concept, this method approximates the space–time solution of the system variables by a linear combination of some known space functions (modes) with undetermined time-dependent coefficients. With this method the space–time system equations can be reduced to a set of time-dependent equations of the modal coefficients by performing spatial integration over the reactor. The various types of modal methods involve the selection or construction of the space functions. The most basic and common functions selected for this purpose are an infinite set of orthogonal or biorthogonal functions. Although this method is much simpler for most one-dimensional problems,[22,23] the general approach is also suitable for systems of higher spatial dimensions[24,25] despite the complexity involved.

Various types of space functions have been proposed for the modal method. Generally, they can be categorized into two major areas: (*a*) the set of the space functions can be the eigenfunctions obtained from solving the eigenvalue (steady-state) equations (sometimes the set of space functions is referred to as the natural modes of the system); examples are the λ modes,[26] ω_p modes, ω_d modes,[27] μ modes,[28] Green's Function modes, and the inhour modes;[29] or (*b*) the set of the space functions can also be arbitrarily chosen, but usually the functions in the selected set are mutually orthogonal (e.g., the Helmholtz modes[30]).

The procedure of the method is well illustrated by Kaplan.[31] Applications to the study of stability and control of reactors can be found in Refs. 32–37.

Pros and Cons. The advantages of the modal method for analyzing stability and control can be summarized as follows:

- The method reduces the space–time reactor system to a set of time-dependent equations that can be analyzed using standard well-developed control theory.
- The spatial variation of the system variables can be calculated by analyzing the coefficient of each spatial mode.
- The procedure is straightforward for linear systems and, therefore, eliminates the complexity in the derivation of the model.

However, despite these advantages, there are serious disadvantages when the reactor system is complex or nonlinear:

- Except in extremely limited cases, the eigenfunctions (natural modes) are very difficult to calculate.
- If the space functions are arbitrarily chosen, instead of calculating the natural modes, many modes will be needed and the resultant time-dependent equations will, in general, be coupled; therefore, in stability and control analysis, a large number of simultaneous equations must be treated—particularly when the system is nonlinear, the task may very well become insurmountable.
- For a nonlinear system, whether the natural modes (for the linear part only) are obtainable or not, the resultant equations will generally be coupled; furthermore, there is no definite knowledge of how many modes are required for a specified accuracy.

In conclusion, the modal method is adequate for simple linear space–time reactor systems. For more complex or nonlinear systems, the method becomes undesirable because of the amount of effort required in the analysis.

NODAL METHOD

The concept of nodal method (coupled core) involves nothing more than considering a space–time reactor system as a finite number of points (nodes) or smaller reactor systems coupled by the interaction between adjacent nodes (e.g., due to flux leakage or heat transfer between interface boundaries). The procedure is to divide the entire reactor system into strategically located smaller regions or zones. The same basic assumption used in the point model (and adiabatic model) is imposed in each and every region, and the final node equations are derived by the same procedure as in the point-model formulation. The coupling coefficients are obtained by means of the boundary conditions given for each region.

The finite-difference technique[38] can be considered as a limiting case of the nodal method. This approach has been used for analog studies[39,40] and digital-computer programs[41,42] for obtaining the space–time solution of reactor systems. There are also cases in which some feedback effects were included in the analyses.[43–45] Despite the simple concept in this approach, it is extremely unsuitable for stability and control analysis. The major drawback is due to the large number of node equations involved in the analyses (e.g., for a simple two-dimensional problem with four equations and a 10 by 10 mesh, 400 equations must be handled).

When the nodes are few and represent gross effects in each region, leakage parameters must be obtained from experiments or from time-independent calculations. Two examples are the determination of the coupling coefficients (*kij*) in Avery's theory of coupled reactors[46] and the determination of the channel transfer coefficients in Wachspress's multichannel flux synthesis.[47,48] The reactivity concept used in the point model can also be modified for the nodal method by introducing a reactivity to each node. Examples of this type of analysis are those by Baldwin,[49] Danofsky and Uhrig[50] on Argonaut reactors, and Cohn[51] and Gamble[52] on reflected-reactor kinetics. Applications of this method to space–time reactor kinetics are described in Refs. 53 and 54; more references can be found in Ref. 55.

Pros and Cons. The advantage of the nodal method, in addition to those of the point model, for analyzing the stability and control of space–time reactor systems is that it does take into account some spatial effects. Disadvantages of the nodal method can be summarized as follows:

- The reliability of the analyses depends on the complexity of the system as well as on how many nodes are taken in formulating the model; in most cases, when the nonlinear feedback is to be included in the analyses, the number of node equations required for the desired accuracy can be very large, which is undesirable in the application of present-day control theory.
- The determination of the coupling coefficients usually poses a problem and, also, it is rather difficult to solve a set of spatial nonlinear equations whether it is time-dependent or not; to obtain the coefficients experimentally is no easy task because validly interpreting the data depends strongly on knowledge of the system solution.

TRANSFER-FUNCTION METHOD

In systems where the linear dynamic processes can be described by a set of ordinary differential equations, the transfer-function representation of the processes is very useful in the sense that the stability and control analyses can be conducted by studying the system parameters without finding the solution of system equations. Intuitively, this concept can be carried over to the general space–time systems. In the study of space–time reactor kinetics, there has been much work done in defining the concept of space-dependent transfer functions. Examples are: the spatial transfer function derived for heat-transfer problems with boundary inputs and for boiling-water reactors by Sanathanan,[56] the transfer function for reactor systems using modal expansion by Haugset,[57] the nodal method by Gage,[58] and the spatial transfer function derived through age equations by Kylstra and Uhrig.[59] The most general study on the concept of space-dependent transfer functions for reactors is by Nomura,[60] who defines the transfer function by the concept of generalized Green's transfer matrix. The resultant transfer function depends on the position of the detectors as well as the inputs. Other analyses including the study of modal interactions in measuring reactor transfer functions are those by Loewe[61] and Naqi Zaidi.[62] Application of these methods to stability analyses for reactor systems has been studied by Guppy,[63] Takeda,[64,65] and Cohn.[105]

In general, because the transfer-function concepts only apply to linear systems, most of the analyses were derived either by treating linear space–time systems or by using perturbation theory to analyze system behavior subject only to small disturbances. Furthermore, the local disturbances induced by the presence of detectors and inputs are not included in the analyses. Therefore, if the method is to be useful as an experimental tool in the study of stability and control of space–time reactor systems, it is necessary to plan, implement, and interpret meaningful experiments.

Pros and Cons. The advantages of the transfer-function method are:

- Data can be obtained experimentally and, when the experiments are repeated at various locations, can be helpful in the basic understanding of space–time stability and control analysis.
- The analyses performed on the transfer-function model can relate the system stability to the system

parameters without the necessity of finding the solution of the system.

• It is equally applicable to the various approaches in the study of space–time systems.

The disadvantage of the method is that it cannot handle nonlinear systems directly, unless the analyses are carried out for various operating conditions of the reactor system. Therefore, it is not desirable to use this method in stability and control analyses in the design stage. However, the method should be suitable for predicting system stability from extrapolation of experiments made at various operating conditions, such as application to existing point-model reactors (e.g., EBWR and EBR-I).

DIRECT METHOD

This method treats the space–time reactor system directly from the governing partial differential equations, rather than reducing the system to a lumped-parameter model described by a set of ordinary differential equations. This direct approach has been studied by many (Wang,[66] Parks,[67] Hsu,[68] Kastenberg[69]) in the fields of power-reactor dynamics, aeroelasticity, and related fields. The basic theories used in the stability analysis of space–time systems are the stability theory of Lyapunov[70] and the use of comparison functions,[71] whereas for control applications the theories used are the maximum principle of Pontryagin,[72] variational techniques,[73] and dynamic programming.[74] The application of these theories to the general lumped-parameter system as well as reactor systems has been very successful; a few selected successful applications are given in Refs. 75–79. The extension of these theories to general distributed-parameter systems was carried out by Zubov[80] and Wang[81,82] for the areas involving stability analysis, and by Butkovskii and Lerner[83,84] and Wang[66] for areas involving optimal control. The extended theories have been applied to space–time reactor systems only relatively few times, the only publications to date being the study of simple linear homogeneous reactor system stability by Lundquist and Weissglas,[85] the work in the stability analyses of general nonlinear reactor systems and optimal control of reactor systems by Hsu,[68,86,87] and stability analysis using the comparison function by Kastenberg.[69,88]

Pros and Cons. The advantages of this direct method are that its use:

• Does not require solving the system equations.

• Provides information about the effects of system-parameter variations on the system stability.

• Does not require engaging in any further approximations beyond those in the derivation of the system equations.

The one disadvantage of the direct method in stability analysis is that both Lyapunov's method and the comparison function are approaches rather than systematic methods, so there usually is no way to develop Lyapunov functionals or comparison functions for either the general linear or nonlinear systems. However, it is possible, with experience, to obtain practical design information for the specific systems of interest.

Research in Other Disciplines

The study of distributed-parameter dynamic systems is not confined to nuclear power-reactor systems. Related research is being conducted in other disciplines. Many of the developments in treating stability and control problems in other fields can be used directly or indirectly for analyzing power reactor systems. Some of the more important developments in other fields, other than those mentioned previously, are discussed briefly here.

In space–time stability analysis, Rakhmatullina[89] applied the direct method to obtain regions of stability for nonlinear heat-conduction equations, Domshlak[90] obtained regions of stability for general parabolic nonlinear systems, Eckhaus[91] discussed stability problems using power-series expansions, and Wang[92] obtained the sufficient asymptotic stability conditions for stable nonlinear parabolic systems with feedback control and transport time delays.

In space–time optimal control, work has increased in recent years. Lure[93] obtained the necessary optimality conditions for the general distributed system using the classical calculus of variations, and Egorov[94] formulated the optimal-problem quasilinear distributed systems and obtained the optimal condition using Rozonoer's method.[95] More recently, Wang and Tung[96] derived a maximum principle for diffusion systems in integral form, and Wismer[97] treated the optimal problem using multilevel control techniques; both papers used spatial discrete approximations. Kolb[98] developed optimal design concepts and techniques using finite integral transform, which is essentially one form of the modal method. Uzgiris[99] obtained the necessary condition for optimality of a linear parabolic equation with nonlinear boundary conditions using the gradient technique as applied to function space. Axelband[100] and Yeh and Tou[101] treated linear distributed systems with bounded controls. Axelband used the convex programming algorithm, whereas Yeh and Tou used conventional dynamic programming techniques. Brogan[102] gives results for the linear diffusion system with distributed control using dynamic programming and variational techniques; Sakawa[103] treated a similar problem with boundary controls. Briggs and Shen[104] treated a simplified nuclear rocket system with constraints on the system states (temperature and thermal stresses).

Because most of the referenced developments have merits in their respective areas, their pros and cons will not be discussed here.

Conclusions

Although the advantages and disadvantages of using the various approaches in the control and stability problems of spatially dependent power-reactor systems have been discussed here in a general way, there is no clear indication that any one method is distinctly superior for the analysis of power reactors in general. The choice of approach for any specific reactor depends on many interacting factors. To make a reasonable choice, one must first carefully define the objectives of his investigation and formulate an accurate mathematical model of the system. Then he must define the geometrical, physical, and mathematical characteristics of the system model and investigate the available analytical, computational, and experimental tools. From this information he then can evaluate the various methods with respect to factors such as the type of approximation required, the computational effort involved, and the respective accuracy, as well as the likely consequences of using the various methods. By weighing every aspect of the evaluation, he can decide which method would be most suitable for the system, as well as the one most likely to yield reasonable results that will achieve his objective.

Most of the references cited here are to work which is theoretical in nature and which constitutes extension of the well-known theories developed for lumped-parameter systems. In our opinion, the theoretical investigations have reached a state of maturity. Although practical application of these theories is still in its infancy because of the computational difficulties in solving the practical problems, the intense interest among the researchers causes us to expect significant progress on practical problems in the near future.

References

1. J. B. Yasinsky and A. F. Henry, Some Numerical Experiments Concerning Space–Time Reactor Kinetics Behavior, *Nucl. Sci. Eng.*, 22(2): 171-181 (1965).
2. A. F. Henry, Analytical Methods in Reactor Kinetics, in Proceedings of the 1960 Idaho Conference on Reactor Kinetics, Oct. 12–14, 1960, Sun Valley, Idaho, USAEC Report IDO-16791, pp. 263-282, July 1962.
3. S. Kaplan, A. F. Henry, S. G. Margolis, and J. J. Taylor, Space–Time Reactor Dynamics, in *Proceedings of the Third International Conference on the Peaceful Uses of Atomic Energy, Geneva, 1964*, Vol. 4, pp. 41-50, United Nations, New York, 1965.
4. W. B. Lowenstein and D. Okrent, The Physics of Fast Power Reactors — A Status Report, *Proceedings of the Second United Nations International Conference on the Peaceful Uses of Atomic Energy, Geneva, 1958*, Vol. 12, pp. 16-37, United Nations, New York, 1958.
5. S. Glasstone and A. Sesonske, *Nuclear Reactor Engineering*, pp. 262-264, D. Van Nostrand Company, Inc., Princeton, N. J., 1963.
6. C. Hsu, Control and Stability Analysis of Spatially Dependent Nuclear Reactor Systems, Ph. D. Dissertation, Purdue University, June 1967.
7. A. F. Henry, Neutron Kinetics, Sec. 5.2 in *Naval Reactors Physics Handbook*, A. Radkowsky (Ed.), Vol. I, pp. 855-864, Superintendent of Documents, U. S. Government Printing Office, Washington, 1964.
8. A. F. Henry, The Application of Reactor Kinetics to the Analysis of Experiments, *Nucl. Sci. Eng.*, 3(1): 52-70 (1958).
9. J. Lewins, Variational Representations in Reactor Physics Derived from a Physical Principle, *Nucl. Sci. Eng.*, 8(2): 95-104 (1960).
10. J. Lewins, A Variational Principle for Nonlinear Systems, *Nucl. Sci. Eng.*, 12(1): 10-14 (1962).
11. H. Hurwitz, Jr., Note on the Theory of Danger Coefficients, USAEC Report KAPL-98, Knolls Atomic Power Laboratory, September 1948.
12. L. N. Ussachoff, Equation for the Importance of Neutrons, Reactor Kinetics and the Theory of Perturbation, in *Proceedings of the International Conference on the Peaceful Uses of Atomic Energy, Geneva, 1955*, Vol. 5, pp. 503-510, United Nations, New York, 1956.
13. D. S. Selengut, Variational Analysis of Multi-Dimensional Systems, USAEC Report HW-59126, Hanford Atomic Products Operation, 1958.
14. B. B. Kadomtsev, The Invariance Principle for a Homogeneous Medium of Any Geometric Form, *Dokl. Akad. Nauk SSSR*, 113(3): 541-543 (1957). English Translation: *Soviet Phys. Dokl.*, 2(1): 71-75 (1957).
15. V. T. Gozani, The Concept of Reactivity and Its Application to Kinetic Measurements, *Nukleonik*, 5(2): 55-62 (1963).
16. J. Lewins, Time-Dependent Variational Principles for Nonconservative Systems, *Nucl. Sci. Eng.*, 20(4): 517-520 (1964).
17. H. B. Smets, Nonlinear Analytical Methods in Nuclear Power Kinetics, Zurich, September 25–26, 1961, USAEC file No. NP-10722, Organization for European Economic Cooperation.
18. A. F. Henry and N. J. Curlee, Verification of a Method for Treating Neutron Space–Time Problems, *Nucl. Sci. Eng.*, 4(6): 727-744 (1958).
19. N. J. Curlee, Nonseparable Space–Time Transients Resulting from Changes in Inlet Coolant Temperature, *Nucl. Sci. Eng.*, 6(1): 1-10 (1959).
20. J. Lewins, A Derivation of the Time-Dependent Adjoint Equations for Neutron Importance in the Transport, Continuous Slowing-Down, and Diffusion Model, *J. Nucl. Energy: Pt. A, Reactor Sci.*, 13(1/2): 1-5 (1960).
21. G. I. Marchuk and V. V. Orlov, The Theory of Adjoint Functions, in *Soviet Progress in Neutron Physics*, P. A. Krupchitskii (Ed.), pp. 24-34, Consultants Bureau, New York, 1963.
22. H. L. Garabedian, Core Kinetics, in *Proceedings of Symposia in Applied Mathematics, April 23–25, 1959*, Vol. XI, pp. 256-288, American Mathematical Society, Providence, R. I., 1961.
23. S. Kaplan, S. G. Margolis, and D. R. Harris, Transient Response of the Spatial Flux Distribution in an Initially Uniform Bare Reactor to Arbitrary Nonuniform Changes in Materials Properties, in Bettis Technical Review, Reactor Physics and Mathematics, USAEC Report WAPD-BT-17, pp. 69-83, Westinghouse Electric Corporation, February 1960.
24. H. L. Garabedian and D. H. Thomas, An Analytical Approach to Two-Dimensional Reactor Theory, *Nucl. Sci. Eng.*, 14(3): 266-271 (1962).
25. H. L. Garabedian and R. E. Lynch, Nonlinear Reactor Kinetics Analysis, *Nucl. Sci. Eng.*, 21(4): 550-564 (1965).
26. G. Birkhoff, Positivity and Criticality, in *Proceedings of Symposia in Applied Mathematics, April 23–25, 1959*, Vol. XI, pp. 116-126, American Mathematical Society, Providence, R. I., 1961.
27. E. R. Cohen, Some Topics in Reactor Kinetics, in *Proceedings of the Second United Nations International Conference on the Peaceful Uses of Atomic Energy, Geneva, 1958*, Vol. 11, pp. 302-309, United Nations, New York, 1958.

28. D. R. Harris and P. S. Lacy, A Simple Approximate Test for Spatial Xenon Stability, *Trans. Amer. Nucl. Soc.*, 3(2): 437-438 (1960).
29. A. F. Henry, The Application of Inhour Modes to the Description of Nonseparable Reactor Transients, *Nucl. Sci. Eng.*, 20(3): 338-351 (1964).
30. A. M. Weinberg and E. P. Wigner, *The Physical Theory of Neutron Chain Reactors*, The University of Chicago Press, Chicago, 1958.
31. S. Kaplan, The Property of Finality and the Analysis of Problems in Reactor Space-Time Kinetics by Various Modal Expansions, *Nucl. Sci. Eng.*, 9(3): 357-361 (1961).
32. D. E. Dougherty, The Space-Time Neutron Kinetics by a Variational Method with Application to Power Reactor Dynamics, USAEC Report KAPL-2217, Knolls Atomic Power Laboratory, December 1962.
33. A. Hitchcock, *Nuclear Reactor Stability*, Temple Press Ltd., London, 1960.
34. G. L. Gyorey, The Effect of Modal Interaction in the Xenon Instability Problem, *Nucl. Sci. Eng.*, 13(4): 338-344 (1962).
35. D. M. Wiberg, Optimal Control of Spatial Xenon Oscillation, *Trans. Amer. Nucl. Soc.*, 7(1): 219-220 (1964).
36. I. Kliger, Optimal Control of Space Dependent Nuclear Reactors, *Trans. Amer. Nucl. Soc.*, 8(1): 233-234 (1965).
37. T. R. England, G. L. Hartfield, and R. K. Deremer, Xenon Spatial Stability in Large Seed-Blanket Reactors, USAEC Report WAPD-TM-606, Bettis Atomic Power Laboratory, April 1967.
38. R. S. Varga, Numerical Solution of the Two-Group Diffusion Equations in x-y Geometry, USAEC Report WAPD-159, Westinghouse Electric Corporation, August 1956.
39. C. N. Kelber, L. C. Just, and N. F. Morehouse, Jr., The Solution of Many Region Reactor Kinetics Problems on an Analog Computer, *Nucl. Sci. Eng.*, 11(3): 285-289 (1961).
40. R. M. Pearce, Method of Studying Xenon Spatial Instability with an Analog Computer, *Nucl. Sci. Eng.*, 11(3): 323-331 (1961).
41. W. R. Cadwell, A. F. Henry, and A. J. Vigilotti, WIGLE — A Program for the Solution of the Two-Group Space-Time Diffusion Equations in Slab Geometry, USAEC Report WAPD-TM-416, Bettis Atomic Power Laboratory, January 1964.
42. J. Agresta and L. B. Borst, Space-Dependent Prompt Kinetics of a Subcritical Reactor, *Nucl. Sci. Eng.*, 7(1): 64-68 (1960).
43. R. L. Crowther and W. H. Wolf, Numerical Method for Analysis of Nonlinear Axial Dynamics of Large BWR, *Trans. Amer. Nucl. Soc.*, 6(2): 210-211 (1963).
44. D. Okrent, J. M. Cook, D. Satkus, R. B. Lazarus, and M. B. Wells, AX-1, A Computing Program for Coupled Neutronics-Hydrodynamics Calculations on the IBM-704, USAEC Report ANL-5977, Argonne National Laboratory, May 1959.
45. J. W. Riese and G. Collier, VARIQUIR — A Two-Dimensional Time-Dependent Multigroup Diffusion Code, Report WANL-TNR-133, Westinghouse Electric Corporation, September 1963.
46. R. Avery, Theory of Coupled Reactors, in *Proceedings of the Second United Nations International Conference on the Peaceful Uses of Atomic Energy, Geneva, 1958*, Vol. 12, pp. 182-191, United Nations, New York, 1958.
47. E. L. Wachspress, Digital Computation of Space-Time Variation of Neutron Fluxes, USAEC Report KAPL-2090, Knolls Atomic Power Laboratory, Oct. 1, 1960.
48. E. L. Wachspress, R. D. Burgess, and S. Baron, Multichannel Flux Synthesis, *Nucl. Sci. Eng.*, 12(3): 381-389 (1962).
49. G. C. Baldwin, Kinetics of a Reactor Composed of Two Loosely Coupled Cores, *Nucl. Sci. Eng.*, 6(4): 320-327 (1959).
50. R. A. Danofsky and R. E. Uhrig, The Kinetic Behavior of the Coupled Regions of the UTR-10 Reactor, *Nucl. Sci. Eng.*, 16(1): 131-133 (1963).
51. C. E. Cohn, Reflected-Reactor Kinetics, *Nucl. Sci. Eng.*, 13(1): 12-17 (1962).
52. D. D. Gamble, The Effect of Reflector Moderated Neutrons on the Kinetics of the Kinetic Experiment Water Boiler Reactor, *Trans. Amer. Nucl. Soc.*, 3(1): 122-125 (1960).
53. C. G. Chezem and R. L. Seale, Temperature Dependent Kinetics of Coupled-Core Reactors, USAEC Report LA-3148-MS, Los Alamos Scientific Laboratory, July 1964.
54. S. J. Gage, F. T. Adler, and P. N. Powers, Investigations on Nonlinear Stability of Coupled Nuclear Systems, in *Neutron Dynamics and Control*, Tucson, Ariz., Apr. 5-7, 1965, D. L. Hetrick and L. E. Weaver (Coordinators), pp. 45-76, AEC Symposium Series, No. 7 (CONF-650413), 1966.
55. C. G. Chezem and W. H. Koehler (Eds.), Proceedings of the National Topical Meeting on Coupled Reactor Kinetics, January 23-24, 1967, at College Station, Texas, Report CONF-670107, Texas A & M Press, 1967.
56. C. K. Sanathanan, On the Synthesis of Space Dependent Transfer Functions, *Inst. Elec. Electron. Eng. Trans. Automat. Contr.*, AC-11(4): 724-729 (1966).
57. K. Haugset, A Study of Space-Dependent Transfer Functions, Norwegian Report KR-107, 1966.
58. S. Gage and F. T. Adler, Approximate Transfer Functions for Coupled-Core Reactor Dynamics, *Trans. Amer. Nucl. Soc.*, 8(2): 502-503 (1966).
59. D. C. Kylstra and R. E. Uhrig, Spatially Dependent Transfer Function for Nuclear Systems, *Nucl. Sci. Eng.*, 22(2): 191-205 (1965).
60. T. Nomura, Some Aspects of Zero Power Reactor Transfer Functions, *J. Nucl. Sci. Technol. (Tokyo)*, 1(2): 41-50 (1964).
61. W. E. Loewe, Space-Dependent Effects in the Response of a Nuclear Reactor to Forced Oscillations, *Nucl. Sci. Eng.*, 21(4): 536-549 (1965).
62. S. M. Naqi Zaidi, The Effect of Detector and Reactivity Oscillator Location in Reactor Transfer Function Measurement, M.S. Thesis, University of Illinois, 1963.
63. C. B. Guppy, Transfer Function Synthesis for Reactor Spatial Dynamics Using the Modal Approach, British Report AEEW-R-197, 1962.
64. K. Mochizuki and A. Takeda, An Analysis of Neutron Flux Spatial Oscillation Due to Xenon Build-Up in a Large Power Reactor Core, *Nucl. Sci. Eng.*, 7(4): 336-344 (1960).
65. A. Takeda, Pt. 1, A Method of Analysis of Reactor Spatial Kinetics of Calder Hall Type Reactors, and Pt. 2, A Study of the Transfer Functions of Spatial Kinetics in the Nuclear Reactor, British Report AERE-Trans-888, 1962.
66. P. K. C. Wang, Control of Distributed Parameter Systems, in *Advances in Control Systems*, C. T. Leondes (Ed.), Vol. 1, pp. 75-173, Academic Press Inc., 1964.
67. P. C. Parks, A Stability Criterion for a Panel Flutter Problem via the Second Method of Lyapunov, in *Proceedings of the AIAA Symposium on Structural Dynamics and Aeroelasticity, Boston, Mass., Aug. 30-Sept. 1, 1965*, pp. 92-95, American Institute of Aeronautics and Astronautics.
68. C. Hsu and R. E. Bailey, Stability Analysis of Nonlinear Reactor Systems, *Trans. Amer. Nucl. Soc.*, 9(2): 457 (1966).
69. W. Kastenberg, Stability Analysis of Nonlinear Space Dependent Reactor Kinetics, Ph. D. Thesis, University of California, Berkeley, 1966.
70. N. N. Krasovskii, *Stability of Motion*, Stanford University Press, Stanford, Calif., 1963.

71. G. Prodi, Stability Questions for Nonlinear Partial Differential Equations of Parabolic Type, (in Italian) *Atti Accad. Naz. Lincei, Rend., Cl. Sci. Fiz., Mat. Natur., Ser. 8*, 10: 365-370, (1951).
72. L. S. Pontryagin et al., *The Mathematical Theory of Optimal Processes*, John Wiley & Sons, Inc., New York, 1962.
73. M. Becker, *The Principles and Applications of Variational Methods*, The M.I.T. Press, Cambridge, Mass., 1964.
74. R. E. Bellman and R. Kalaba, Dynamic Programming and Modern Control Theory, Academic Press Inc., New York, 1965.
75. E. P. Gyftopoulos, Applications of Geometric Theory to Nonlinear Reactor Dynamics, *Nucl. Sci. Eng.*, 10(3): 254-268 (1961).
76. H. B. Smets, *Problems in Nuclear Power Reactor Stability*, Presses Universitaires, Bruxelles, 1962.
77. J. Chernick, A Review of Nonlinear Reactor Dynamics Problems, USAEC Report BNL-774, Brookhaven National Laboratory, July 1962.
78. J. J. Roberts and H. P. Smith, Jr., Time Optimal Solution to the Reactivity-Xenon Shutdown Problem, *Nucl. Sci. Eng.*, 22(4): 470-478 (1965).
79. I. Kliger, Synthesis of an Optimal Nuclear Reactor Control System, in *Neutron Dynamics and Control*, Tuscon, Ariz., Apr. 5–7, 1965, D. L. Hetrick and L. E. Weaver (Coordinators), pp. 110-136, AEC Symposium Series, No. 7 (CONF-650413), 1966.
80. V. I. Zubov, The Methods of Lyapunov and Their Applications, USAEC Report AEC-tr-4439, 1957.
81. P. K. C. Wang, Stability Analysis of Elastic and Aeroelastic Systems via Lyapunov's Direct Method, *J. Franklin Inst.*, 281(1): 51-72 (1966).
82. P. K. C. Wang and M. L. Bandy, On the Stability of Equilibrium of a Diffusion System with Feedback Control, Research Note No. NF-56, IBM Research Laboratory, San Jose, Calif., June 1964.
83. A. G. Butkovskii and A. Ya. Lerner, The Optimal Control of Systems with Distributed Parameters, *Automat. and Remote Contr., (USSR) (Engl. Transl.)*, 21(6): 472-477 (1960).
84. A. G. Butkovskii, Optimum Processes in Systems with Distributed Parameters, *Automat. and Remote Contr., (USSR) (Engl. Transl.)*, 22(1): 13-21 (1961); A Maximum Principle for Optimum Systems with Distributed Parameters, 22(10): 1156-1169 (1961); Some Approximate Methods for Solving Problems of Optimal Control of Distributed Parameter Systems, 22(12): 1429-1438 (1961); Broadened Principle of Maximum for Optimal Control Problems, 24(3): 292-304 (1963).
85. S. Lundquist and P. Weissglas, A Method for Determination of Spatial Stability, *Nuc. Sci. Eng.*, 15(4): 474-475 (1963).
86. C. Hsu, Stability Analysis of Reactor Systems via Lyapunov's Second Method, *Trans. Amer. Soc. Mech. Eng., Ser. D, J. Basic Eng.*, 89(2): 307-310 (June 1967).
87. C. Hsu and R. E. Bailey, Optimal Control of Spatially-Dependent Nuclear Reactors, *Trans. Amer. Nucl. Soc.*, 10(1): 253-254 (1967).
88. W. E. Kastenberg, On the Stability of a Reactor with Positive Feedback, *Trans. Amer. Nucl. Soc.*, 10(2): 567 (1967); W. E. Kastenberg and P. L. Chambre, On the Space–Time Behavior of an Adiabatic Reactor, *Trans. Amer. Nucl. Soc.*, 10(2): 567-568 (1967).
89. L. L. Rakhmatullina, On the Problem of Stability of the Solution of the Nonlinear Heat-Conduction Equation, *Prikl. Mat. Mekh.*, 25(3): 591-592 (1961), in Russian; *J. Appl. Math & Mech.*, pp. 880-883, in English.
90. Iu. I. Domshlak, On the Asymptotic Stability of the Solution of a Nonlinear Parabolic System, *Prikl. Mat. Mekh.*, 27(1): 166-167 (1963), in Russian; *J. Appl. Math. & Mech.*, pp. 238-240, in English.
91. W. Eckhaus, *Studies in Nonlinear Stability Theory*, Springer Tracts in Natural Philosophy, No. 6, Springer-Verlag, New York, Inc., 1965.
92. P. K. C. Wang, Asymptotic Stability of Distributed Parameter Systems with Feedback Controls, *Inst. Elec. Electron. Eng. Trans. Automat. Contr.*, AC-11(1): 46-54 (1966).
93. K. A. Lure, The Mayer-Bolza Problem for Multiple Integrals and the Optimization of the Performance of Systems with Distributed Parameters, *Prikl. Mat. Mekh.*, 27(5): 842-853 (1963), in Russian; *J. Appl. Math & Mech.*, pp. 1287-1299, in English.
94. A. I. Egorov, On Optimal Control of Processes in Distributed Objects, *Prikl. Mat. Mekh.*, 27(4): 688-696 (1963), in Russian; *J. Appl. Math. & Mech.*, pp. 1045-1058, in English.
95. L. I. Rozonoer, The Maximum Principle of L. S. Pontryagin in the Theory of Optimal Systems, *Automat. and Remote Contr. (USSR) (Engl. Transl.)*, 20(10): 1288-1302 (1959); 20(11): 1405-1421 (1959); 20(12): 1517-1532 (1959).
96. P. K. C. Wang and F. Tung, Optimum Control of Distributed-Parameter Systems, *Trans. Am. Soc. Mech. Eng., Ser. D, J. Basic Eng.*, 86(1): 67-79 (March 1964).
97. D. A. Wismer, Jr., Optimal Control of Distributed Parameter Systems Using Multi-Level Techniques, Ph. D. Thesis, University of California, Los Angeles, Report AD-646096, November 1966.
98. R. C. Kolb, Optimal Control of Linear Distributed-Parameter Systems, Ph. D. Thesis, Montana State University, *Diss. Abstr.*, 66-10846 (1966).
99. S. C. Uzgiris, Control of Distributed Parameter Systems with Nonlinear Boundary Conditions, Ph. D. Thesis, Illinois Institute of Technology, *Diss. Abstr.*, 66-10482 (1966).
100. E. I. Axelband, The Optimal Control of Certain Classes of Linear Distributed Parameter Systems, Ph. D. Thesis, University of California, Los Angeles, *Diss. Abstr.*, 66-4741 (May 1966).
101. H. H. Yeh and J. T. Tou, Optimum Control of a Class of Distributed-Parameter Systems, *Inst. Elec. Electron. Eng. Trans. Automat. Contr.*, AC-12(1): 29-37 (February 1967).
102. W. L. Brogan, Optimal Control Theory Applied to Systems Described by Partial Differential Equations, Ph. D. Thesis, University of California, Los Angeles, *Diss. Abstr.*, 65-12701 (1965).
103. Y. Sakawa, Optimal Control of a Certain Type of Linear Distributed Parameter Systems, *Inst. Elec. Electron. Eng. Trans. Automat. Contr.*, AC-11(1): 35-41 (January 1966).
104. D. L. Briggs and C. N. Shen, Distributed Parameter Control of a Nuclear Rocket with Thermal Stress Constraints, *Trans. Amer. Soc. Mech. Eng., Ser. D., J. Basic Eng.*, 89(2): 300-306 (June 1967).
105. C. E. Cohn, R. J. Johnson, and R. N. Macdonald, Calculating Space-Dependent Transfer Functions Using Statics Techniques, *Nucl. Sci. Eng.*, 26: 198 (October 1966).

Coolant Ejection Mechanisms for Use in Analyzing Fast Reactor Safety

By Hans K. Fauske

During steady-state operation, the coolant in a liquid-metal-cooled fast breeder reactor (LMFBR) is considerably below its boiling temperature throughout the core. But abnormal reactor behavior (reactivity perturbations and coolant-system failures) might greatly increase coolant temperature due to rapid heat insertion, a decrease in flow, or both, and might initiate boiling. When this occurs, reactivity might increase, but the rate of increase depends primarily on how rapidly sodium is ejected from fuel-coolant channels. This article reviews various models that have been proposed to describe liquid ejection from reactor coolant channels. A previous article[1] evaluated our knowledge of the superheat problem of liquid metals, a prerequisite for describing the ejection or expulsion of the liquid sodium from the reactor core.

Rapid Channel Voiding

Two basically different approaches have been adopted in theoretical studies of transient void formation: (1) vapor growth according to thermodynamic equilibrium[2–5]—zero liquid superheat before as well as during the void formation—and (2) vapor growth based on nonequilibrium[6–8]—liquid superheating might occur in the single- and the two-phase regions. The various two-phase flow patterns assumed in these analyses are summarized in Fig. 1.

Equilibrium Models

Models pertaining to equilibrium vapor growth include TRANSFUGUE-I (Ref. 2), BURP (Ref. 3), the MacFarlane analysis (Ref. 4), and TRANSFUGUE-II (Ref. 5).

TRANSFUGUE-I

The equations that describe this model[2] are:
Continuity:

$$\frac{\partial \rho}{\partial t} + \frac{\partial}{\partial z}(\rho u) = 0 \qquad (1)$$

Momentum:

$$\rho \frac{\partial u}{\partial t} + \rho u \frac{\partial u}{\partial z} + g\rho + \frac{f\rho u^2}{2D_e} + \frac{\partial P}{\partial z} = 0 \qquad (2)$$

Energy:

$$\gamma\phi(z,t) - \rho \frac{\partial h}{\partial t} - \rho u \frac{\partial h}{\partial z} = 0 \qquad (3)$$

This set of equations applies to a homogeneous two-phase mixture where the density is defined by:

$$\rho = \frac{\rho_l \rho_g}{\rho_g (1-x) + \rho_l x} \qquad (4)$$

Because thermodynamic equilibrium is assumed, the vapor quality is:

$$x = \frac{h - h_l}{h_{fg}} \qquad (5)$$

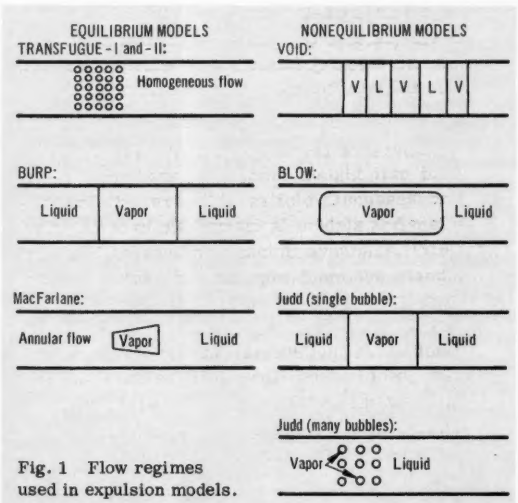

Fig. 1 Flow regimes used in expulsion models.

Because numerical instabilities occur in solving these equations, the following additional restrictions were imposed: (1) constant vapor density and (2) saturation temperature constant everywhere in the channel. These restrictions imply that the calculated voiding rate becomes essentially independent of the momentum equation and is not modified as a result of pressure buildup (increased vapor density and saturation temperature). Thus, for the flow regime chosen, the TRANSFUGUE-I model will overestimate the void growth in the case of zero initial superheat. The pressures calculated from TRANSFUGUE-I for a typical loss-of-flow transient are shown in Fig. 2 together with sodium vapor pressures corresponding to calculated temperatures (Fig. 3). As pointed out in Ref. 2, a considerably larger pressure is necessary for this type of void growth (energy controlled) than is available from the only source of pressure, namely, the vapor pressure of sodium.

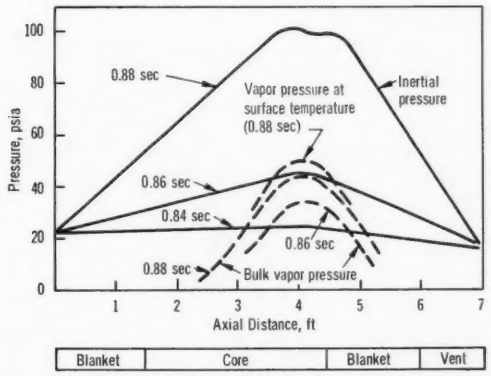

Fig. 2 Inertial and vapor pressures resulting from a typical loss-of-flow transient, as calculated by TRANSFUGUE-I code.[3]

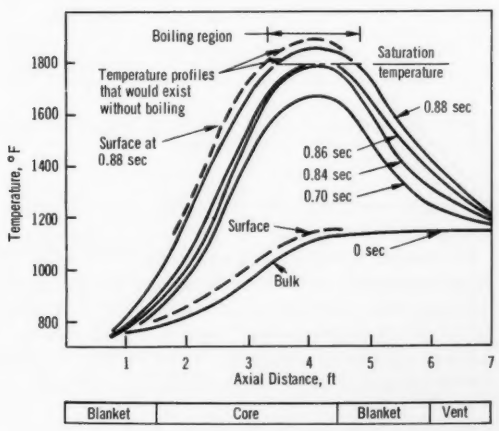

Fig. 3 Sodium temperatures calculated to occur during typical loss-of-flow transient.[3]

THE BURP MODEL

The occurrence of strong self-pressurization effects from TRANSFUGUE-I calculations of power and loss-of-flow transients and numerical instability problems resulted in another model called BURP.[3] The assumptions used to construct this model are: (1) the void spreads axially along the channel from a single starting point (Fig. 1) (note that the vapor is in contact with the heated surface), (2) the pressure in the void region is equal to the highest vapor pressure of the bounding liquid, (3) the self-pressurization effect suppresses boiling away from the growing void region, and (4) the void fraction within the vapor region is 100% (Ref. 3).

Figure 4 illustrates core voiding and pressure buildup for the loss-of-flow transient (same condition as used in Fig. 2 for TRANSFUGUE-I). Being consistent with the vapor pressures, the maximum pressures shown in Fig. 4 are considerably less than those calculated from TRANSFUGUE-I. However, because energy considerations are not included in the analysis, the method used for estimating the bubble pressure becomes questionable. Furthermore, if a

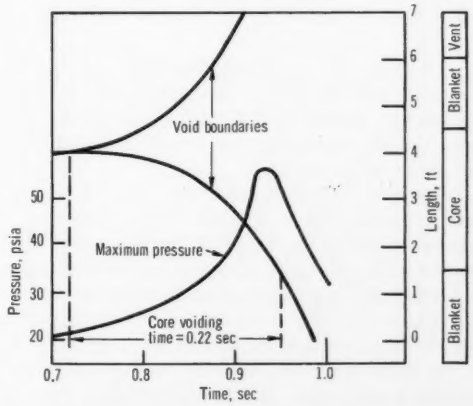

Fig. 4 Maximum pressure and location of void boundaries after boiling in a flow transient as calculated with the BURP model.[3]

liquid layer is present on the heated wall (most likely the case and will be discussed later), the BURP model will predict too small a voiding rate, since evaporation of this layer will increase the vapor pressure over that predicted and will result in larger expulsion rates.

THE MacFARLANE ANALYSIS

This model[4] represents improvements over the TRANSFUGUE-I code in three areas: (1) the ref-

erence pressure (or saturation temperature) along the channel varies according to the steady-state profile during the two-phase transient rather than being fixed at a constant value, (2) an annular flow model is assumed, allowing for slip rather than equal phase velocities (Fig. 1), and (3) a space–time dependent vapor density (feedback from inertia and friction considerations) is used rather than a constant value throughout the channel.

The governing equations are:

Continuity:

$$\frac{\partial}{\partial t}\left[\alpha\rho_g + (1-\alpha)\rho_l\right] + \frac{\partial}{\partial z}\left[\alpha\rho_g u_g + (1-\alpha)\rho_l u_l\right] = 0 \quad (6)$$

Momentum:

$$\frac{\partial}{\partial t}\left[\alpha\rho_g u_g + (1-\alpha)\rho_l u_l\right] + \frac{\partial}{\partial z}\left[\alpha\rho_g u_g^2 + (1-\alpha)\rho_l u_l^2\right] + g\left[\alpha\rho_g + (1-\alpha)\rho_l\right] + \frac{\partial \tau}{\partial z} + \frac{\partial P}{\partial z} = 0 \quad (7)$$

Energy:

$$\gamma\phi(z,t) - \frac{\partial}{\partial t}\left[\alpha\rho_g h_g + (1-\alpha)\rho_l h_l\right] - \frac{\partial}{\partial z}\left\{G\left[xh_g + (1-x)h_l\right]\right\} = 0 \quad (8)$$

The well-known Lockhart–Martinelli analysis[9] is used for estimating the void fraction for a given equilibrium quality (Eq. 5) and liquid–vapor density ratio, which represents the equation of state for the two-phase mixture.

The improvements made in this analysis should result in a somewhat smaller voiding rate than that calculated from the TRANSFUGUE-I model for the same initial conditions. However, numerical instabilities were also encountered in the MacFarlane analysis; therefore it was necessary to effectively decouple Eqs. 7 and 8 to eliminate inertia and friction feedback on the saturation temperature. As a result, pressure buildup larger than that available from the vapor pressure is calculated (see Figs. 5 and 6, which represent typical power excursions), again probably resulting in a conservative estimate of the core voiding rate for the case of zero initial superheat and the flow regime chosen. This model has been incorporated in a more complicated calculation that includes the reactor kinetics equations and reactivity feedback.[10]

In the MacFarlane analysis, as well as in the TRANSFUGUE-I model, two-phase compressibility effects were neglected, and the momentum equation is used in the so-called "momentum integral" form.[11] This technique implies that pressure is effectively eliminated as an unknown in the momentum equation and is simply integrated across specified volume boundaries. In the case of high-pressure systems

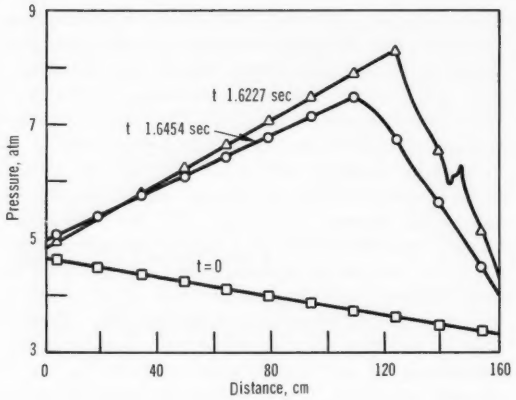

Fig. 5 Pressure profiles at various times, as calculated by the MacFarlane analysis.[10]

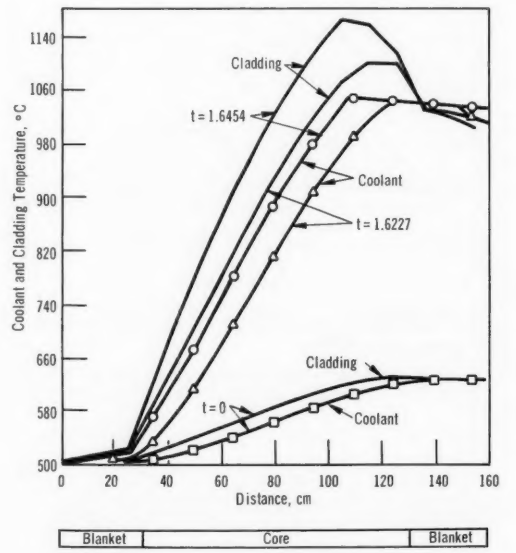

Fig. 6 Coolant-temperature profiles at various times as calculated by the MacFarlane analysis.[10]

(thermal reactors), this technique can be considered a valid approximation.

In typical low-pressure systems (LMFBR's) with large transients, however, the method becomes questionable. Since large pressurization effects are likely to occur within the coolant channels with corresponding local momentum changes, these must be accounted for in the analysis.

TRANSFUGUE-II

This code[5] is basically the same as the TRANSFUGUE-I code with the following improvements: (1)

the elimination of the numerical instability problems, making feedback from pressure changes to vapor density possible (it is not clear to this reviewer whether correction to the vapor quality is made), (2) the inclusion of a variable two-phase heat-transfer coefficient, and (3) the conversion from FORTRAN IV to FORTRAN H. A detailed description of this analysis, in particular the treatment of two-phase compressibility effects and numerical techniques used, would be welcome.

Nonequilibrium Models

As illustrated in Ref. 1, a considerable amount of experimental data have become available on liquid-metal superheat, clearly indicating that large superheats can occur before boiling is initiated. Models taking into account incipient superheat include VOID,[6] BLOW,[7] and Judd's analyses.[8]

THE VOID MODEL

This model[6] represents the first attempt to take into account superheating of the liquid metal before boiling is initiated. For a specified superheat, vapor growth and pressure within the channel are computed by solving simultaneously the continuity, momentum, and energy equations describing a one-dimensional bubble-growth model that treats bubbles (assumed proportional to the active nucleation site density) as slabs of liquid and vapor (see Fig. 1). The heat transfer across each liquid–vapor interface is calculated using an empirical relation between the liquid and the vapor temperatures. The strong effect of superheat on the voiding rate calculated from this model is shown in Fig. 7. The amount of superheat present when boiling occurs, together with the rate of superheat release, governs the driving pressure for liquid-sodium ejection. These factors also determine whether the reactor heat flux is an important parameter in subsequent vapor production leading to complete voidage of the coolant channels (Fig. 7).

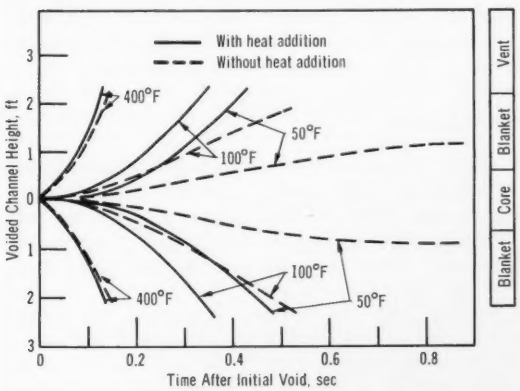

Fig. 7 Core flow-blockage effects of superheat and heat addition, as calculated by the void model.[6]

The choice of flow pattern used in this model is, however, questionable. For example, assuming heat transfer to take place only from liquid–vapor interfaces perpendicular to the flow direction (disregarding the possibility of a liquid layer adjacent to the wall) might conceivably lead to underestimation of vapor growth and liquid expulsion velocities for a given superheat.

THE BLOW CODE

Experimental observations of potassium and sodium ejections from single channels,[12] suggesting that the void growth occurs as a single bubble that grows and eventually occupies the entire cross section except for a thin liquid film remaining on the heated wall (see Fig. 1), led to development of the BLOW code.[7] It uses the well-known one-dimensional equations describing heat conduction in the fuel pin and cladding and Newton's law describing the ejection of liquid. The assumed boiling process that supplies vapor to the expanding bubble from the liquid surface layer is verified by applying the kinetic theory of gases. Predicted values of the voiding rates from this model were compared with the potassium-ejection experiments.[12] Incipient superheat values were calculated by matching the ejection behavior. Figure 8 shows

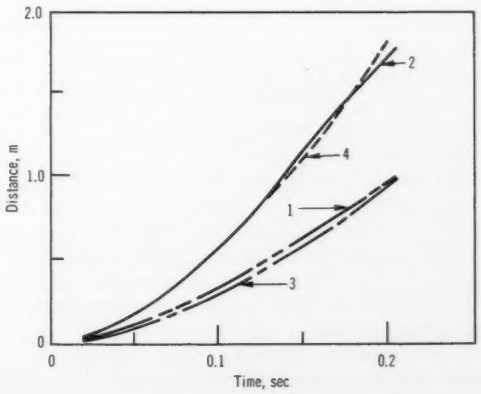

Fig. 8 Natural-convection kinetic behavior during boiling. Curves 1 and 2 are experimental data;[12] curves 3 and 4 are calculated with the BLOW code.[7]

ejection starting from natural convection with 65°C initial superheat as compared to 29°C measured, and Fig. 9 shows ejection initiated from forced convection with 25°C superheat as compared to 11°C measured. In other words, if measured superheats are used, the BLOW code will underestimate the experimental ejection rates. However, quoting Ref. 7, "Because of the difficulty of measuring the exact temperature at

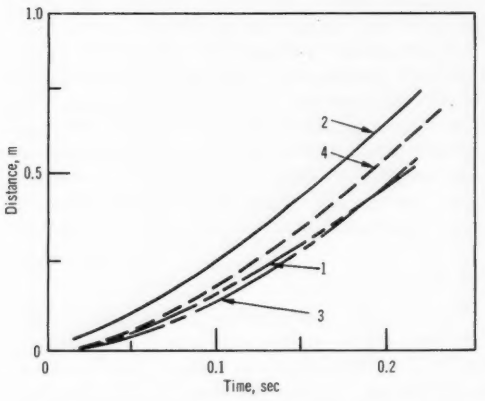

Fig. 9 Forced-convection kinetic behavior during boiling. Curves 1 and 2 are experimental data;[12] curves 3 and 4 are calculated with the BLOW code.[7]

the point of bubble nucleation, the discrepancy between the measured and the assumed superheat temperature is not too difficult to explain." It is perhaps possible to explain parts of the deviations as being due to oversimplification of the flow regime. As an example, if the effects of initial bubble formation and liquid film thickness were included in the analysis, they might improve the predictions.

JUDD'S ANALYSES

Judd[8] was not sure whether one bubble or many bubbles control the expulsion (data on metallic and nonmetallic fluids[13–15] show both flow regimes). He therefore examined both cases (Fig. 1).

His single-bubble solution is quite similar to the BURP model,[3] except for: (1) consideration of initial superheating and (2) the bubble growth can be heat-transfer as well as inertia limited. (For a similar treatment of the bubble-growth problem, see Ref. 14.) Again, the shortcoming of this approach, as pointed out by Judd, is that of ignoring the possibility of a liquid layer in contact with the heated wall.

In the analysis assuming many bubbles, it was found that the number of bubbles taking part in the expulsion has a small effect and depends mainly on the superheat. The increased surface area due to many bubbles leads to expulsion controlled primarily by inertia. Again, the latter analysis could lead to underestimation of the voiding rate, since the predicted driving pressure for the liquid slugs is considerably less than the vapor pressure corresponding to the temperature of the superheated liquid.

Recommendations for Improvements

So that critical-heat-flux limits (vapor in contact with the heated surface), nonequilibrium, and compressibility effects can be evaluated, the basic requirement for improving the proposed voiding models is reliable information about the flow regimes throughout the voiding period. The importance of considering the two-phase compressibility effects was pointed out in Ref. 16, which reported sodium-ejection experiments that verified the single-bubble expulsion theory (liquid film on the heating surface) but also verified that condensation occurs as the bubble or vapor slug moves into colder regions of fluid, resulting in two-phase choking controlling the expulsion rate at the lower liquid–vapor interface. Reference 16 also discussed water experiments carried out to simulate sodium expulsion; the philosophy can be summarized by quoting the paper: "The obtained results have shown that there was no basic difference between water and sodium vaporization, if similar initial conditions are chosen. Particularly the dynamics of ejection is similar and the importance of the role played by the critical flow phenomena was shown."

It appears, therefore, that much of the detailed information needed to refine existing voiding models can be obtained by using nonmetallic fluids that are considerably easier and less expensive to handle. This approach was verified by recent experiments[17,18] in which extensive data on flashing flow of sodium and water were obtained, suggesting that no major differences existed and that the expulsion or flashing leading to critical flow is controlled hydrodynamically rather than thermally. However, as yet no satisfactory theoretical predictions are available for the two-phase choking phenomenon in the low-quality region.

To evaluate accurately the magnitude of the compressibility effects requires a good knowledge of how pressure waves propagate in two-phase mixtures. Very few experimental data are available in this area,[19] and recent data obtained using two-component mixtures[20] illustrate the strong dependency of flow regime on the propagation velocity of pressure waves (Fig. 10). These findings emphasize the importance of knowing the flow regimes throughout the entire voiding period of a reactor coolant channel.

Conclusions

From this brief review of proposed models dealing with rapid channel voiding, it can be concluded that:

- In the case of zero initial liquid superheat, TRANSFUGUE-I and the MacFarlane analyses will generally result in conservative estimates of the voiding rates (assuming the flow regimes used are correct), with the former predicting the largest values, whereas the BURP model will probably underestimate the voiding rate if the heated surfaces remain wetted. It should be noted that experimental verification for these models is still lacking.
- In the case of sizable liquid superheat (the actual value of superheat present under reactor conditions

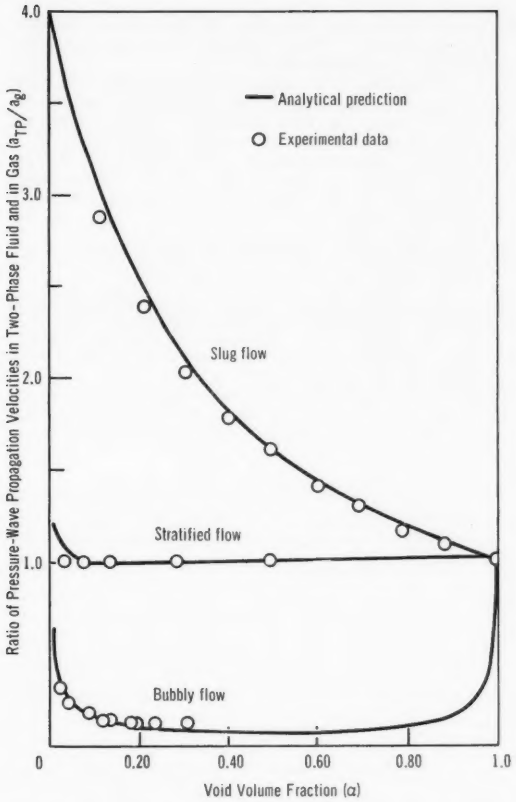

Fig. 10 Measured and calculated pressure-wave propagation velocities in air–water mixtures.

remains to be determined, see Ref. 1), most likely none of the equilibrium models will yield a dependable description of the voiding problem.

• Of the models taking into account liquid superheating, the BLOW code appears the most attractive because of its simplicity and extensive experimental verification. However, none of these models account for the two-phase expulsion that is likely to follow the piston-type ejection from a channel blocked at the inlet.

• Additional refinements of the models require detailed information about the flow regimes throughout the voiding process such that heat-transfer limitations, nonequilibrium, and compressibility effects can be accounted for.

• At the present time, all the sodium boiling data have been obtained in single-channel experiments, and these have provided a basis for developing some of the one-dimensional expulsion models. Whether these models can adequately describe the coolant motion in a fuel subassembly depends on results of experiments with multipin clusters.

Nomenclature

a_g = pressure-wave propagation velocity in gas
a_{TP} = pressure-wave propagation velocity in two-phase fluid
D_e = equivalent diameter
f = friction factor
g = acceleration of gravity
G = total mass flow rate
h = fluid enthalpy
h_g = vapor enthalpy
h_l = liquid enthalpy
h_{fg} = latent heat of vaporization
P = pressure
t = time
u = fluid velocity
u_g = vapor velocity
u_l = liquid velocity
x = vapor quality
z = distance
$\phi(z,t)$ = heat flux at channel wall
α = volume fraction of gas or vapor
ρ = fluid density
ρ_g = vapor density
ρ_l = liquid density
τ = frictional pressure
$\partial\tau/\partial z$ = frictional pressure gradient
γ = ratio of channel perimeter to cross-sectional area

References

1. H. K. Fauske, Superheating of Liquid Metals in Relation to Fast Reactor Safety, *Reactor Fuel-Process. Technol.*, 11(2): 84-88 (Spring 1968).
2. R. C. Noyes, J. G. Morgan, and H. H. Cappel, TRANSFUGUE-I, A Digital Code for Transient Two-Phase Flow and Heat Transfer, USAEC Report NAA-SR-11008, Atomics International, July 1965.
3. R. C. Noyes, H. Lurie, and A. A. Jarrett, The Development and Growth of In-Core Voids Due To Boiling During Fast Reactor Transients, in Proceedings of the Conference on Safety, Fuels, and Core Design in Large Fast Power Reactors, October 11–14, 1965, USAEC Report ANL-7120, Argonne National Laboratory, pp. 881-889, 1965.
4. D. R. MacFarlane, Transient Sodium Boiling Calculations-II, *Nucl. Eng. Design*, 6: 103-114 (1967).
5. D. Logan et al., Boiling Liquid Metals and Two-Phase Flow Investigations, in Proceedings of the International Conference on the Safety of Fast Reactors, Aix-en-Provence, France, September 19–22, 1967 (to be published).
6. W. G. Meinhardt, Calculating Vapor Growth in a Superheated Liquid Metal Within a Heated Channel, *Trans. Amer. Nucl. Soc.*, 9(2): 566-567 (1966).
7. W. Peppler et al., Sodium Boiling and Fast Reactor Safety, in Proceedings of the International Conference on the Safety of Fast Reactors, Aix-en-Provence, France, September 19–22, 1967 (to be published).
8. A. M. Judd, Boiling and Condensation of Sodium in Relation to Fast Reactor Safety, in Proceedings of the International Conference on the Safety of Fast Reactors, Aix-en-Provence, France, September 19–22, 1967 (to be published).
9. R. W. Lockhart and R. C. Martinelli, Proposed Cor-

relation of Data for Isothermal Two-Phase Two-Component Flow in Pipes, *Chem. Eng. Prog.*, 45(1): 39-48 (January 1949).
10. D. R. MacFarlane et al., Theoretical Studies of the Response of Fast Reactors During Sodium Boiling Accidents, in Proceedings of the International Conference on the Safety of Fast Reactors, Aix-en-Provence, France, September 19–22, 1967 (to be published).
11. J. E. Meyer, Hydrodynamic Models for the Treatment of Reactor Thermal Transients, *Nucl. Sci. Eng.*, 10(3): 269-277, July 1961.
12. G. Grass et al., Das Sieden von Flussigen Alkalimetallen, *Atomkernenergie*, 12: 101-110 (1967).
13. G. Friz, Coolant-Ejection Studies with Analogy Experiments, in Proceedings of the Conference on Safety, Fuels, and Core Design in Large Fast Power Reactors, October 11–14, 1965, USAEC Report ANL-7120, Argonne National Laboratory, pp. 890-894, 1965.
14. P. G. Kosky, Some Aspects of Boiling and Vapor Voidage Growth Problems in a Liquid-Metal-Cooled Reactor, in Proceedings of the International Conference on the Safety of Fast Reactors, Aix-en-Provence, France, September 19–22, 1967 (to be published).
15. R. M. Singer, The Expulsion of Liquid from a Rapidly Heated Channel, USAEC Report ANL-7337, Argonne National Laboratory, May 1967.
16. B. Le Gonidec et al., Experimental Studies on Sodium Boiling, in Proceedings of the International Conference on the Safety of Fast Reactors, Aix-en-Provence, France, September 19–22, 1967 (to be published).
17. H. K. Fauske, Two-Phase Compressibility in Liquid Metal Systems, in Proceedings of the International Conference on the Safety of Fast Reactors, Aix-en-Provence, France, September 19–22, 1967 (to be published).
18. H. K. Fauske et al., Sodium Flashing Experiment, *Trans. Amer. Nucl. Soc.*, 10(2): 693 (1967).
19. H. K. Fauske, Propagation of Pressure Disturbances in Two-Phase Flow, in Proceedings of the Symposium on Two-Phase Flow Dynamics, Eindhoven, Netherlands, September 4–9, 1967, USAEC Report CONF-670912 (to be published).
20. R. E. Henry and H. K. Fauske, Propagation Velocity of Pressure Waves in Two-Phase Mixtures and the Dependency on Flow Regimes, *Trans. Amer. Nucl. Soc.*, 11(1): 364-365 (1968).

Compact Power Concept Features a Fast Reactor, Heat Pipes, and Direct Converters

By John J. Roberts and Edward J. Croke

A simple, durable, and lightweight power generator might result if a compact fast reactor fueled by ^{239}Pu in a new high-temperature form were combined with heat pipes, the latest development in heat-transfer technology. Described here is a conceptual design for such a heat source that could take advantage of advancements in the technology of thermoelectric or thermionic energy converters. The passive self-regulating nature of the system could permit unattended operation. A major objective of the 1-kw(e) design is the potential for straightforward uprating of power to at least 10 kw(e).

Although the design of the system has not been optimized or pointed toward a specific application, its possible features and performance are described here because they might be of interest in exploring the feasibility of various lightweight power sources. We believe that reactor systems of this type could compete with other power systems where light weight, reliability, and reasonable cost are important.

Fuel Material. The design involves a new and unproved fuel material, plutonium monophosphide (PuP), in which ^{239}Pu would be the fissionable constituent. Because ^{239}Pu is a by-product of the expanding number of water-cooled reactors being built by utilities, it will be available in useful quantities.[1] This fuel should cost from 20 to 70% of the equivalent in radioisotopes for power in the 25- to 125-kw(t) range. A reasonably firm cost prediction[2] of $10/g for ^{239}Pu implies a fuel inventory cost of about $380,000 per reactor, a figure that is essentially independent of the thermal-power level. Fuel burnup will be less than 0.05% for each 10,000 kw-hr of electricity generated.

Heat Pipes. Heat pipes in both the reactor core and the space radiator would offer unique advantages for a 1- to 20-kw(e) system that bridges the gap between a simple but low-power [0.3 to 0.5 kw(e)] conduction-cooled nuclear-thermoelectric generator[3,4] and the more complicated but higher-power [0.5- to 350-kw(e)] liquid-metal-cooled space power thermoelectric or turboelectric systems such as SNAP-10A or SNAP-50. Heat pipes used to extract heat from the core and reject it to the hot shell, to thermoelectric converters, and to space would avoid the compromises of reliability and operating life which occur with systems that have multiple liquid-metal coolant loops and high-temperature rotating machinery. Moreover, meteor damage would be less drastic in a heat-pipe radiator constructed in modules than in a conventional liquid-metal radiator or even a vapor-chamber fin radiator.[5]

Converters. Recent improvements in thermoelectric and thermionic devices give these static converters special appeal for remotely sited electric generators. The demonstrated[3] feasibility of thermoelements having hot-junction temperatures as high as 1200°C permits higher radiator temperatures, lower system weights, and greater radiation stability (due to self-annealing) of thermoelectric materials than previously were considered for space power generators.[6]

Although the minimum practical emitter temperature for thermionic diodes has dropped[7] to around 1200°C, which is only a little higher than the maximum temperatures of existing designs for nuclear reactors and radioisotopic energy supplies, in the 1200°C range the state-of-the-art of thermoelectric converters is more advanced than it is for thermionic generators. But the availability of a reliable high-temperature source will spur the development of thermionic[7] devices with probable efficiencies of 15%.

Although thermoelectric devices[3] are only 4% efficient, their availability led us to choose them for the reference design described here.

Weight. In the 1- to 5-kw(e) range, the specific weight of radioisotopic thermoelectric power generators is typically about 1000 lb/kw(e). As shown in Table 1, existing designs for unshielded SNAP-type

Table 1 WEIGHTS AND POWERS FOR COMPACT POWER GENERATORS

Power			Total system weight, lb	Specific weight, lb/kw(e)
Thermal, kw(t)	Electric, kw(e)	Conversion efficiency, %		
Thermoelectric Version of Fast Reactor System				
25	1	4	525	525
125	5	4	1700	340
Thermionic Version of Fast Reactor System				
46	5	15	500	100
92	10	15	730	73

thermoelectric generators that employ thermal reactors weigh more than 800 lb/kw(e) in this power range. An unshielded SNAP-8 reactor–thermoelectric generator weighs 633 lb/kw(e) at 1 kw(e) and 293 lb/kw(e) at 20 kw(e).[1] But our reference fast reactor heat-pipe thermoelectric system would weigh only about 435 lb/kw(e) for a 1-kw(e) system or 290 lb/kw(e) for a 5-kw(e) system. Because the reactor and heat pipes might supply the converter elements with up to 150 kw(t) at 1200°C, more efficient thermionic diodes could replace the thermoelectric elements and produce up to 20 kw(e), at which power the total unshielded-system weight would be about 75 lb/kw(e). (The lithium hydride moderator in SNAP-8 has a vapor pressure[4] of 5 atm at 1100°C, so its use with a thermionic converter does not seem feasible.)

Potential Applications. The use of a ^{239}Pu-based fuel in an unusually simple design that employs in-core heat pipes and a heat-pipe radiator could produce a relatively lightweight and low-cost system that should be intrinsically reliable. Thus this fast reactor power supply could compare very favorably with radioisotopic generators and SNAP reactors in the 1- to 20-kw(e) range.

As interest in communication and other satellites, manned space laboratories, and space probes rises, a flexible reactor power system that could be adapted for varying purposes would be highly desirable. The concept described here is intended to be such a device. No attempt has been made to optimize the design for a specific power or mission. Undersea or terrestrial versions of the system would be tailored to other means of heat rejection than thermal radiation.

System Description

Heat generated by fission of the ^{239}Pu in each of 36 unclad plutonium monophosphide[8] fuel elements in the reactor core is conducted (by helium) and radiated across a 2-mil gap to a heat pipe that extends through the center of the fuel element (Figs. 1 to 3). This reactor-system heat pipe is a niobium tube whose wicks consist of channels in the wall and a niobium screen mesh in which lithium flows as the working fluid. Within the heat pipe, the hot vaporized lithium travels from the reactor core, through the reactor vessel, around two 90° bends, and down into a hot shell beneath the reactor. The hot shell is a cylinder formed by niobium webs welded between the 36 heat pipes. The 1200°C heat from the pipes is conducted from the hot shell to 2222 thermocouples (thermoelectric converters) mounted on the outer surface of the shell (Figs. 1 and 3). The 510°C outer surfaces of the thermoelectric converters are fastened to the radiator shell. The radiator, which consists of 100 rectangular-cross-section heat pipes containing potassium as the working fluid, rejects the heat at 500°C to space.

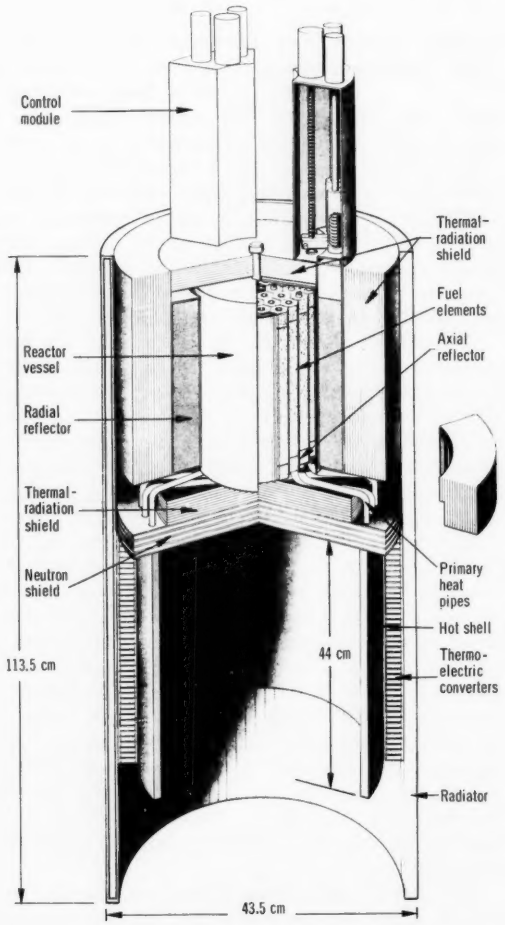

Fig. 1 Compact fast reactor 1-kw(e) power generator has heat pipes to convey heat from fuel elements to hot shell on which are mounted thermoelectric converters. Radiator has longitudinal heat pipes.

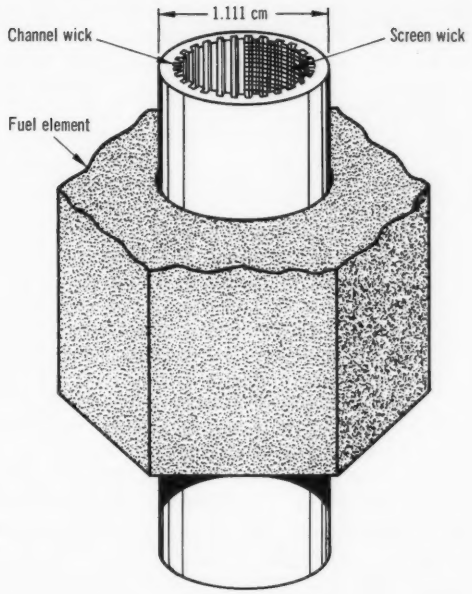

Fig. 2 Heat pipe from reactor system to hot shell is a niobium tube with wicks in the form of channels in the wall and a niobium screen mesh.

When cooled by the thermocouples, the lithium condenses to a liquid and returns to the reactor core by capillary action in the wick.

THE REACTOR

As shown in Fig. 1, the reactor consists of fuel elements, reflectors, reactor vessel, shields, and reflector-type control elements.

Fuel Elements. Each of the 36 unclad fuel elements measures 30 cm long, is 2.6 cm across the hexagonal flats, and has a central hole 1.12 cm in diameter. The fuel material is plutonium monophosphide (PuP), a novel compound[8] whose thermodynamic, chemical, and physical properties apparently are superior to those of plutonium dioxide (PuO_2) or plutonium monocarbide (PuC), as is shown in Table 2. At the operating temperature the fuel density is 8.41 g/cm^3. The 84.9 lb of fuel makes up 67.5 vol.% of the core.

Plutonium monophosphide, a dark-gray metallic-appearing ceramic, has been prepared in high-purity 40-g samples by reacting the metal hydride with the phosphide.[8] Because the monophosphide is the only stable high-temperature compound in the PuP system, the stoichiometric composition was obtained easily. With a fluid-bed technique, this same method can be used for producing the fuel elements.

In the 1-kw(e) thermoelectric version of the system, the maximum temperature in the fuel is 1269°C, which is well below the melting or dissociation temperature. The PuP compound is extremely stable—up to 1500°C in vacuum and 1700°C in 1 atm argon; the evaporation and dissociation rates are negligible.[9] At 2600°C the compound melts and decomposes rapidly.[8] The linear expansion coefficient (11.9×10^{-6}/°C) and the thermal conductivity [0.09 watt/(cm)(°C)] are nearly invariant with temperature.[9,10]

The PuP fuel elements do not have to be clad because of (1) the low fuel burnup (<0.05% at 10,000-

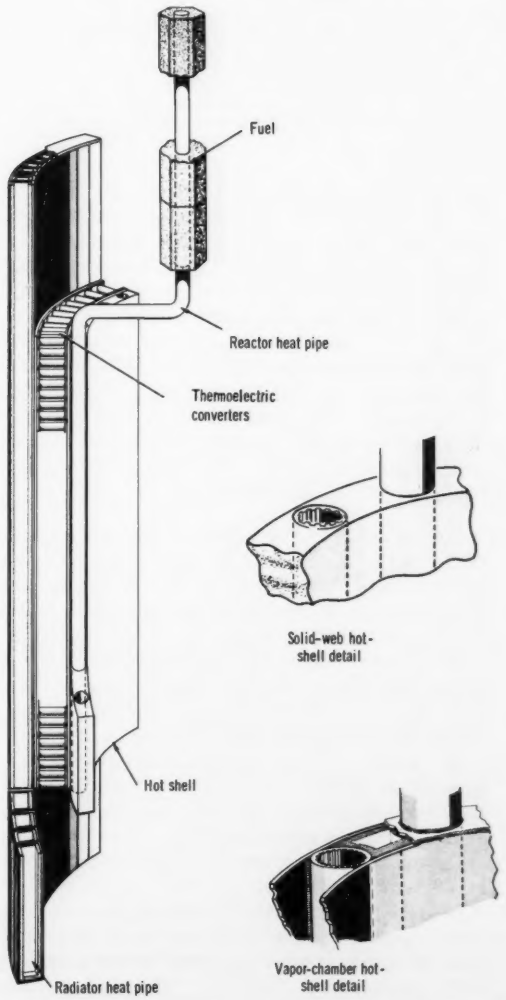

Fig. 3 Arrangement of heat pipes from reactor, hot shell, thermoelectric converters, and radiator heat pipes. Reference design has solid-type hot shell with single web between adjacent heat pipes (at upper right). Advanced-design hot shell has a double web that forms a vapor chamber between the heat pipes (lower right); with wicks and lithium in the chambers, the heat and temperature are distributed more evenly than with single web.

Table 2 PROPERTIES OF CANDIDATE FUEL MATERIALS

Fuel	Theoretical density, g/cm³	Melting point, °C	Thermal conductivity, watts/(cm)(°C)	Bare sphere: Critical radius, cm	Bare sphere: Critical mass, kg	Refs.
Metallic ^{235}U	18.8	1132	0.536 at 900°C	8.4	46	4
Metallic ^{233}U	18.8	1132	0.536 at 900°C	5.8	15	4
Metallic ^{239}Pu	19.7	680	0.209 at 600°C	5.0*	10	4
^{235}UC	12.3	2400	0.251	11.8	84	4
$^{235}UO_2$	10.0	2750	0.025 at 900°C	14.2	120	4, 16
$^{235}UO_2$–20 vol.% Mo	10.1		0.24 at 870°C	16.2†	168	14
^{239}PuC	13.6	1654	0.1 at 400°C	7.6‡	22	13
$^{239}PuO_2$	10.0	2400	0.025 at 900°C	9.3	34	4
^{239}PuC–20 vol.% ZrC	11.12	~2000		8.9	33	4
$^{239}PuO_2$–20 vol.% Mo	9.69	<2000		10.8	51	14
^{239}PuP	9.89	2600	0.09	10.3	45	8, 10

*Enrichment 96%.
†Theoretical density 94%.
‡Theoretical density 90%.

hr design life), (2) the excellent stability of PuP, and (3) the fact that the coolant flows within the sealed heat pipes rather than in contact with the fuel elements, which eliminates corrosion or erosion mechanisms in the fuel. In addition, because helium thermally couples the fuel element with the heat pipe, the material development problems usually involved with high-temperature bonding of cladding and fuel are avoided. These characteristics permit a relatively simple design and facilitate system fabrication, assembly, and testing. The high-temperature compatibility of PuP and the niobium heat-pipe material remains to be investigated.

Fuel Selection. The nuclear criteria for the compact reactor are similar to those proposed by MacFarlane[4] and others for low-power conduction-cooled systems; i.e., a fast assembly reflected, if at all, for purposes of power flattening or neutron shielding. MacFarlane showed that, although some moderated cores have lower critical masses than cores that have pure fuel, the low melting points of most lightweight diluents are an overriding disadvantage.

To study a single feasible reactor system, we selected an optimal reference fuel. Table 2 compares the characteristics of available candidate fuel materials. Plutonium monophosphide, a novel fuel that is exceptionally well suited to high-temperature fast reactors, was chosen.

Because the desired thermal-to-electric converters would operate at 1200°C, which means that the fuel must be stable up to at least 1400°C, the pure metals were unacceptable. Although ^{235}U systems probably would be cheaper than those with plutonium-based fuels, as Table 2 shows, they would be less compact. Thus all ^{235}U compounds were eliminated as candidates. Uranium-233 compounds were ruled out because ^{233}U is unlikely to be available in sufficient quantities.

Among the plutonium compounds, PuC is undesirable because of its relatively low melting point and poor compatibility with most structural materials above 1300°C (Ref. 11). Although PuO_2 has low thermal conductivity, the maximum fuel temperature (~1500°C) at the outer surface of a PuO_2 fuel element would be considerably below the melting point of the fuel; however, at 1500°C, dissociation effects[12] would compromise fuel-element performance significantly. Moreover, with PuO_2 fuel, the reactor design could not be uprated to 5 to 10 kw(e) because the fuel temperature would be excessive.

The combination PuP–ZrC was considered because studies of uranium carbide have shown that the melting point of UC increases almost linearly when ZrC is added to form a solid solution; although a similar effect might be predicted for PuC–ZrC, this mixture has not been prepared,[13] so it would not be an appropriate choice for this design. Similarly a PuO_2–20 vol.% Mo cermet might have better thermal conductivity and stability than plutonium dioxide,[14] but no data are available for this material.

Axial Reflector Pieces. To the upper and lower ends of each fuel element are fastened 5-cm-high beryllium oxide reflector pieces (Fig. 1), whose cross-sectional dimensions are the same as those for the fuel elements.

REACTOR VESSEL

The core containment cylinder is the main structural member of the system. Made of Nb–1% Zr, the 32.8-cm-high vessel has a 30.3-cm outer diameter, 0.25-cm-thick sidewalls, and 0.5-cm-thick upper and lower caps.

A hexagonal niobium insert within the vessel fits around the core and supports and aligns the lower ends of the core heat pipes and the fuel elements. Also mounted on this insert is a Nb–1% Zr radial shield the same height as the fuel elements which reduces the radiative heat transfer from the core to the reflector and vessel wall. Six ribs protrude

radially from the vessel to support the radial reflector and the six segments of the hot shell; the axial thermal shields and the radiator shell also attach to these ribs.

RADIAL REFLECTOR

A 5-cm-thick, 30-cm-high, 29.9-cm-OD radial reflector of beryllium oxide surrounds the reactor vessel. By reflecting neutrons back into the core, this 65.5-lb cylinder reduces the fuel loading (from ~60 kg for a bare core to 38 kg) and total mass. This combination of reflector and core (whose active length is 30 cm and critical diameter is 16.6 cm) is near the optimum from a weight standpoint. The reflector also flattens the core radial power profile, which tends to equalize the thermal load on the core heat pipes, which in turn ensures a more uniform temperature along the circumference of the hot shell.

The reflector also serves as a radiation shield for the thermoelectric converters.

Nuclear Calculations. The reactor criticality calculations were performed with the SNARG one-dimensional multigroup Sn code using the S4 option. Higher-order approximations only negligibly improved the estimated critical masses or multiplication constants. Multigroup diffusion theory does not apply because the core radius is less than five mean free paths. Hansen and Roach[15] 16-group cross sections were obtained from ANL Set 201 augmented to include ^{31}P.

Although power peaking could occur near the outer edge of the core, this problem is avoided if the reflector is less than 8 cm thick (Fig. 4). Within the constraints imposed by requirements for neutron shielding and the necessity for power flattening without flux peaking, the reflector thickness was chosen to minimize reactor weight. The variations of reactor height, mass, and ^{239}Pu inventory with reflector thickness are shown in Fig. 5 for the actual core configuration. Because this core plan required a BeO reflector at least 1.5 cm thick to achieve criticality, the weight curve rises sharply for thicknesses below 4 cm. The minimum core and reflector weight corresponds to a BeO-reflector thickness of 5 cm, the choice for this preliminary design.

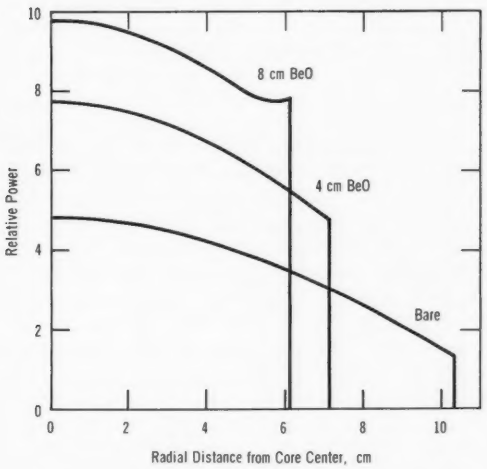

Fig. 4 Power peaking at the core edge is negligible if reflector thickness is less than 8 cm.

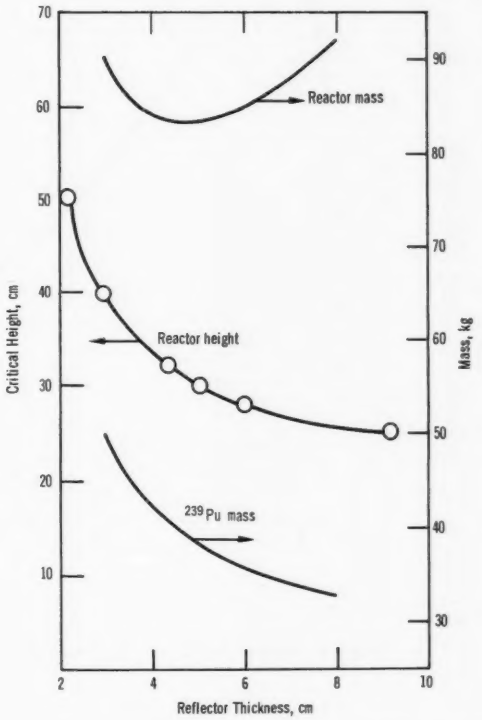

Fig. 5 How reflector thickness affects reactor height, mass, and ^{239}Pu inventory.

The neutron dose rate at the surface of the hot shell would not necessarily be reduced by thickening the reflector because the power density in the core increases in proportion to the core volume reduction associated with the reflector saving (Fig. 6).

Reflector Materials. Table 3 lists some of the reflector materials considered for the compact fast reactor. Beryllium oxide best satisfies the major requirements of a high melting point, a low dissociation rate, a low density, and good neutron-scattering properties. Graphite is a close second choice.

Graphite, with thermal conductivity[16] as high as 0.6 watt/(cm)(°C), might be preferred over BeO

[0.2 watt/(cm)(°C)] for a purely conduction-cooled reactor design,[3] but this advantage is unimportant for a system in which heat pipes provide the primary heat-transfer path.

Beryllium carbide was eliminated because its dissociation rate[16] is equivalent to 1×10^{-3} g/(sec)(cm^2) at 1200°C, whereas that of BeO is only 3×10^{-13} g/(sec)(cm^2). The latter figure implies a loss of only 0.6 g during the 10,000-hr mission life of the reactor.

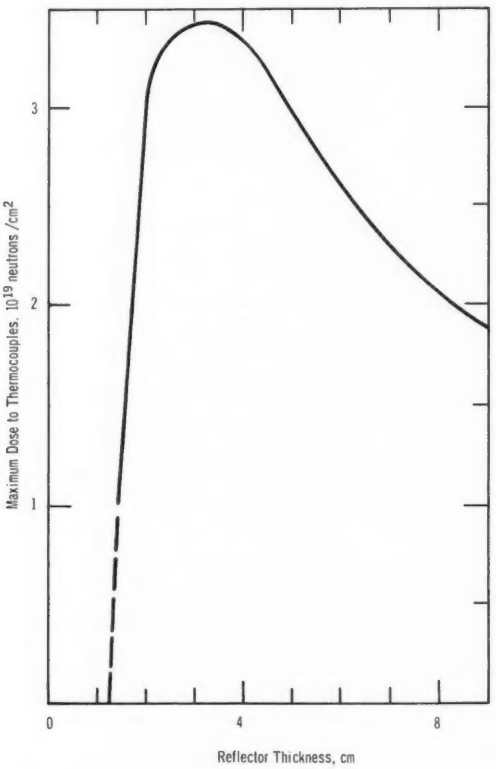

Fig. 6 Neutron dose to thermocouples during 2.5×10^5 kw-hr operation [10,000 hr at 25 kw(t)] as a function of reflector thickness.

AXIAL THERMAL-RADIATION SHIELDS

As shown in Figs. 1 and 3, each heat pipe undergoes two 90° bends between the core (evaporator section) and the hot shell (condenser section). In this transition region a 4-cm-thick axial thermal-radiation shield of Nb–1% Zr laminations is installed to reduce the axial radiative heat loss to ~2% of the core thermal power. A similar 37.5-cm-diameter shield suppresses radiation heat losses at the opposite end of the core. The temperature at the outer radiating surface of these shields is 364°C.

STRUCTURE AND RADIAL THERMAL SHIELDING

The main structural member of the system is the core containment vessel. Six equidistant radial ribs that protrude from the vessel provide mounting and structural support for the reflector segments and for the six segments of the hot shell. These ribs also provide attachment points for the axial thermal shields and the radiator shell. Within the containment vessel is a hexagonal niobium insert that fits around the core and provides support and alignment for the lower ends of the heat pipes. Also mounted on this insert is laminar radial shielding that is similar in structure to the axial shield. The radial shielding minimizes the thermal radiative heat transfer from the core to the reflector. As shown in Fig. 1, this type of thermal shielding is also employed to minimize heat loss from the exterior surface of the radial reflector.

NEUTRON SHIELD

A shadow shield, if needed for the mission, would be mounted atop the reactor. Weight and effectiveness would be similar to SNAP systems.

REACTOR CONTROL

The reactor is designated to operate unattended. Both the temperature and power coefficients of re-

Table 3 PROPERTIES OF CANDIDATE REFLECTOR MATERIALS

Material	Theoretical density, g/cm^3	Melting point, °C	Reflector savings for PuC sphere with 4-cm reflector, cm	Mass of 4-cm reflector, kg	Refs.
C	1.6	Sublimes*	1.03	6.0	16, 21
Be	1.85	1284	1.83	5.7	4, 21
Be_2C	2.4	Dissociates†	2.01	7.1	16
BeO	3.025‡	2550	2.02	8.9	16
LiH		688			4
ZrH_2		1093			4
Ni	8.9	1455	1.29	31.4	21
Fe	7.86	1539	1.06	29.2	21

*$P_{atm} = 10^{-14}$ at 1300°C.
†$P_{atm} = 4 \times 10^{-4}$ at 1300°C.
‡But 2.6 g/cm^3 at the 1200°C operating temperature of the radial reflector.

activity are estimated to be negative, which ensures stability at all times and enables passive control of the system during normal steady-state operation. Motion of the control elements for startup and shutdown can be preprogrammed to proceed automatically.

Reactivity Coefficients. The axial temperature coefficient ($-6 \times 10^{-6}/°C$) was calculated by expanding a 15-cm half-slab of homogenized core material by a factor ($1 + \alpha_{Pup} \Delta T$) and diluting the fuel number densities by their reciprocal.

Two thermal-expansion effects of a temperature increase in the core influence the radial temperature coefficient: (1) the fuel pieces expand into the interelement voids and (2) the elements move outward because they are held by the heat pipes, which in turn are positioned by the lower end cap of the niobium reactor vessel. The first mechanism cannot be incorporated into the nuclear model because this effect does not change the homogenized fuel number densities of the core material. On the other hand, the expansion of the core container, which displaces the elements radially, can be modeled by increasing the radii of the fuel annulus. This effect results in a radial temperature coefficient of $-3.5 \times 10^{-5}/°C$.

Startup. To initiate large reactivity changes for reactor startup or shutdown, three segments of the radial reflector are lowered or raised by small stepping motors (Figs. 1 and 7). The movable reflector segments provide the best startup-control scheme in terms of reactivity worth, weight, and simplicity. Movable neutron-absorber rods or vanes were rejected because they would not provide enough reactivity control in a design that minimizes system weight.

The number and size of reflector segments that would be movable for control purposes were decided on the bases of necessary reactivity variation and structural considerations. As Fig. 8 shows, the total worth of the 5-cm-thick radial reflector is 22.1% Δk. Although the curve of differential reflector worth shows that a slab of BeO immediately adjacent to the core is worth more than one at the outer edge of the reflector, practicality required that the control segments include the full 5-cm reflector thickness. The hexagonal array of the fuel elements and heat pipes and the location of internal structural supports favored a 60° span for each control segment.

The reactivity decrement from criticality at zero power to full power can be estimated by multiplying the temperature coefficient ($-4.1 \times 10^{-5}/°C$) by the rise from the 30°C ambient to the 1220°C nominal operating temperature. With a shutdown margin of 6% Δk assumed to be adequate, the required reactivity control is 11.1% Δk, which corresponds to three full-length (30 cm) 60° reflector segments.

Reactor startup is accomplished by slowly inserting two of the three 60° reflector segments, each of which is connected to a small stepping motor by a screw drive (Fig. 7). When fully inserted, these two pieces bring the reactor critical at an equilibrium temperature of ~300°C. At this temperature, lithium is still frozen in the heat pipes, and heat transfer from the core is by pure conduction, so the reactor power is very low. Then the third 60° segment is inserted, under the feedback control of a temperature

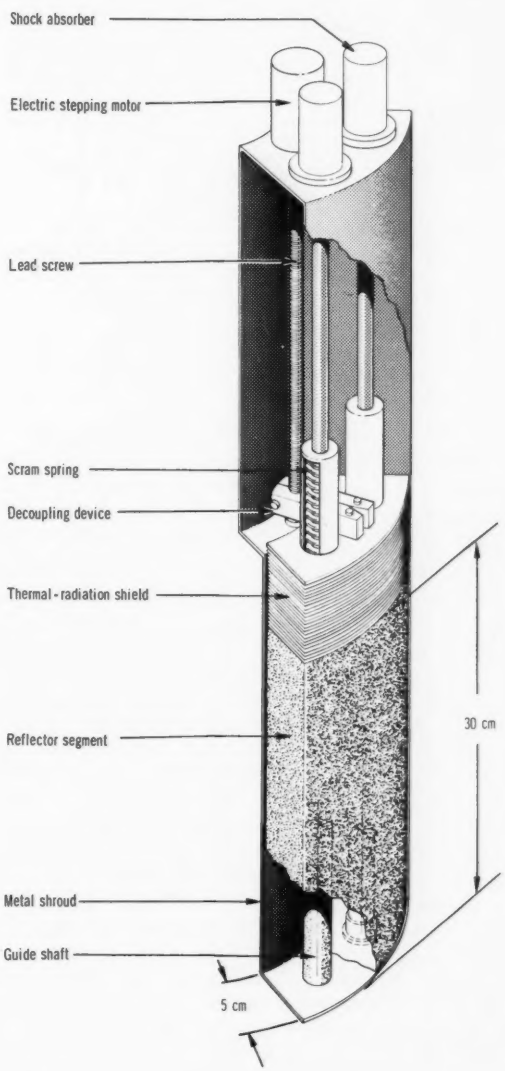

Fig. 7 For reactor control during startup and shutdown, each of three 60° segments of the BeO radial reflector is lowered or raised by stepping motor (2°/step) connected to the reflector piece by a screw drive (10/in. pitch).

sensor, to bring the reactor up to its 1220°C operating temperature.

The entire startup occurs slowly enough for uniform heatup of the system, which passes through a series of quasi-equilibrium criticality-temperature states during the startup sequence. The desired heatup rate is attained by presetting the frequency of the pulses that activate the stepping motors.

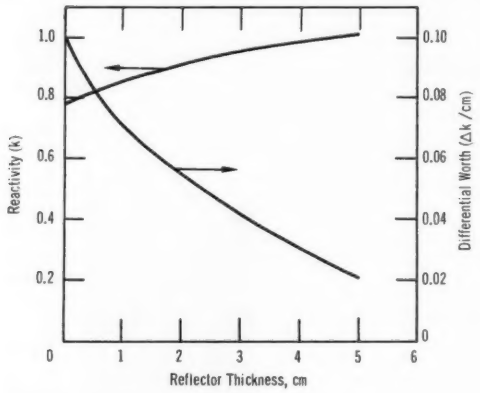

Fig. 8 Reactivity effectiveness as a function of thickness of beryllium radial reflector.

When the system stabilizes at its operating temperature and power, the startup controller is permanently deactivated. Then steady-state operation is maintained by means of passive temperature-coefficient control.

Steady Operation. During steady operation at power, the negative temperature coefficients of reactivity compensate for the small, gradual reactivity loss due to fuel burnup. Any reactivity reduction decreases the power and fuel temperature, promptly causing the fuel to compress axially, and, after a delay for the lessened heat transmission to cool the niobium reactor vessel, thermal contraction causes the fuel elements to be displaced radially closer together. If the fuel temperature increases for some reason, the thermal expansion has the opposite reactivity effect and thus reduces the power.

During the 10,000-hr mission life, 2.5×10^5 kw-hr of thermal power would be produced, and 13.2 g of ^{239}Pu (2.19 cm^3 of the homogenized core material) would be burned up. This burnup, less than 0.05%, would not affect fuel properties. The reactivity decrement corresponding to this fuel loss is 2.67×10^{-4} Δk, which can be compensated by a 6.5°C drop in the core temperature. If the maximum allowable temperature decrease during a 10,000-hr mission life were 50°C, the maximum reactor power at the end of the mission would be 192 kw(t), fuel temperature permitting.

HOT SHELL

The hot shell, a 44-cm-long cylinder that has a 33.5-cm outside diameter, is formed by solid niobium webs between the condenser sections of the 36 lithium-bearing heat pipes (see Figs. 1 and 3). Like the heat pipes, the webs are Nb–1% Zr alloy. The shell is 1.3 cm thick and operates at 1200°C.

The solid-web hot-shell configuration (Fig. 3) is the simplest to design, although not necessarily the optimal one. By using a double web to form a vapor chamber between adjacent pipes, and by putting lithium and wicks within the vapor chamber, we could distribute the heat and temperature more evenly. The more complex double-web shell also would be lighter, but the solid-web hot shell was selected for the reference design because of its simplicity and because the solid webs provide moderately greater shielding for the thermoelements.

REACTOR HEAT PIPES

Lithium in 36 heat pipes transfers the heat from the reactor core to the hot shell. As shown in Figs. 1 and 3, the 30-in.-long evaporator section of each heat pipe is in the center of a fuel element in the reactor. After making two 90° bends below the core, each heat pipe extends down into the hot shell. The transition section is 23 cm long; the heat-pipe condenser section within the hot shell is 44 cm long. All 36 heat pipes have 1.111-cm outside diameters and 0.076-cm walls and are made of Nb–1% Zr alloy. Each pipe is sized to accommodate the 0.88-kw(t) peak power generated in each of the six fuel elements in the inner ring of the reactor core, although the average power per fuel element in the core is 0.764 kw(t).

At full power the lithium in the reactor heat pipes operates at 1200°C and 5.3 psia. Along the length of the pipe, the vapor pressure and temperature drop 0.0235 psi and 0.655°C in passing from the evaporator to the condenser.

By capillary action, wicks within the heat pipes return the liquid lithium from the condenser section in the hot shell to the evaporator section within the reactor core; the liquid pressure drops 0.1544 psi in the return. There are two types of wicks in each heat pipe: channels and screen mesh. The channels, of which there are 51 equally spaced around the inside surface of the 0.762-mm-thick pipe wall (Fig. 2), extend the length of the pipe and are 0.51 mm deep and 0.204 mm wide. To prevent the high-velocity lithium vapor from interacting with the surface of the liquid lithium in the open channels during startup from low temperatures, which would tend to retard liquid flow and prevent startup,[17] there is a single layer of Nb–1% Zr screen (Fig. 2) against the inner surface of the pipe. This 0.22-mm-thick screen has an equivalent pore radius of 0.08

mm, a permeability of 12, and a porosity (void fraction) of 0.5.

Working Fluid. The reactor-system heat pipes operate at 1200°C to heat the thermoelement hot junctions to that temperature. Lithium was selected as the optimum heat-pipe fluid for 1200°C operation because: (1) its sufficiently high vapor pressure above 900°C, its high surface tension, and its low liquid density make it an excellent fluid for use in an efficient capillary pump; (2) its vapor pressure at 1200°C is low (~5 psi), so the pipe wall can be thin enough to give both low weight and low temperature drop across the pipe walls; (3) the high latent heat of vaporization of lithium permits a small pipe diameter, which, among other benefits, reduces potential startup instability problems; and (4) the great heat-transfer capacity of a lithium pipe lends itself to a system design that can be uprated to higher powers with minimal modification of the heat pipes.

Pipe Material. From the limited number of refractory metals compatible with lithium at 1200°C (niobium, tantalum, and molybdenum and their alloys), Nb–1% Zr was chosen for the heat pipe and wick. This selection was based primarily on heat-pipe tests at the Los Alamos Scientific Laboratory.[18] Those tests verified the compatibility of the Li–Nb combination at temperatures in excess of 1100°C for operating times up to 3500 hr, including a number of restart cycles. Lithium and niobium are compatible at temperatures as high as 1150°C for up to 6500 hr (Ref. 19). The LASL tests included runs at temperatures as high as 1300°C; however, 10,000-hr compatibility remains to be verified experimentally.

Sizing the Heat Pipes. The excellent thermal properties of lithium make it easy for small-diameter heat pipes and wicks to carry the design power; they also keep the heat flux across the pipe surface low enough to preclude boiling within the wick.

It is also important that the pipe diameter be large enough to: (1) keep the PuP fuel temperature below 1700°C, (2) ensure a near-uniform temperature distribution on the hot-shell surface that contacts the thermocouples, and (3) permit the system to be uprated from its initial design power of 27.5 kw(t) to at least 125 kw(t) without significantly modifying the reactor design.

The fuel-temperature limitation is not a problem with the 36-fuel-element configuration because the 6 elements in the central ring do not get hotter than 1269°C when the reactor operates at 25 kw(t). Figure 9 shows how the peak fuel temperature at the core midplane would vary with reactor power for fuel elements of five sizes. Note that, for the 2.6-cm across-flats hexagonal fuel elements, the 1700°C limiting temperature for the PuP fuel would be reached at a thermoelectric power of 7.2 kw(e) [180 kw(t)]. Figures 10 and 11 show the axial and radial distributions of temperature in the core.

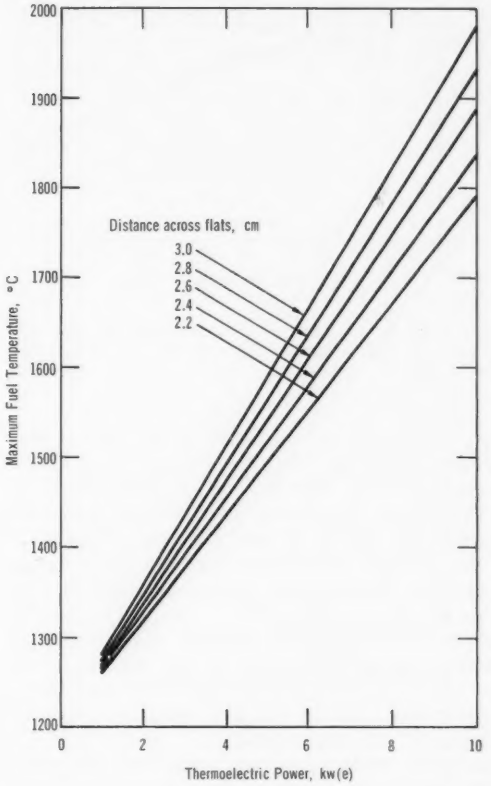

Fig. 9 Maximum fuel temperature reached in fuel elements of five sizes as a function of system electricity generation (for 4% efficient thermoelectric conversion).

The governing criterion for the size of the heat pipes proved to be that associated with temperature uniformity on the surface of the hot shell on which the converters are mounted. A 20°C maximum allow-

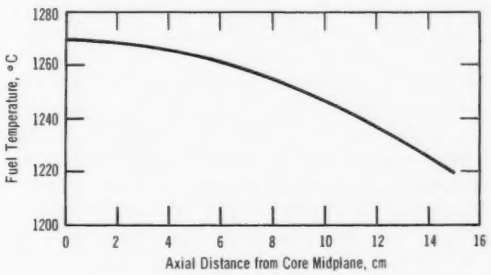

Fig. 10 Axial distribution of temperature in outer edge of fuel element in center ring of core when the reactor is operating at 27.5 kw(t).

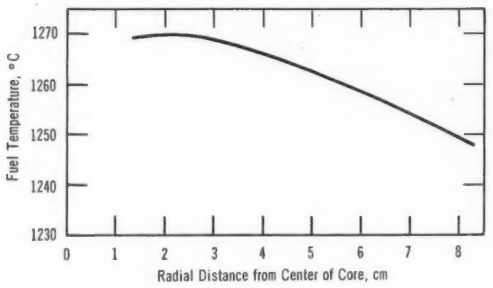

Fig. 11 Radial distribution of temperature in fuel elements along core midplane when the reactor is operating at 27.5 kw(t).

able circumferential variation of the 1200°C temperature was established (arbitrarily) for the solid-single-web shell. With the shell diameter the same as that of the 29.9-cm-OD reactor radial reflector, and with the number of heat pipes established as 36 by the number of fuel elements, the pipe diameter determined the thickness and circumferential width of the web joining adjacent heat pipes. On the premise that the inner surface behaves adiabatically, the smallest heat-pipe diameter (outer) that would limit the circumferential variation to 20°C was determined to be 1.111 cm ($^{7}/_{16}$ in.). With this dimension established, the heat pipe easily met the other requirements, which were considerably less stringent.

The theory of heat pipes in Ref. 20 considers heat-pipe equations in which the liquid and vapor in the heat pipe flow either adiabatically or under conditions of uniform heat input and extraction. In the compact-reactor core, however, with a "chopped cosine" axial power distribution, this assumption is not valid for the evaporator section of the lithium pipe, although it does apply to the condenser section. For design of the in-core heat pipe, the liquid and vapor pressure-drop equations were integrated over the evaporator length on the basis of a chopped-cosine power profile using the integrated average radial Reynolds number, which approximates the actual case more closely than does the assumption of a uniform power input. The condenser section was sized on the assumption of uniform power extraction.

The channel-type wicks in each heat pipe are sized to carry the full 0.88-kw heat load of a central fuel element. However, an additional ~148 watts of heat-transfer capacity is provided by the single-layer screen-type wick within the pipe. But the screen is counted on only to serve as a barrier between the liquid and the vapor to prevent instabilities during the low-temperature portion of startup, even though a screen wick is superior to a channel wick as a capillary pump. Because the radius of curvature of the liquid meniscus is effectively infinite in the axial direction for a channel wick, the capillary forces are approximately half those in a screen-mesh wick. However, unlike the screen, under no circumstances can the channels milled in the pipe wall detach from the wall and cause hot spots. The channel wick also can be designed more readily than a screen wick because the channel flow characteristics (flow area, hydraulic diameter, etc.) can be defined more accurately.

The 0.102-mm effective capillary pore radius of the channel is sufficient to wick the liquid lithium to a height of 45 cm against earth gravity. This wicking height corresponds to the length of the condenser leg of the heat pipe so the core-heat-pipe subassembly can function in earth gravity for ground-testing the space system. It also means that the system can be adapted readily for terrestrial or undersea use.

THERMOELECTRIC CONVERTERS

The $^{3}/_{8}$-in.-diameter thermoelectric converters, of which there are 2222, are mounted on the outer surface of the 1200°C hot shell (Figs. 1 and 3). These 1200°C thermocouples are of the type developed by Monsanto Research Corp.[3] With its 510°C cold junction at the radiator surface, each of these 4% efficient converters produces 0.495 watt of 40-volt electricity when the reactor power is 25 kw(t).

RADIATOR

The radiator that rejects heat at 500°C to space consists of 100 rectangular cross-section heat pipes that form a 113.5-cm-long cylindrical shell around the thermoelectric converters and reactor (Figs. 1 and 3). Although the full 113.5-cm length of the outer wall serves as the condenser section, only the 44-cm-long portion of the inside wall in contact with the thermocouples functions as the evaporator section.

The gross dimensions of the radiator were dictated by (1) the 39.5-cm outside diameter of the converter array, (2) the 510°C cold-junction temperature of the reference thermocouples, and (3) the desire to reject 26.4 kw(t) at 500°C with an effective emissivity of 0.85 from a 4% efficient thermoelectric system.

Radiator Heat Pipes. Each heat pipe has a 1.35- by 2.0-cm cross section, is made of Inconel tubing having a 0.051-cm (20-mil) wall, contains potassium as the working fluid, and has screen-mesh-type wicks of Inconel (Fig. 12). Inconel was selected mainly because of its long-term compatibility with potassium, but also because of its reasonably good resistance to penetration by meteors (Fig. 13). The screen-mesh wicks are 0.314 cm thick along the inner and outer walls of the radiator rectangular pipes; the wicks on the lateral walls are 0.157 cm thick. Wick porosity is 0.5, pore radius is 0.025 cm, and permeability is 12. With each of the 100 radiator heat pipes trans-

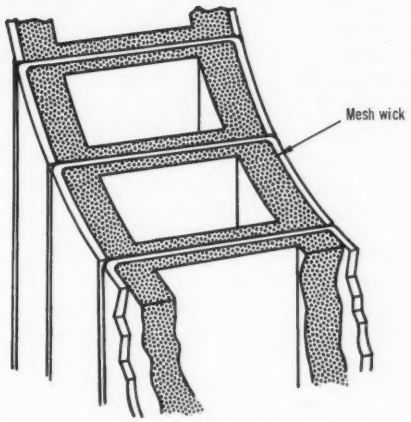

Fig. 12 Cutaway of radiator heat pipes, showing screen-mesh-type wicks.

mitting 0.264 kw(t), the operating pressure is 0.5 psia, the vapor pressure and temperature drop are 0.005 psia and 2.93°C, the liquid pressure drop is 0.005 psia, and the total temperature drop across the radiator wall is 11.9°C.

Fluid Flow. The configuration and operation of the radiator heat pipes are unusual in several respects. The heat pipes are double-ended, so heat is added in the central portion of the pipe, and the vapor flows axially in two directions as well as transversely (Figs. 1 and 3). The transverse flows of vapor and liquid within the rectangular pipe are considerably more complex and less symmetric than they would be in a circular pipe. The vapor produced in the evaporator section on the inner radius of the radiator shell condenses on the entire outer radius and flows back to the evaporator section through the upper, lower, and lateral wicks. No satisfactory analytical description has been developed for this complicated flow pattern. For this study the basic heat-pipe theory of Ref. 20 was adapted to determine the sizes of the wick and vapor passages.

Unlike the primary heat pipes in the reactor and hot shell, in which the excellent wicking properties of lithium permit the system to be tested in an "upright" position, as shown in Fig. 1, ground tests of the radiator heat pipes (and thus of the overall integrated system) have to be conducted with the system in a horizontal attitude. For the radiator heat pipes to be tested vertically, the radiator-wick pore structure would have to lift the potassium 56.75 cm (half the radiator height) to ensure that the lower half of the evaporator would be wetted. To do this, the wick pore radius would have to be 0.04 mm, which is extremely small. Even if this pore radius could be attained in practice, a thick wick in a large pipe with a large ratio of width to length would be required to keep the liquid pressure drop well below the potassium vapor pressure (~0.5 psi at 500°C). However, with a pore radius of 0.025 cm, the wicking height is ~8 cm, which results in a design for the radiator heat pipe that has 1.34- by 2-cm cross section; so ample margin exists for capillary pumping in a horizontal attitude ground test of the integrated system.

Radiator Fluid. The selection of an optimal fluid for the radiator heat pipes was less obvious than it was for the heat pipes in the reactor and hot shell. Lithium is not suitable for the 500°C radiator because its vapor pressure is too low below 800 to 900°C for an effective heat pipe. So the choice rested among: (1) the lower-temperature liquid metals, such as Na, K, Cs, and Rb (Hg was ruled out because of its questionable wetting properties); (2) the higher-temperature organic materials, such as the diphenyls (e.g., Dowtherm); and (3) the molten salts.

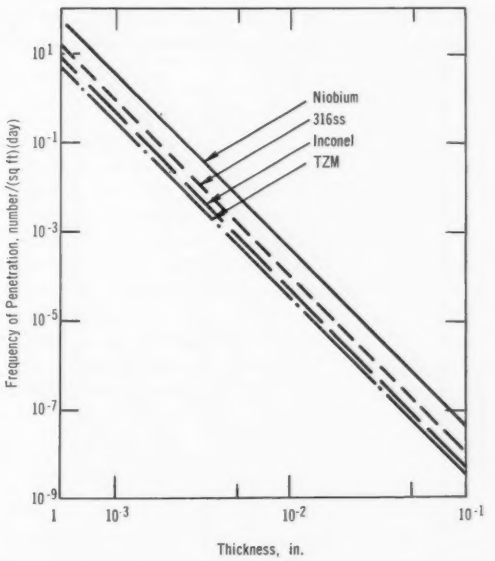

Fig. 13 Probable incidence of meteor damage to heat pipes of four materials as a function of wall thickness. Correlation of Ref. 22 was used to adapt data of Ref. 23 to materials of interest for this study.

To aid in the selection of the best heat-pipe fluid, figures of merit were estimated on the basis of the relations in Ref. 20 for the limiting heat-transfer capacity of an optimized heat pipe operating with uniform power input and extraction in a 0-g environment. This figure of merit for an operating mode with a high radial Reynolds number is

$$F_H = L(\rho_v \rho_l \gamma^2/\mu_l)^{1/4}$$

and for a low radial Reynolds number is

$$F_L = L\gamma(\rho_v\rho_l)/(\mu_v\mu_l)^{1/2}$$

where L = latent heat of vaporization
ρ = density
μ = viscosity
γ = surface tension
v, l = vapor and liquid

As shown in Fig. 14, Na, K, Rb, and Cs are approximately competitive in the ~500°F range of interest. Potassium was selected because of its better performance during startup from low temperatures, although above 500°F sodium clearly is superior to the other liquid metals. Cesium was eliminated because its relatively low surface tension makes it less effective than potassium as a capillary pump.

Heat-pipe experiments at LASL have demonstrated the performance of sodium and potassium.[17]

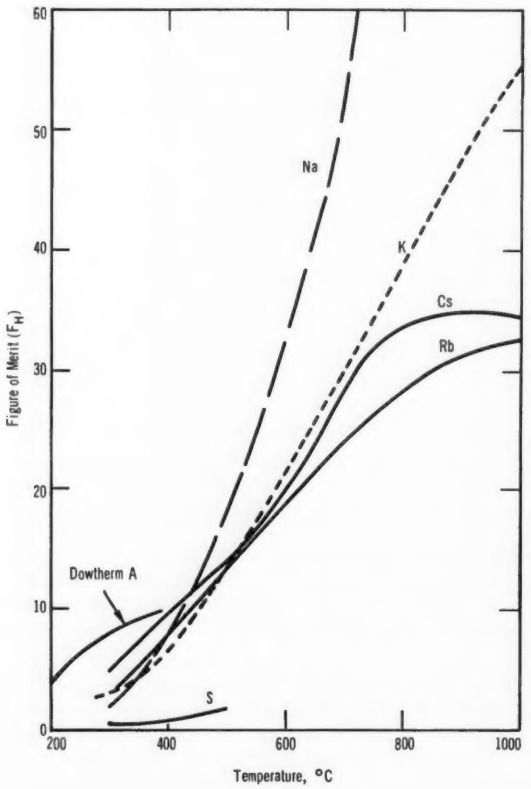

Fig. 14 Selection of potassium as the reactor heat-pipe fluid was made partly on the basis of a figure of merit (F_H) that assumes uniform power input and extraction in a 0-g environment.

Meteor Invulnerability. Relative invulnerability to damage by meteors is a major advantage of a heat-pipe radiator constructed of an aggregate of independent cells. This concept involves 100 independent cells, so the puncture of any one heat pipe would reduce the radiator capacity by less than 1%.

Although meteor-penetration data are not yet fully reliable, Fig. 13 indicates that our system would encounter a meteor sufficiently large to puncture the 20-mil-wall Inconel heat-pipe radiator approximately once in 2 years. Inasmuch as the radiator has been designed oversize by 10%, a reasonable attrition of heat pipes can be tolerated, so no meteor armor should be required. In contrast, although an advanced-concept vapor-chamber[5] finned Rankine-cycle radiator also would offer some invulnerability to meteor damage, it would require some meteor armor to protect the liquid-metal passages from a catastrophic puncture.

Assembly and Testing

The mechanical design of the reactor system enables straightforward assembly and handling. After the 36 reactor heat pipes are installed in the vessel (Figs. 1, 3, and 15) and welded to the flanges on the niobium heat-pipe bellows, the core is assembled in the vessel by sliding the fuel hexagons over the heat pipes. The central position, in what is basically a 37 fuel-element array, is left vacant to simplify the routing of the heat pipes to the hot shell.

After the core is assembled, the reactor vessel is purged and welded gastight under 1 atm helium. Then the three 60° movable reflector segments that constitute the startup control system are installed as three separate modules (Fig. 7), each of which includes a reflector segment, a stepping motor, a driving motor, and a covering shroud. To prevent unintentional startup of the reactor during shipment, prelaunch activities, and before the attainment of orbit, each reflector segment is held in the withdrawn position by a scram spring. During operation, the scram spring is restrained by a magnetic latch. With the three stationary reflector segments in place but the movable segments withdrawn, the shutdown reactivity margin is 6%. If the three stationary segments also are removed during shipment and handling, the bare core has a shutdown safety margin of 20%.

For component development and system tests, the nuclear and nonnuclear parts of the system are separable. Electric heating can be used to test the assembled system without the fuel elements.

Because the fuel is not bonded to the heat pipes in the reactor (heat transfer across the 2-mil gap between the fuel and pipe is by radiation and, mostly, conduction through the helium), no problem is posed by the differential thermal expansion between the PuP

fuel and niobium pipe during startup. With the niobium bellows welded on each heat pipe where it emerges from the reactor vessel, thermal stresses caused by differential expansion do not compromise the integrity of the pipes or vessel.

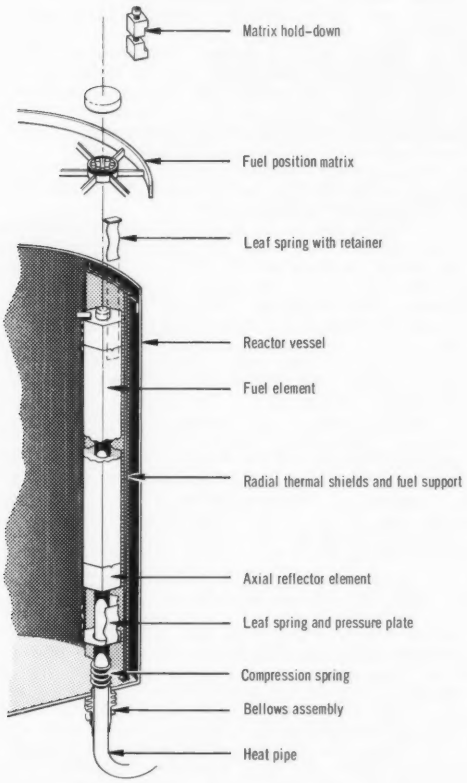

Fig. 15 Alignment and support system for fuel element.

Optimization and Uprating

As for any conceptual design, the design parameters and performance characteristics described for this 1-kw(e) compact fast reactor power generator are subject to considerable refinement. Nevertheless, the predicted weight (Table 1) of less than 450 lb for a 4% efficient 1-kw(e) thermoelectric generator indicates the performance potential of this concept. Doubtless, further design and development studies would modify the system performance and weights somewhat.

If the conceptual design were carried to the preliminary-design stage, it would be worthwhile to optimize the complete system. An obvious improvement would result from a combined core, reflector, and reactor heat-pipe optimization. Desirable optimization steps such as power flattening in the core and improved mechanical design would have to be balanced against material temperature limits and the ability to increase the design power. Furthermore, design changes such as the use of smaller heat pipes and a modified hot-shell structure would significantly reduce the specific weight, particularly for a high-power [5 kw(e)] version.

The power of the 1-kw(e) thermoelectric system can be uprated to 5 kw(e) without significantly altering the reactor design, although the hot shell and radiator would be enlarged. As shown in Table 1, the specific weight of the 5-kw(e) thermoelectric generator system would be reduced to ~290 lb/kw(e). The maximum fuel temperature associated with a 5-kw(e) output would be 1590°C [vs. 1269°C for 1-kw(e) operation], which is still within the range of stable performance for plutonium monophosphide under 1 atm helium.[9] Other system temperatures would be essentially unchanged; passive temperature-coefficient control would still be feasible. The reactor heat pipes in the 1-kw(e) system have been designed oversize to accommodate the 5-kw(e) power.

THERMIONIC VERSION

The same optimization steps would apply to a thermionic version of the system (the same hot shell would serve as the emitter heat source), where reactor-system performance improvements would be even more significant because the superior efficiency of the thermionic system (15% vs. 4% for the thermoelectric) would reduce system specific weight to about 100 lb/kw(e) for a 4.25-kw(e)-output generator. If the reactor were used with a 1-kw(e) 15% efficient thermionic generator, the radiator length could be reduced from 113.5 cm to ~30 cm.

IMPROVED HOT SHELL

The solid-web hot-shell configuration (Fig. 3) selected for the reference design is the simplest but not necessarily the optimal design for the hot shell. As shown at lower right in Fig. 3, the vapor-chamber-web concept would be employed to achieve a virtually uniform temperature along the hot-shell surface. Then the hot-shell configuration would be somewhat more complex, in that the web structure between the heat pipes would contain lithium and would be lined with wicking material similar to that in the pipes from the reactor. This aggregate of vapor-chamber webs would weigh ~12 kg less than the solid shell. Because approximately the same wicking height (44 cm) is involved, the wicks in the vapor-chamber webs would have the same pore size as the wicks in the reactor pipes, but the liquid and vapor pressure drops associated with the web would be considerably less because the distance over which heat is transferred is much smaller (~0.5 cm).

We gratefully acknowledge the assistance of Ralph Carter, who solved many of the mechanical design problems; Jay Norco, who aided in the nuclear and thermal calculations; and Owen Kruger, who advised on reactor fuels technology.

This article is an adaptation of a paper presented at the Intersociety Energy Conversion Engineering Conference, which was held in Miami, Fla., in August 1967. Details of a similar space power system concept are also provided in Argonne National Laboratory Report ANL-7422, A Heat-Pipe-Cooled Fast-Reactor Space Power Supply.

References

1. Milton Shaw, AEC Programs and Requirements for Plutonium, in Commercial Plutonium Fuels Conference, March 1–2, 1966, Washington, D. C., USAEC Report CONF-660308, pp. 6-13.
2. Glenn T. Seaborg, Plutonium — Past, Present, Future, in Commercial Plutonium Fuels Conference, March 1–2, 1966, Washington, D. C., USAEC Report Conf-660308, pp. 60-68.
3. Monsanto Research Corp., Dayton Laboratories, High Temperature Thermoelectric Research, Report AFAPL-TR-64-135 (AD-609051), Oct. 30, 1964.
4. D. R. MacFarlane, A 200-Watt Conduction-Cooled Reactor Power Supply for Space Application, USAEC Report ANL-6694, Argonne National Laboratory, March 1963.
5. H. C. Haller and S. Lieblein, Feasibility Studies of Space Radiators Using Vapor Chamber Fins, in *Proceedings of Joint Atomic Energy Commission/Sandia Laboratories Heat Pipe Conference*, June 1, 1966, Albuquerque, N. Mex., USAEC Report SC-M-66-623, Vol. 1, p. 51, Sandia Corporation, October 1966.
6. J. C. Danko, G. R. Kelp, and P. V. Mitchell, Irradiation Effects on Thermoelectric Materials, *Advanced Energy Conversion*, Vol. 2, pp. 79-85, Pergamon Press, London, 1962.
7. G. N. Hatsopoulos, Thermionic Energy Conversion, in Proceedings of the Intersociety Energy Conversion Engineering Conference, Los Angeles, Calif., pp. 238-244, September 1966.
8. O. L. Kruger and J. B. Moser, Preparation of the Sulphides and Phosphides of Plutonium, *J. Inorg. Nucl. Chem.*, 28: 825-832 (1966).
9. O. L. Kruger, Argonne National Laboratory, to J. J. Roberts, personal communication, January 1966.
10. Argonne National Laboratory, Metallurgy Division Annual Progress Report for 1965, USAEC Report ANL-7155.
11. International Symposium on Compounds of Interest in Nuclear Reactor Technology, University of Colorado, August 3–5, 1964, Boulder, Colo., USAEC Report CONF-506.
12. R. N. Mulford and L. E. Lamar, The Volatility of Plutonium Oxide, in Proceedings of the Second International Conference on Plutonium Metallurgy, April 19–22, 1960, Grenoble, France, pp. 411-421.
13. J. Leary, Los Alamos Scientific Laboratory, to J. J. Roberts, personal communication, January 1967.
14. S. Paprocki et al., Preparation and Properties of UO_2 Cermet Fuels, USAEC Report BMI-1487, Battelle Memorial Institute, December 1960.
15. G. E. Hansen and W. H. Roach, Six and Sixteen Group Cross Sections for Fast and Intermediate Critical Assemblies, USAEC Report LAMS-2543, Los Alamos Scientific Laboratory, November 1961.
16. *Reactor Handbook, 2nd ed.*, Vol. I, Materials, C. R. Tipton, Jr. (Ed.), Interscience Publishers, New York, 1960.
17. J. E. Kemme, Heat Pipe Capability Experiments, USAEC Report LA-3585, p. 33, Los Alamos Scientific Laboratory, October 1966.
18. J. Deverell and J. E. Kemme, High Temperature Thermal Conductance Devices Using the Boiling of Lithium or Silver, USAEC Report LA-3211, p. 26, Los Alamos Scientific Laboratory, October 1964.
19. A. Romano, A. Fleitman, and C. Klamut, Evaluation of Li, Na, K, Rb, and Cs Boiling and Condensing in Nb–1% Zr Capsules, *Nucl. Appl.*, 3(2): 110 (February 1967).
20. T. P. Cotter, Theory of Heat Pipes, USAEC Report LA-3246, Los Alamos Scientific Laboratory, Mar. 26, 1965.
21. Reactor Physics Constants, 2nd ed., USAEC Report ANL-5800, Argonne National Laboratory, July 1963.
22. J. L. Summers, Investigation of High Speed Impact: Regions of Impact and Impact at Oblique Angles, Report NASA-TN-D-94, National Aeronautics and Space Administration, 1959.
23. R. E. English, Potassium Rankine Systems Technology, in Space Power Systems Advanced Technology Conference, Report NASA-SP-131, p. 237, National Aeronautics and Space Administration, Lewis Research Center, August 1966.

Research and Development on Aqueous Processing

By C. E. Stevenson and D. M. Paige

Silicon in U–Al alloy has little effect on rate of dissolution, but its presence in suspended solids may result in surface activity in solutions of such alloys. Tests are being made to determine conditions for the electrolytic dissolution of sodium-bonded EBR-II fuel elements. Semicontinuous dissolution of Zircaloy fuels in HF at the Idaho Chemical Processing Plant (ICPP) was not accompanied by excessive corrosion. Methods are discussed for the recovery of americium, curium, and neptunium from Shippingport reactor fuel. The radiation deterioration of extraction solvents is reviewed, and results of initial operation of the Eurochemic plant are presented.

The performance of a centrifugal solvent extraction contactor, which has been operated with radioactive fuel solutions for 1 year, is discussed. A monitor for detecting traces of fissionable material left in the hulls from shear–leach processing of tubular-clad ceramic fuels is described.

Process Methods

EFFECT OF SILICON UPON THE REPROCESSING OF U–Al ALLOY FUELS

In a continuation of earlier studies[1] at the ICPP upon the effect of minor metallic constituents on the rate of dissolution of U–Al alloys in HNO_3, Paige and Rohde[2] recently examined the metallurgical structure of both aluminum and 22 to 32% U–Al alloys that contain up to 11% silicon, the dissolution rates of such alloys in boiling 6.6*M* HNO_3 containing 0.007*M* $Hg(NO_3)_2$, and the surface activity of the suspended siliceous solids resulting from dissolution of the alloy. Silicon is added in the fabrication of U–Al cores for plate-type fuel elements, such as those for the Engineering Test Reactor (ETR), to stabilize the UAl_3 phase and to prevent the formation of UAl_4, which is present as hard, brittle intermetallic particles.

Dissolution rates of the alloys were found to be related to the metallurgical composition, i.e., the phases present. The observed rates decreased in the following order: Al > UAl_3 > $U(Al,Si)_3$ > UAl_4 > Si. All alloys tested, however, dissolved at rates that were practical for processing. Some tendency for the preferential dissolution of aluminum was noted, so that the possibility of enrichment of undissolved residues in uranium must be considered. Silicon present in the alloy as the intermetallic $U(Al,Si)_3$ dissolves, but silicon present in excess of one atom per atom of uranium apparently is not contained in the intermetallic and does not dissolve. This undissolved residue may require removal during reprocessing. Because the presence of even a small amount of silicon results in sufficient surface activity to require treatment (e.g., with gelatin) to obtain good extraction behavior, the concentration of silicon in the alloy is not important from this standpoint. Surface activity appears to be due to the presence either of polysilicic acid or of colloidal silica in the form of particles less than 35 μ in diameter.

AQUEOUS PROCESSING OF EBR-II FUEL

The fuel used in Experimental Breeder Reactor II (EBR-II) at the National Reactor Testing Station in Idaho is highly enriched uranium alloy which is clad in stainless steel and which is bonded to the stainless steel with sodium. For the past several years, all fuel from this reactor has been reprocessed remotely by a pyrochemical process and refabricated into new fuel elements at the Fuel Cycle Facility immediately adjacent to the reactor.[3] Small quantities of scrap from this process have been recovered at the ICPP.[4] To reduce the dependence of the reactor upon the continued operation of the Fuel Cycle Facility as its fuel source, and to make additional hot-cell space available for the handling of materials irradiated experimentally in EBR-II, it is now planned to provide for aqueous processing at the ICPP of all fuel discharged by EBR-II. The proposed process method includes electrolytic dissolution in HNO_3, followed by TBP and

hexone extraction. Although extensive studies of the electrolytic dissolution of fuels of various types have been made at the ICPP,[5] new equipment will be required for this purpose, and pilot-scale studies are now under way.[6]

An EBR-II fuel element consists of a uranium-alloy rod, 0.144 in. in diameter by 13.5 in. long, contained in a cladding tube of 304L stainless steel with a 9-mil-thick wall; a 6-mil annulus containing a sodium bond for heat-transfer purposes separates the rod from the cladding. The uranium alloy is described as "fissium" and consists of 95 wt.% uranium at an enrichment of 52.2% with the balance being 2.5 wt.% Mo, 1.9 wt.% Ru, 0.3 wt.% Rh, 0.2 wt.% Pd, 0.1 wt.% Zr, and 0.01 wt.% Nb. The latter elements represent metallic fission products not removed by the pyrochemical process. Individual fuel elements are assembled into bundles of 91 with a hexagonal sheath and other structural components of stainless steel. Because of the sodium bond in the fuel element, the safety aspects of the reaction of the dilute HNO_3 dissolution reagent with sodium were investigated. In the dissolution of single fuel elements (less than 1 g of sodium in each), the rate of the sodium reaction was sufficiently low that no safety problem was apparent. Consideration has also been given to the possible corrosion of the cladding and reaction of sodium during extended underwater storage. However, five fully irradiated fuel pins (~ 1 at.% burnup) have been retained for 10 months in the ICPP storage basin with no indication of penetration of the cladding.

In pilot-plant studies, two 10-day continuous dissolving cycles have been carried out in which about 1200 lb of stainless-steel tubing was dissolved (no sodium or fuel was present) using an insulated niobium basket in a 6- by 18- by 24-in. titanium vessel (the cathode), and a platinum-coated niobium anode. An average dissolution rate of 1.3 kg/hr was achieved with a current efficiency of 0.5 g/amp-hr at varying acid concentrations. The principal problem encountered was the accumulation of a heavy sludge of particles of iron, chromium, and nickel bound together with silicic acid or silica gel. The addition of gelatin to the dissolution reagent did not reduce the sludge accumulation. Further studies will include evaluation of the safety aspects of the sodium reaction and investigation of methods for reducing or disposing of the sludge.

CORROSION IN PROCESSING ZIRCONIUM-TYPE FUELS WITH HF

The hydrofluoric acid dissolution process, used in the processing of Zircaloy-clad and -alloyed enriched uranium fuels at ICPP, requires the use of vessel materials of limited corrosion resistance to the combination of reagents that must be used at various steps in the process. For example, aqueous HF, to which relatively few alloys are resistant, is required for dissolution of zirconium. Other reagents include small amounts of HNO_3, which were used originally in the batch process to oxidize uranium and facilitate its dissolution, and $Al(NO_3)_3$ solution containing 0.02*M* chromic acid, the complexing agent that is added to the dissolver solution to enable solvent extraction of the uranium with TBP. Monel-400 is used for the dissolving vessel, and Carpenter-20, for the complexing tank. The solutions are handled thereafter in 347, 348, 316, 304L, or 304 stainless-steel equipment.

To increase fuel throughput, the process has recently been modified to permit semicontinuous dissolution in 6.5*M* HF to which H_3BO_3 is added to a concentration of 4 g of boron per liter for nuclear safety. The 0.03*M* HNO_3 initially contained in the dissolver solution was found to be unnecessary in later operations. Results of operating the semicontinuous process were reported previously.[7,8] Following that campaign, Zimmerman and Hoffman at ICPP conducted an evaluation of vessel corrosion which had occurred. The results of this evaluation have been reported recently.[9]

The estimated rate of metal loss of the Monel-400 dissolver, based on examination of a pipe specimen, was 7.5 mils/month of exposure over about a 2-month period. This included losses incurred both in actual dissolution and in decontamination of the vessel. Decontamination was effected with hot (60 to 92°C) 7*M*–20*M* HF, 0.05*M*–0.1*M* chromic acid, and 6.0*M* H_2SO_4 solutions over a time period of 244 hr. From laboratory data the H_2SO_4 decontaminant was most corrosive (7 to 9 mils/month at 114°C). The total corrosion was not considered excessive since the dissolving vessel was constructed with a 188-mil corrosion allowance. Cyclic tests indicated that chromic acid corrosion of Monel-400 is increased by prior exposure to 20*M* HF.

The 304L stainless-steel evaporator, used to concentrate the product of solvent extraction, was also examined since there is some carry-over of fluoride to this unit. The evaporator also utilizes boron-containing 304 stainless-steel plates for nuclear safety. After 14,500 hr of exposure to product solutions from processing both zirconium-alloy and aluminum-alloy fuels (the latter solutions were fluoride-free), the estimated loss from the vessel wall was only 0.02 mil and that from the boron steel was 1.0 mil. A corrosion rate of 0.2 mil/month for the boron plates was calculated from the boron concentration of the evaporator product.

RECOVERY OF AMERICIUM AND CURIUM FROM SHIPPINGPORT REACTOR FUEL

The Shippingport pressurized-water power reactor utilizes a seed-and-blanket type of core, in which a ring of highly enriched uranium seed elements is surrounded by a blanket of natural uranium oxide. In the blanket, plutonium is formed and partially consumed.

Since the blanket is retained in this reactor for several years, appreciable amounts of the transplutonium isotopes americium and curium are also formed. A brief description was recently given by Rathvon, of the Atlantic Richfield Hanford Co., of the recovery at the Hanford Redox Plant of the americium and curium in connection with plutonium extraction from the first Shippingport blanket processing operation.[10] The blanket elements processed consisted of 13.5 tons of uranium (as UO_2) in zirconium-alloy tubes and were estimated to contain 63 kg of plutonium, 1.2 kg of ($^{241}Am + {}^{243}Am$), and 0.07 kg of ^{244}Cm. The decladding and dissolution processes were previously described.[11] After chemical decladding, the core material was dissolved in acid, and the uranium, plutonium, and neptunium were separated by solvent extraction with hexone. Americium and curium were then batch-extracted from the fission-product waste solution, with 30% TBP in a paraffinic diluent, stripped from the solvent with dilute HNO_3, and concentrated by evaporation. Approximately 93% of the americium and curium were recovered by this means. No process details were given.

NEPTUNIUM–PLUTONIUM RECOVERY FROM PUREX WASTE

The accumulated, neutralized high-activity-level wastes from Purex processing operations at Hanford, which have been allowed to concentrate by self-boiling, contain significant amounts of neptunium and plutonium. These were accumulated prior to modification of the Purex process to provide for neptunium recovery.[12] The transuranium elements are largely contained in a sludge in the waste-storage tanks. Because plans have been made to sluice the sludge from the tanks with water to recover ^{90}Sr from it, consideration has also been given to recovery of plutonium, as well as ^{237}Np, which is the starting material for the production of the isotopic power source ^{238}Pu (Ref. 13). The conceptual recovery process that has been developed is based on coextraction of the transuranics from a nitric acid solution of the sludge with a diluent solution of di-2-ethylhexyl phosphoric acid (D2EHPA) and TBP. The utility of the D2EHPA reagent for heavy-element recovery has been discussed previously.[14] Salt constituents of the sludge solution consist principally of the nitrates of iron, aluminum, and sodium at a total NO_3^- concentration of about $3M$ (Ref. 13). The transuranics are present at concentrations of 1 to $5 \times 10^{-5} M$.

The principal process operations consist of a sequence of batch contacts involving D2EHPA extraction–oxalic acid stripping (this permits use of available tankage for extraction), followed by evaporative concentration. This sequence of operations is repeated on the concentrated solution to provide further removal of uranium, iron, and other contaminants. Because of its strong complexing action, oxalate must be destroyed following the extraction sequences; this is accomplished by boiling the strip solution with HNO_3 and H_2O_2. A simplified process diagram is shown in Fig. 1.

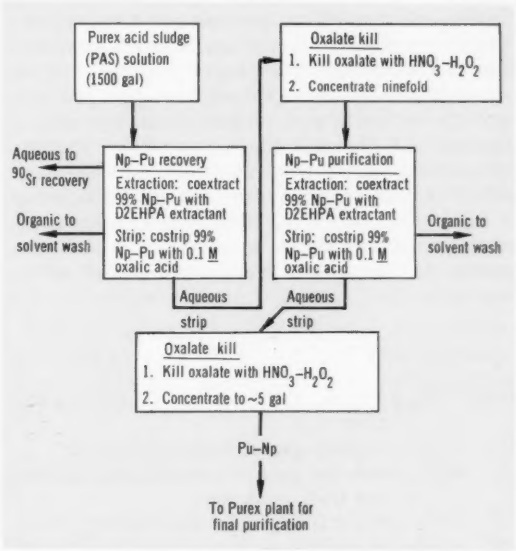
Purex acid sludge (PAS) solution (1500 gal)
Oxalate kill
1. Kill oxalate with HNO3–H2O2
2. Concentrate ninefold
Aqueous to 90Sr recovery
Np–Pu recovery
Extraction: coextract 99% Np–Pu with D2EHPA extractant
Strip: costrip 99% Np–Pu with 0.1 M oxalic acid
Np–Pu purification
Extraction: coextract 99% Np–Pu with D2EHPA extractant
Strip: costrip 99% Np–Pu with 0.1 M oxalic acid
Organic to solvent wash
Organic to solvent wash
Aqueous strip
Aqueous strip
Oxalate kill
1. Kill oxalate with HNO3–H2O2
2. Concentrate to ~5 gal
Pu–Np
To Purex plant for final purification

Fig. 1 Batch D2EHPA Np–Pu recovery process concept.[13]

For effective and simultaneous coextraction of neptunium and plutonium, it would be desirable to adjust their valence states to the highly extractable quadrivalent state; however, all attempts to do this were unsuccessful. In the alternative procedure that was developed, Pu(IV), as found in the sludge solution, is first extracted into the $0.1M$ D2EHPA–$0.1M$ TBP solution in a paraffinic diluent. After allowing the two phases to separate, but without removing the organic phase, the aqueous phase is treated with $0.03M$ ferrous sulfamate–$0.01M$ hydrazine to reduce neptunium to Np(IV). Recontacting then extracts the neptunium without loss of plutonium.

DETERIORATION OF EXTRACTION SOLVENTS UNDER IRRADIATION

The limited irradiation stability of solvents used for the extraction and purification of fertile and fissionable materials has been indicated to be a factor of potential significance in defining the applicability of solvent extraction for fuel reprocessing.[15] This is of particular concern in planning for the processing of fast reactor fuels because burnups of the order of 100,000 Mwd/metric ton may be achieved in U–Pu ceramic fuels, and because economic considerations associated with the large fuel inventory in a fast reactor may make it highly desirable to process fuels

after as short a cooling period as 1 month. Estimates of irradiation density in the aqueous feed to such processes are as high as 100 watts/liter. Blake[16] has recently summarized the available information on methods of estimating the irradiation dose to solvents, as well as the literature on solvent deterioration at expected levels, and has noted the specific effects of iodine and plutonium. It is observed that most of the reported data leads to erroneous and exaggerated predictions of solvent damage in processing; this is due in part to unavoidable confusion of chemical and radiation effects and in part to difficulties in estimating process doses realistically. A method of calculation is presented which is based on an equation developed for the radiation dose experienced in mixing. This is illustrated by the following equation applying to the operation of a mixer–settler contactor:

$$E_m = T_m \ (D_\beta + GD_\gamma)\, P$$

where E_m = organic-phase dose in mixing, watt-hr/liter
T_m = organic-phase residence time, hr
D_β, D_γ = beta and gamma power density in aqueous feed, watts/liter
G = fraction of gamma absorbed
P = aqueous feed-volume fraction in mixer

An equation is also provided for exposure during phase disengagement. Literature data indicating exposures experienced in processing various thermal reactor fuels, where levels of up to 3 to 4 watt-hr/liter per pass were noted, are evaluated on the basis of these equations. In comparison, estimated values for fast reactor fuel processing with short cooling are estimated to be only of the order of 0.1 watt-hr/liter per pass. This value is thought to be quite tolerable in consideration of the successful operation of extraction processes that provided adequate solvent-treatment equipment at accumulated solvent doses of tens of watt-hours per liter.

In considering the effects of alpha radiation from high plutonium concentrations in fast reactor fuels, it was concluded that such radiation can contribute up to 10% of the total first-cycle dose in processing fast reactor fuels. In later extraction cycles the alpha effects are more significant. The prediction of the possible effects of the take-up of iodine by the solvent in processing short-cooled fuels is made difficult by a lack of information of the behavior of iodine following dissolution.

RESULTS OF EUROCHEMIC PLANT OPERATION

The results of the first year's experience in processing a variety of reactor fuels in the Eurochemic plant were described by R. Rometsch[17] at the 1967 annual meeting of the American Institute of Chemical Engineers (AIChE) in New York in November 1967. This meeting was discussed briefly in the preceding issue of *Reactor and Fuel-Processing Technology*.[18] The Eurochemic plant structure and its process flow sheets were described in the Spring 1965 issue of *Reactor Fuel Processing*.[19] In the first year of operation,[17] fuels from seven different reactors located in four countries were processed successfully (see Table 1). The core materials included both unalloyed uranium and U–Mo alloy varying in enrichment from natural uranium to 1.6% ^{235}U. Fuels clad in both aluminum and magnesium were handled satisfactorily, the former cladding being removed with NaOH and the latter with H_2SO_4. A total of 34.5 tons of uranium was processed in 208 on-stream days, with a plutonium recovery of 18.86 kg.

Much of the material had undergone quite a long cooling period (3 to 9 years) so that high fission-product decontamination was not required. However, for the 3-month cooled material from the BR-1 reactor, a first-cycle ruthenium decontamination factor of $>10^3$ and a beta decontamination factor of 5×10^3 were obtained for uranium. For Diorit, FR-2, and BR-1 fuels, minimum first-cycle zirconium decontamination factors were 70, 40, and 29, respectively.

Table 1 FUELS PROCESSED DURING THE FIRST YEAR'S OPERATION OF THE EUROCHEMIC PLANT[17] (JUNE 1966–JULY 1967)

	Source of irradiated fuel (reactor and country)							
	EL-1 France	EL-2A France	EL-2B France	EL-3 France	Diorit Swiss	FR-2 W. Germany	BR-1 Belgium	Total quantities
Core	U	U	U	U/Mo	U	U	U	
Cladding	Al	Mg	Mg	Al	Al	Al	Al	
Enrichment, %	Nat.	Nat.	0.72–0.86	0.72–1.6	Nat.	Nat.	Nat.	
Burnup, Mwd/metric ton	25	200	300	1800	1300	750	300	
Years cooled	9	2.5	3	5	1.6	1.6	0.25	
U, tons	2.0	3.8	5.6	8.4	6.1	6.7	1.9	34.5
Pu, kg	0.03	0.65	1.06	5.12	6.9	4.1	0.61	18.86
Process time, days	17	31	37	39		84		208

Plutonium was separated from uranium in the first cycle by a factor of 10^4. Product specifications, following two extraction cycles, a silica-gel treatment of the uranium, and final plutonium purification by oxalate precipitation, were met for both uranium and plutonium.

It was felt that this initial operating period had adequately demonstrated the workability of the Eurochemic multifuel plant concept, the feasibility of chemical decladding a variety of materials, and the operability of the natural-recirculation dissolver used. Somewhat more active waste was obtained than had been anticipated. This resulted principally from decladding operations, which amounted to 2 to 2.7 m^3 of U per ton for the Diorit, FR-2, and BR-1 processing runs.

NEW AQUEOUS PROCESSING PLANT

In a February 1968 news release,[20] Allied Chemical Corporation announced that it intended to file an application with the AEC for construction of a nuclear fuel-reprocessing plant designed to process spent fuel from U. S. power reactors. The plant will employ a modified aqueous process, will have a capacity of 5 metric tons per day, and is expected to be operational in 1973. Primary consideration is being given to a location on the site of the AEC's Savannah River plant near Aiken, S. C. No other details were released.

Plant and Equipment Design and Operation

PERFORMANCE OF CENTRIFUGAL MIXER–SETTLER

In spent-fuel processing, using solvent extraction, it has become more and more desirable to use a contactor that minimizes solvent exposure to fission-product radiation. This becomes even more desirable in processing breeder reactor fuel because economics are improved by processing short-cooled fuel and thereby decreasing inventory charges. At a recent AIChE symposium on reprocessing irradiated fuels[18] D. S. Webster presented a paper that related experiences using a centrifugal mixer–settler for separating plutonium and uranium from radioactive fission products.[21]

The unit tested is an 18-stage contactor made up of three 6-stage units, the design of which was previously described in *Reactor Fuel Processing*.[22]

The hydraulic capacity was tested prior to radioactive operations, and throughput rates up to the equivalent of 27 tons/day (70 gal/min) were achieved without excessive entrainment. Mass-transfer performance was also checked out in these cold runs, and less than 0.03% of the uranium remained in the waste stream.

The performance of the unit, after a year's operation on radioactive fuels with fission-product gamma activity ranging from 50 to 200 curies/liter, was compared with that of conventional mixer–settler units:

1. Mechanical reliability has been excellent (one defective unit was replaced remotely early in the run).
2. Frequent shutdowns of the Purex process (over weekends) required only 15 to 30 min of solvent and scrub flow vs. 4 to 5 hr for pump-mix mixer–settlers.
3. Steady-state operation on startup was reached in 20 min vs. 16 hr.
4. Decontamination for the new unit was roughly equivalent; however, evaluation of decontamination performance is continuing.
5. The short residence time lowered the gross gamma activity in the solvent to one-fifth of former values. (Higher-activity-level feeds will be tested.)

This 1 year of operation, then, has demonstrated the advantages that were expected of the centrifugal mixer–settler; the demonstration of mechanical reliability will require longer operating time.

DELAYED-NEUTRON MONITOR FOR ^{235}U IN LEACHED HULLS

One problem associated with the shear–leach processing[23] for spent fuels is making sure that no undissolved fuel is discarded with the hulls. When fuel material, such as UO_2, is clad in stainless-steel or Zircaloy tubing, there is always the possibility that both ends of a short piece may be crushed closed by the shear, and hence not be leached by the acid.

Strain et al.[24] have designed and evaluated a monitor to detect amounts of ^{235}U as low as 10 mg in the presence of a gamma-radiation field of 10^5 r/hr.

High levels of beta–gamma radiation can be expected from both stainless steels (^{60}Co, ^{51}Cr, and ^{58}Co) and Zircaloy (^{95}Zr and ^{95}Nb). Table 2 gives an

Table 2 DOSE RATES ESTIMATED FOR THREE SIZES OF FUEL LEACHING BASKETS THAT CONTAIN IRRADIATED STAINLESS-STEEL HULLS[24]

[Basis: Fuel Enrichment, 2% ^{235}U; Burnup, 20,000 Mwd/ton; Irradiation Time, 6×10^7 sec; Irradiation Flux, 3×10^{13} neutrons/(cm^2)(sec); Basket Length, 150 cm; Depth of Hulls in Basket, 150 cm]

Basket diameter, cm	Decay time, days	Dose rate,* r/hr
13	14	1.2×10^4
	30	9.05×10^3
	60	7.65×10^3
	120	5.91×10^3
20	14	2.51×10^4
	30	1.91×10^4
	60	1.62×10^4
	120	1.26×10^4
25	14	3.85×10^4
	30	2.95×10^4
	60	2.49×10^4
	120	1.93×10^4

*At 8 cm from the outer surface of basket.

indication of the various levels of radiation expected from various-sized batches of stainless-steel hulls.

Four methods of detection were considered: (1) fission-product analysis by gamma spectrometry, (2) counting of neutrons produced by bombarding beryllium with the 2.18-Mev gamma radiation from $^{144}Ce-^{144}Pr$, (3) differential gamma-ray absorption of fuel and cladding, and (4) delayed-neutron monitoring.

The delayed-neutron monitoring method was selected for detailed evaluation and appeared to have the following advantages over the other three techniques: (1) variation in the type of cladding has no effect; (2) the analysis is independent of burnup or cooling time; (3) large quantities of hulls can be analyzed rapidly; and (4) the analytical results can be handled by computers or nontechnical personnel.

The theory of this method is that, when a fissionable material such as ^{235}U is bombarded by thermal neutrons, fission occurs, accompanied by the formation of short-lived products that decay by emission of neutrons. Most of these radionuclides are isotopes of bromine and iodine, for example, ^{87}Br, ^{89}Br, ^{137}I, etc., whose half-lives range from 0.23 to 54 sec. An average of 0.02 delayed neutron is produced per ^{235}U fission. This method has been demonstrated to detect 7×10^{-9} g of ^{235}U per liter in a 0.5*M* nitric acid solution after exposure in a reactor operating at 2.5 Mw and a neutron flux of 2.1×10^{12} neutrons/(cm^2)(sec) (Ref. 25).

The neutron generator used in the evaluation study was a commercially available Cockcroft–Walton machine. The 14.7-Mev neutrons produced were moderated by paraffin or polyethylene to provide a source of thermal neutrons; however, the authors proposed water for a permanent installation.

The delayed neutrons could be detected by measuring the products of neutron-capture reactions by means of such instruments as: (1) ^{235}U fission chamber, (2) ^{3}He-filled proportional counter, (3) $^{10}BF_3$-filled proportional counter, and (4) ^{10}B-lined counters.

A fission chamber was not considered practical for incorporation in the monitor because there is sufficient ^{235}U in the fission chamber to produce an appreciable background of delayed neutrons when the fission chamber is subjected to neutron bombardment.

Proportional counters containing ^{3}He or ^{10}B make use of the reactions $^{3}He(n,p)^{3}H$ or $^{10}B(n,\alpha)^{7}Li$ to detect neutrons. The positively charged particles ionize the filler gas within the counter, thereby producing an electronic pulse that can be amplified and recorded.

Various experiments and calculations by the authors led to the choice of a recently developed boron-lined chamber, which, combined with an electronic system having a nanosecond response, was used successfully to count neutrons in a gamma flux of 10^5 r/hr.

Two prototype monitors were built and tested. One was designed with separate compartments for irradiation and detection; the other had a single compartment.

The double-compartment monitor was designed to assay small batches of leached hulls that had been removed from the leachant and the rinse tanks by means of a cup conveyor. In a proposed in-cell installation of such a system (see Fig. 2), the hulls

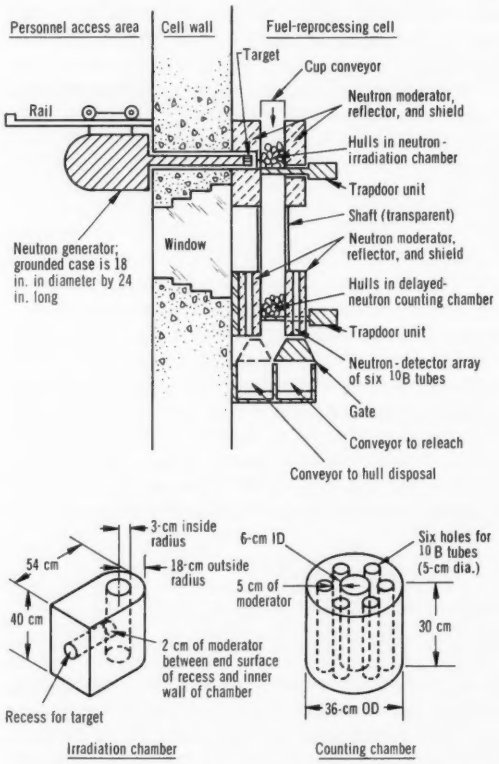

Fig. 2 Proposed in-cell installation of double-compartment leached-hull monitor.[24]

from a single cup are deposited in the monitor for the period of time required for assaying for fissionable residues and are then dropped upon one of two continuous conveyors. These conveyors either return the hulls to the leaching tank for further treatment or transfer them to a collector for subsequent disposal.

The sensitivity of the double-compartment prototype monitor for detecting ^{235}U is demonstrated in Table 3.

In a variation of the shear–leach process, the hulls are carried through the leach and rinse steps in a porous, stainless-steel basket 20 cm in diameter and up to 150 cm long. The capacity of each basket is approximately 50 kg (several thousand hulls). A single-compartment monitor was designed to assay the leached hulls without removing them from the basket.

Table 3 SENSITIVITY OF DOUBLE-COMPARTMENT MONITOR[24]

Sample	Repetitive analysis (counts/20 sec)*	Average*
Background (20 hulls)	5, 9, 6, 4, 7, 6	6
1 mg of ^{235}U	17, 15, 15	16
5 mg of ^{235}U	32, 47, 52, 54, 48	47
6 mg of ^{235}U	38, 38, 60, 58	49
100 mg of ^{235}U	520, 583, 686, 506, 910, 662, 687	650

*Background not subtracted.

A proposed in-cell installation of this monitoring unit is shown in Fig. 3; the prototype single-compartment monitor is shown in Fig. 4.

The authors include detailed discussions of each component of the system and conclude that 1 mg of ^{235}U could be detected with the two-compartment device and 10 mg of ^{235}U, with the single-compartment system. The double-compartment system has the advantage of speeding up the process, since analysis and disposal of leached hulls could start at any point in the process. In comparison, the single-compartment system, which operates on larger units or baskets of hulls, may require recirculation of an entire basket if undissolved ^{235}U is detected.

The single-compartment model, however, would require less cell space, would be mechanically simpler, and lower in cost. The authors estimate the cost

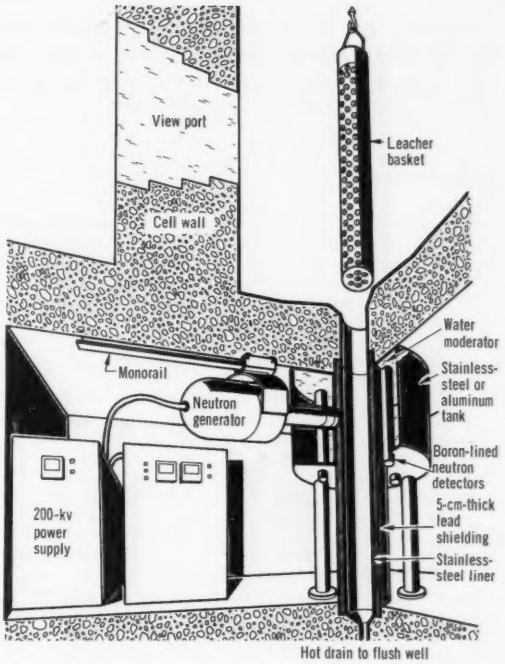

Fig. 3 Proposed installation of the single-compartment leached-hull monitor.[24]

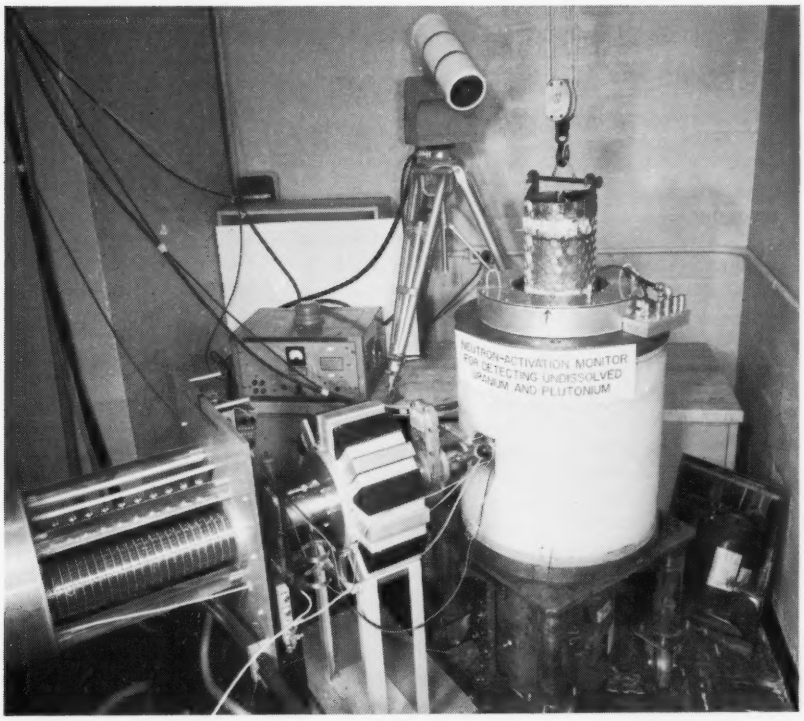

Fig. 4 Prototype single-compartment leached-hull monitor.[24] The target of the neutron generator is inserted in the polyethylene moderator. The radiation shield for the ^{60}Co gamma source can be seen beneath the moderator support.

to be less than $50,000 for the entire system. They also point out that the delayed-neutron monitor system might have other applications, such as analysis of uranium-containing process streams.

References

1. *Reactor Fuel Process.*, 9(1): 16 (Winter 1965–1966).
2. B. E. Paige and K. L. Rohde, Effect of the Metallurgical Composition of Aluminum–Uranium Silicon Fuels upon Chemical Reprocessing, paper presented at 155th National Meeting of the American Chemical Society, San Francisco, Mar. 31–Apr. 4, 1968.
3. *Reactor Fuel Process.*, 9(4): 220 (Fall 1966).
4. *Power Reactor Technol. Reactor-Fuel Process.*, 10(2): 153 (Spring 1967).
5. *Reactor Fuel Process.*, 9(2): 75 (Spring 1966).
6. J. A. Buckham, Idaho Nuclear Corporation, private communication, April 1968.
7. *Power Reactor Technol. Reactor-Fuel Process.*, 10(2): 153 (Spring 1967).
8. *Reactor Fuel Process.*, 9(3): 147 (Summer 1966).
9. C. A. Zimmerman and T. L. Hoffman, Corrosion Evaluation of Equipment Used for Reprocessing Zirconium Alloy Nuclear Fuels, USAEC Report IN-1134, Idaho Nuclear Corporation, February 1968.
10. H. C. Rathvon, The Redox Plant and Its Application to Americium–Curium Recovery from Shippingport Fuels, USAEC Report ISO-SA-46, Atlantic Richfield Hanford Co., Oct. 12, 1967.
11. *Reactor Fuel-Process. Technol.*, 11(2): 93-94 (Spring 1968).
12. *Reactor Fuel Process.*, 7(2): 97 (Spring 1964).
13. W. W. Schulz, D2EHPA Extraction Recovery of Neptunium and Plutonium from Purex Acid Sludge Solutions, USAEC Report BNWL-583, Pacific Northwest Laboratory, March 1968.
14. *Reactor Fuel Process.*, 8(2): 82 (Spring 1965).
15. *Reactor Fuel Process.*, 7(3): 172 (Summer 1964).
16. C. A. Blake, Jr., Solvent Stability in Nuclear Fuel Processing: Evaluation of the Literature, Calculation of Radiation Dose, and Effects of Iodine and Plutonium, USAEC Report ORNL-4212, Oak Ridge National Laboratory, March 1968.
17. T. J. Barendregt, E. Detilleux, and R. Rometsch, Aqueous Reprocessing in a Multi-Purpose Plant, paper presented at American Institute of Chemical Engineers Symposium on Recent Advances in Reprocessing of Irradiated Fuel, New York, Nov. 26–30, 1967.
18. *Reactor Fuel-Process. Technol.*, 11(3): 146 (Summer 1968).
19. *Reactor Fuel Process.*, 8(2): 83-85 (Spring 1965).
20. Allied Chemical Corporation, press release, Feb. 29, 1968.
21. D. S. Webster, A. S. Jennings, A. A. Kishbaugh, and H. K. Bethman, Performance of Centrifugal Mixer–Settlers in the Reprocessing of Nuclear Fuel, paper presented at American Institute of Chemical Engineers Symposium on Recent Advances in Reprocessing of Irradiated Fuel, New York, Nov. 26–30, 1967.
22. *Reactor Fuel Process.*, 7(3): 176-179 (Summer 1964).
23. *Reactor Fuel Process.*, 9(2): 78-81 (Spring 1966).
24. J. E. Strain, W. J. Ross, G. A. West, and J. W. Landry, The Design and Evaluation of a Delayed-Neutron Leached-Hull Monitor, USAEC Report ORNL-4135, Oak Ridge National Laboratory, February 1968.
25. W. H. Davies and R. F. Coleman, The Determination of Traces of Uranium by Delayed-Neutron Emission, British Report AWRE-0-88/64, November 1964.

Volatility Processes

By G. J. Vogel and J. W. Simmons

Fluid-Bed Fluoride-Volatility Processes for Ceramic Oxide Fuels

Fluid-bed fluoride-volatility processes are under development for the recovery of uranium and plutonium from irradiated UO_2 fuel. The processes reported here use approximately the same steps—chemical removal of cladding, oxidation of the ceramic oxide to a fine powder, fluorination to form volatile actinide hexafluorides, and purification of hexafluorides prior to their conversion to oxide for recycle to the reactor. At different sites, different fluorination agents (F_2, BrF_5, ClF_3, and ClF) are being evaluated. Development work at the Oak Ridge Gaseous Diffusion Plant (ORGDP), Oak Ridge National Laboratory (ORNL), Centre d'Étude de l'Énergie Nucléaire (Mol, Belgium), Argonne National Laboratory (ANL), Battelle Memorial Institute, and Fontenay-aux-Roses is reviewed.

Two general review articles were published recently. Fluidized-bed fluoride-volatility reprocessing methods being developed at ANL are described in a proceedings,[1] and another article describes fluoride-volatility methods under development at AEC laboratories for the reprocessing of plutonium-containing fuels.[2]

DECLADDING AND OXIDATION OF OXIDE FUELS

An experimental program is under way at ORGDP to determine the processing conditions and equipment requirements for optimum batch decladding and oxidation of UO_2 pellets.[3,4] In one run, a 76-kg simulated fuel element (a 6-in.-square array of sixty 4-ft-long tubes loaded with 53 kg of annular UO_2 pellets) was processed through the decladding and oxidation steps in a semiworks-scale fluid bed (45.5 kg of 48- to 100-mesh alumina). In this run, decladding by treatment of the Zircaloy with 20 to 50 vol.% HCl followed by oxidation with 10.5 to 21 vol.% oxygen resulted in an overall HCl utilization of 29% during decladding and in elutriation from the reactor of 97% of the uranium charged. The elutriated material contained essentially no alumina, as is necessary if transfer by elutriation is to become practical.

Four oxidation runs were performed in the same equipment with the charge consisting of ~55 kg of alumina or magnesium fluoride powder and 65 kg of UO_2 pellets (either annular or solid pellets).[4] It was concluded from the results of these runs that the reactor can be operated successfully through the decladding and oxidation steps with either alumina or magnesium fluoride as the bed material, that a superficial gas velocity of ~2.5 ft/sec is needed for oxidation of a $2\frac{3}{4}$-ft-deep bed of solid pellets, and that a gas velocity of ~1.5 ft/sec is needed for a $2\frac{3}{4}$-ft-deep bed of annular pellets.

Reaction of stainless-steel cladding with $HF-O_2$ in a fluidized bed produces oxides of stainless-steel constituents. Reaction of Zircaloy cladding with $HF-O_2$ may produce ZrO_2 shards.[5] The decladding gas mixture may react with the fuel oxide also, producing particulate fluorides and oxides in a proportion dependent upon the composition of the gas.

Two decladding runs were made at ORNL[5] in which Zircaloy-clad fuel elements were declad with 20 to 40 vol.% $HF-O_2$. A fuel assembly consisting of four 12-in.-long, 0.4-in.-OD Zircaloy tubes containing UO_2 pellets was used in each run. Runs were performed at 550°C in the presence and absence of a fluidized bed of alumina. Although it may be mandatory to remove heat in this step by means of a fluidized bed, results indicated that exposure of the oxide to a fluidized bed should be minimal to minimize the amount of fines produced and to minimize uranium and plutonium losses.

Bartlett and associates[6] patented a process for fluid-bed removal of zirconium cladding from fuel elements with a gas composed of 20 to 90 vol.% oxygen and 10 to 80 vol.% hydrogen fluoride at 500 to 800°C. At Argonne it was found that a gas mixture containing at least 2 parts by volume of hydrogen fluoride to 1 part by volume of oxygen does not react with the UO_2 pellets.[7] A high-HF gas mixture

would thus react with and remove stainless-steel or Zircaloy cladding without affecting the UO_2.

At Mol, one process cycle under investigation involves decladding of stainless-steel-clad UO_2 by reaction of the cladding with HF–oxygen mixtures at 500 to 600°C. A series of nine 1-hr experiments was carried out[8] at 590°C to determine the effect of concentration of the gaseous reagents on (1) the rate of the decladding reaction and (2) the degree of pulverization of the uranium dioxide fuel pellets. There was no fluidized bed in the reaction vessel. Results showed that hydrogen fluoride concentrations of 40 to 65% gave satisfactory decladding rates and that with 65% HF in the gas mixture the rate of pulverization of the oxide pellets was at a maximum.

Fuel assemblies, each consisting of nineteen 20-cm-long stainless-steel-clad fuel elements packed with natural UO_2, were chemically declad at Mol.[9] In two tests the gas mixtures contained 15 to 40% HF, 28 to 60% O_2, and 0 to 53% N_2. Heat transfer between the center of an assembly and the fluid bed was poor, and the temperature at fuel-element surfaces ranged from 500 to 800°C, indicating that the 2-mm distance between fuel elements in these assemblies was inadequate. Study of chemical decladding was continued, using assemblies containing seven fuel elements 5 mm apart.[10] Each fuel element consisted of a 304L stainless-steel tube containing 20 depleted UO_2 pellets. Initial tests showed that prefluorination of the alumina bed with HF prevented agglomeration of alumina particles during the decladding step. Four tests (three with prefluorinated alumina and one test with none) were performed at bed temperatures up to 650°C using 40% HF–60% O_2 as the reagent. Although heat transfer was very poor in the test in which alumina was absent, decladding was complete in this and the three other tests, and the uranium dioxide was pulverized and transformed into UO_2F_2 and UF_4. The authors concluded that it is probably not necessary to perform the decladding reaction in a bed of fluidized alumina.

In a series of fluid-bed tests at Mol[11] in which 4000-g charges of compacted uranium dioxide–2% fissium in 2000 to 4500 g of Al_2O_3 were oxidized at 500°C with 20 to 30% oxygen in a 10-cm-diameter reactor, only a small variation in temperature was observed along the bed height, and the uranium content in the alumina increased uniformly as a function of time. At the end of the tests, no agglomerates were found and only a low percentage of unreacted UO_2 was present. The decrease in the proportion of alumina to one-third of the total charge did not pose new problems.

FLUORINATION WITH FLUORINE

A series of experiments was performed at ANL in which 0.3- to 1.2-g charges of simulated spent fuel pellets containing UO_2, PuO_2, and nonradioactive fission-product oxides were fluorinated with fluorine in a 2-in.-diameter fluidized-bed reactor.[12] Each experiment was evaluated primarily on the amount of plutonium remaining in the alumina bed following recycle fluorination with 90 vol.% fluorine at 350 to 550°C or 450 to 550°C. It was found that a 12-hr recycle-fluorination sequence gave as good plutonium removal as a 20-hr sequence. In other experiments in which various pellet-to-alumina weight ratios were used, it was found that the fraction of plutonium retained by the alumina decreased with an increase in the pellet-to-alumina charge ratio in the range 0.3 to 1.2. In another experiment a single bed of alumina was used to process three batches of pellets; the plutonium retention on the final bed was 1.2% of that charged, which was the minimum value attained for this series of experiments. Another beneficial effect resulting from the reuse of alumina for several batches of fuel pellets is the reduction of the amount of solid waste. To minimize the amount of plutonium not reacted because of holdup on the upper cooler sections of the reactor, workers at ANL[13] performed an experiment with a bed consisting entirely of –100 mesh alumina instead of normally used 48 to 100 mesh. After precoating of the off-gas filters with alumina, it was expected that the bulk of the plutonium fines would be returned to the reaction zone by blowback of the filters. At the end of this run, excessive amounts of plutonium were found in the bed and on the upper sections of the reactor, and this fact indicates that the use of –100-mesh alumina as the bed does not decrease plutonium holdup in the upper sections of the reactor.

Three tests were performed at ANL[13] to evaluate the removal of low concentrations of plutonium from alumina-bed samples by leaching with nitric acid, as an alternative to extensive fluorination of the bed. Samples containing 0.164 wt.% plutonium were leached for 2, 3, or 5 hr with 6*N* HNO_3 at 100°C. The percentages of plutonium removed by leaching in the three tests were 95.1, 99.8, and 99.8%.

Three campaigns of PuF_4 fluorination experiments were performed at ANL to demonstrate that PuF_6 can be produced and transported readily and collected quantitatively in a 3-in.-diameter fluid-bed reactor facility. The results of two of the three campaigns were reported earlier.[14] The third campaign, like the other two, consisted of three separate fluorination runs (fluorination of about 260 g of PuF_4 with fluorine in each run), followed by a cleanup run in which plutonium deposited in the equipment was recovered by fluorination with fluorine.[15] Three-hour fluorinations were used in this campaign instead of 5-hr fluorinations used earlier, and the mean production rate was 4.1 lb of PuF_6/(hr)(sq ft) instead of 2.4 lb of PuF_6/(hr)(sq ft) obtained in the earlier campaigns. The fluorination rates, although substantially lower than those for uranium, are adequate for practical appli-

cations. A material balance for the third campaign shows that 98.9% of the plutonium charged was accounted for.[16] This value is within the range (96 to 104%) expected for a good material balance.

Other engineering-scale studies were performed in the same ANL equipment to develop information on the basic behavior of PuF_6 in the fluorination pilot plant.[17] Emphasis of the work was directed toward the step in which PuF_4 is fluorinated with fluorine for plutonium recovery. The material balance for six engineering-scale experiments and an additional engineering-scale plutonium-transfer experiment was 98.7%, which is considered to be satisfactory.[13] In two experiments, fluorination efficiency (defined as the amount of PuF_6 produced in a given period divided by the theoretical amount produced at equilibrium) was determined. Efficiency was near 50% at the start of each experiment and decreased rapidly as the plutonium content of the bed diminished. In the plutonium-transfer experiment, successful transfers of UF_6 and PuF_6 were carried out with 160.2 g of UF_6 and 89.4 g of PuF_6. Recoveries were 99% and 98.4%. The results indicated that, with proper conditioning of equipment (prefluorination with fluorine or perhaps even with PuF_6), the transport of PuF_6 in engineering-scale equipment is feasible.

Instrumental methods for plutonium analysis of fluoride-volatility process streams are under development[13,17] at ANL as possible alternatives to chemical analytical methods. A water-moderated neutron detector using ^3He proportional counters was constructed and was tested with plutonium fluorides. Its specific neutron counting rate was determined to be 20,800 ± 400 counts/min per gram of PuF_4, which is sufficiently sensitive and accurate for some process uses and indicates any changes in plutonium concentration at low levels with suitable uniformity to permit useful comparisons. A second type of neutron detector evaluated was a portable instrument with neutron shielding to minimize interference from any plutonium fluorides unavoidably near the process equipment being surveyed. Practical levels of directional discrimination could not be achieved without sacrificing the portability feature of the latter detector.

FLUORINATION WITH ClF_3 AND ClF

Workers at Centre d'Étude de l'Énergie Nucléaire (CEN) at Mol, Belgium, are developing a fluid-bed process for the recovery of uranium and plutonium from $(U,Pu)O_2$ fuel. A proposed flow sheet[8] provides for the reaction of compacts of $(U,Pu)O_2$ with a chlorine fluoride to selectively fluorinate uranium to volatile uranium hexafluoride. Plutonium is recovered in the following step as PuF_6 by reaction of the residue with fluorine.

To be an effective agent for separating uranium from plutonium, a chlorine fluoride should react with uranium to form UF_6 but should not form PuF_6. A thermodynamic study was carried out to allow estimation of the PuF_6 concentrations that would be in equilibrium with various fluorinating agents. On the basis of Fig. 1 (Ref. 9), which shows that insignificant amounts of PuF_6 are formed when ClF is in equilibrium with plutonium at temperatures of interest, ClF is being considered as a selective fluorinating agent. This reagent may be used as the selective fluorinating agent for uranium if the fuel is pulverized prior to the fluorination step. If the fuel is not pulverized, ClF_3 may be used as the selective fluorinating agent.[18]

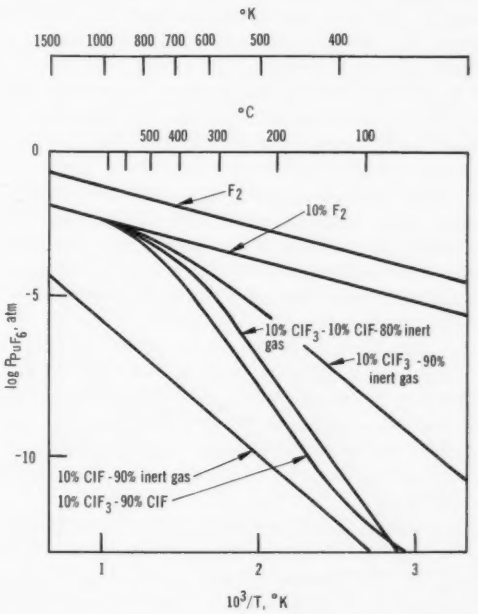

Fig. 1 Partial pressure of PuF_6 in equilibrium with ClF_3–ClF mixtures or F_2 as a function of the temperature (atmospheric pressure).[9]

In the investigations reported here, decladding of the oxide fuel at Mol was accomplished by reaction with $HF-O_2$, which also pulverized the fuel to form mixed oxide and fluoride. After one stainless-steel-clad fuel assembly had been declad, the oxidized uranium and decladding products were reacted with 10 to 25% ClF at 250 to 450°C to volatilize the uranium.[10] Most gases from the reaction (but not UF_6) were sorbed on a bed of sodium fluoride at 350°C. Analysis of samples from the bed indicated that volatile compounds of nickel, iron, and chromium had formed during the reaction with ClF.

Laboratory-scale tests were performed at Mol[8] to determine the extent of reaction of plutonium tetrafluoride with ClF_3 and ClF at selected temperatures.

Little plutonium was volatilized when PuF_4 was contacted with 30% ClF_3 in argon below 300°C. In four other tests,[8] ClF was contacted with 50-mg samples of PuF_4 at 550°C. In two tests in which the gas mixture was 30% ClF in argon and in two other tests in which the mixture was 20% ClF–30% oxygen in argon, no volatilization of plutonium was observed.

Other laboratory tests[10] were performed to determine the effect of high plutonium concentration in $(U,Pu)O_2$ pellets on fluorination by ClF_3. One investigation was carried out with an alumina bed using high-density fuel pellets. Upon fluorination at 300°C of pellets containing 0 to 20% PuO_2, fluorination and volatilization of uranium from the alumina bed were complete. However, with plutonium contents of 20% or greater, the rate of uranium volatilization was sharply reduced. No volatilization of plutonium was observed during volatilization of the uranium. It was concluded that ClF_3 at 300°C can be used for direct fluorination of high-density mixed-oxide pellets. At the end of the runs, the residue was observed to be pulverized.

In another investigation, UO_2–15% PuO_2 microspheres were fluorinated with 30% ClF_3 in argon. As determined with a thermobalance, the rate of volatilization of the uranium was much lower than the volatilization rate for pure uranium dioxide in the same physical state.

The influence of various ratios of ClF to ClF_3 (in the fluorination gas) on the rate at which PuF_4 is fluorinated at 350°C was also studied at Mol.[10] At high ClF concentrations (70 to 90%) in the fluorination gas, the rate of plutonium volatilization decreased to one-tenth the rate observed when no ClF was present.

Experiments were performed at Mol[8] to determine the effects of (1) temperature, (2) flow rate of the gases, and (3) concentration of the fluorinating agent (in nitrogen) on the quantity of uranium reacting with the fluorinating agent. Three series of experiments were performed in a 3.75-cm-diameter column; (1) the fluidized-bed fluorination of a UF_4–UO_2F_2–alumina mixture with ClF, (2) the fluidized-bed fluorination of a UF_4–UO_2F_2–alumina mixture with ClF_3, and (3) the fluorination of UO_2 with ClF_3. In each run of a series, the same total amount of fluorinating agent was fed. With increased temperature, a significantly greater reaction occurred in each series of experiments. Increasing the gas flow rate decreased the total amount of reaction in the runs in series 1 and 3 above but increased the total amount of reaction in series 2. In series 2 and 3, an increased concentration of the fluorinating agent gave a decrease in the total amount of reaction, whereas in series 1 the concentration of the fluorinating agent had no significant effect. Other tests at Mol[8] in which a UF_4–UO_2F_2–alumina mixture was fluorinated with 15, 25, 35, and 50% ClF showed that the reaction rate is a linear function of ClF concentration.

In a series of 16 tests,[10] the quantity of UO_2 reacted with 35% ClF_3 in a fluid bed was determined for two values of each of four variables: fluorination temperature (100 or 300°C), the presence or absence of fissium, the amount of alumina (0 or 20% of the UO_2 weight), and the ratio of height to diameter of the bed (3 or 6). The reaction time and amount of gaseous reagent were the same in all tests. The maximum amount of UO_2 was reacted in the test carried out at 300°C with a charge of 1000 g of UO_2 containing no fissium, in the presence of 200 g of alumina, and in a bed with a height-to-diameter ratio of 6.

In other tests at Mol,[10] UO_2 pellets were fluorinated with 26 or 31% ClF_3 in a 10-cm-diameter fluid-bed reactor, and the height of the reaction zone was measured. With a gas flow of 6 cm/sec, the reaction zone had a height of about 20 cm.

Behavior of Neptunium

In some conceptual versions of the fluid-bed fluoride-volatility process, a gas stream containing UF_6, PuF_6, NpF_6, and other volatile fluorides would be passed through a fixed bed of NaF (operated at 100 to 400°C in various steps of the process).[15] Neptunium hexafluoride would be removed from the gas stream by the reaction

$$3NaF(s) + NpF_6(g) \rightleftharpoons 3NaF \cdot NpF_5(s) + \tfrac{1}{2}F(g) \quad (1)$$

The neptunium can be subsequently recovered from the $3NaF \cdot NpF_5$ complex as NpF_6 by fluorination with fluorine.

Data on the extent to which NpF_6 would be taken up or released by a bed of NaF over a range of fluorine pressures is needed for a proposed method of separating NpF_6 from UF_6. The equilibrium constant

$$K_p = (P_{NpF_6})/(P_{F_2})^{1/2}$$

for the fluorination of $3NaF \cdot NpF_5$ by fluorine has been determined at a pressure of 700 torrs and temperatures[19] of 250 to 400°C. It can be expressed as a function of temperature by the equation

$$\log K_p\ (\text{atm}^{1/2}) = \frac{-3.147 \times 10^3}{T(°\text{K})} + 2.784$$

Several measurements, made at 350°C with fluorine pressures varying from 150 to 1500 torrs, showed that $\log P_{NpF_6}$ was a linear function of $\log P_{F_2}$ with a proportionality coefficient of 0.49, which is comparable to the value of $\frac{1}{2}$ expected for reaction 1. The value of the equilibrium constant, K_p, at 350°C was 5.52×10^{-3} $\text{atm}^{1/2}$.

From the values of the equilibrium constant, the following values for thermodynamic functions for the fluorination of $3NaF \cdot NpF_5$ have been calculated over

the range 250 to 400°C: mean enthalpy change, 14.4 kcal/mole NpF_6; mean entropy change, 12.7 cal/(mole NpF_6)(°K). The standard free-energy change at 298°K was 10.6 kcal/mole NpF_6.

Oxidation and Hydrofluorination of Carbide Fuels

At Mol the pulverization of uranium monocarbide by reaction with HF, O_2, water vapor, CO_2, and mixtures of these reagents in a fluid bed, followed by fluorination of the pulverized material, is being investigated.[11] Compact UC in the form of high-density pellets was completely converted to U_3O_8 with 44 vol.% oxygen at 500°C in one test and was completely converted to UO_2F_2–UF_4–uranium oxide mixtures in two other tests in which HF–O_2 was used as the fluorinating agent at 450 or 500°C.

Purification of Uranium Hexafluoride and Plutonium Hexafluoride

In the fluid-bed fluoride-volatility processing of reactor fuel materials, volatile UF_6 and PuF_6 are produced by reaction of the fuel with gaseous fluorinating agents. Uranium may be separated from plutonium by selective fluorination with ClF, ClF_3, or BrF_5; or, alternatively, uranium and plutonium may be simultaneously volatilized by reaction with fluorine and separated from each other in a subsequent step. In these reactions, volatile-fluoride compounds of certain fission products are also produced and appear in the UF_6 and PuF_6 process streams. Some of the recent work on developing methods for removing the fission-product contaminants from process streams is described below.

PURIFICATION OF URANIUM HEXAFLUORIDE

An earlier issue of this review[20] discussed the use of NaF and MgF_2 sorbents to remove volatile impurities from uranium hexafluoride prior to its return to the gaseous diffusion complex. A paper has been published describing the investigation.[21]

PURIFICATION OF PLUTONIUM HEXAFLUORIDE

Cleveland[22] briefly described the methods, advantages, and disadvantages of several techniques for separating plutonium from irradiated uranium in fluoride-volatility processes.

The French are investigating the selective chemical reduction of plutonium hexafluoride with carbon dioxide.[23] Tests showed that uranium hexafluoride and niobium pentafluoride apparently are stable in the presence of carbon dioxide and that ruthenium pentafluoride reacts only slowly. Mixtures of UF_6 (30 to 60 torrs), PuF_6 (30 to 70 torrs), and CO_2 (600 to 950 torrs) were reacted at 200, 300, and 350°C and resulted in complete reduction of PuF_6 in 15 min, 1 min, and 30 sec, respectively.

Workers at ORNL are studying a purification procedure in which PuF_6 reacts with LiF to form a complex from which PuF_6 can later be conveniently recovered by treatment with fluorine.[20,24,25] The technique of purifying PuF_6 process-gas streams based on the sorption of PuF_6 on granulated LiF is also being studied at ANL.[16,19,26] Two experiments were performed[26] in which mixtures of ruthenium fluorides and plutonium fluoride were passed through a static LiF bed to determine whether stabilities of the complexes differ sufficiently so that (1) a large fraction of the ruthenium would be fixed as the solid complex and (2) a large fraction of the plutonium would remain in the vapor phase. In a 10-hr experiment with the bed at 300 to 400°C, the ruthenium decontamination factor was 2.5×10^2, and 1% of the plutonium was retained in the bed. In a 7-hr experiment at 300°C, the corresponding values were 9×10^2 and 26%.

Two additional experiments were performed[16] at ANL in which a gaseous mixture of PuF_6, ruthenium fluoride, and fluorine was passed through LiF beds at 400 and 500°C to determine the effect of bed temperature on the decontamination factor (DF) and on plutonium retention in the bed. Results of these and earlier experiments show that the best temperature for PuF_6–ruthenium fluoride separation is between 200 and 500°C.

In further work at ANL,[19] a PuF_6–fluorine mixture was reacted with LiF at 300°C until the complex that formed contained 29.4 mole % PuF_4. X-ray powder-diffraction analysis of the solid showed the presence of the $LiF \cdot PuF_4$ complex. The sample was then heated to 400°C, fluorinated with fluorine, and weighed at intervals. A change in the rate of weight loss was observed during fluorination, suggesting that a second plutonium-containing complex was present in the final stage of fluorination. The presence of $4LiF \cdot PuF_4$ was confirmed by X-ray analysis of samples taken after the change in reaction rate.

Several runs were performed at ANL in which the loading capacity of LiF for ruthenium fluoride was determined[16] at 300, 350, and 400°C. The loading capacities expressed as milligrams of ruthenium per gram of LiF were 9 to 13 at 300°C, 17.3 at 350°C, and 9 at 400°C.

A comparison was made of the behavior of ruthenium fluoride species generated by the fluorination with a 3:1 fluorine–oxygen mixture of (1) ruthenium metal and (2) ruthenium dixode.[16] The volatile product was trapped in a cold trap at −78°C and then transpired by increasing the cold-trap temperature in 50°C steps from 0°C to 150°C. The products of both starting materials behaved similarly—for example, both volatilized at about 100 to 150°C.

To determine whether sublimation of PuF_6 from a cold trap at 0°C or 50°C, leaving ruthenium behind, might be a feasible technique of separating plutonium

from ruthenium, ruthenium fluoride and UF_6 (a stand-in for PuF_6) were transpired from a cold trap at 0, 50, 100, and 150°C (Ref. 19). Decontamination factors greater than 5.9×10^2 were calculated for four experiments.

REACTION OF MIXED HEXAFLUORIDES WITH SILICON TETRACHLORIDE

Speeckaert[27] at Mol has proposed separating uranium from plutonium by converting them to chlorides. Uranium hexafluoride and plutonium hexafluoride are converted to the chlorides by reaction with $SiCl_4$:

$$UF_6 + 1.5SiCl_4 = UCl_6 + 1.5SiF_4$$

$$\Delta G^\circ_{298} = -96 \text{ kcal/mole}$$

$$PuF_6 + 1.5SiCl_4 = PuCl_3 + 1.5SiF_4 + 1.5Cl_2$$

$$\Delta G^\circ_{298} = -120 \text{ kcal/mole}$$

The separation of uranium and plutonium would be based on the difference of vapor pressures of the chloride species formed. The highest chlorides formed at UCl_6 and $PuCl_4$–$PuCl_3$. The ratio of the vapor pressures of UCl_6 and $PuCl_4$ at 300°C is about 10^8, and the corresponding ratio for UCl_6 and $PuCl_3$ is many orders of magnitude larger.

SEPARATION OF URANIUM FROM PLUTONIUM IN MOLTEN SALT

The problem of separating uranium from plutonium and converting them to the dioxides for recycle to the reactor was examined at Mol.[11] A process based on oxidizing uranium and plutonium in a medium of molten alkali chlorides was chosen. Plutonium and uranium hexafluorides may be dissolved in a molten-salt bath such as NaCl, KCl, or LiCl. Upon oxidation with HCl–O_2, HCl–air, Cl_2–O_2, or an alkali nitrate, uranium is converted to soluble uranyl fluoride and PuO_2 precipitates. Removal of the PuO_2 by filtration is followed by electrolysis to deposit UO_2 on a cathode. In tests carried out with a LiCl–KCl eutectic at 500°C, the quantity of plutonium dissolved in the salt after PuO_2 precipitation was generally found to be satisfactorily small. In tests in which uranium was charged in the proportion of 9 parts to 1 part of plutonium, no uranium was detected in the PuO_2 product.

Filter Studies

The experience at ANL with automatic blowback systems for primary filters in fluid-bed reactors has been reviewed in a topical report.[28] The effects of variables such as pulse duration, interval between pulses, pressure of blowback gas, and design of the nozzle-venturi assembly were investigated. It was observed that successful operation has been achieved with a wide variety of laboratory and pilot-plant units.

Battelle–Columbus[29] studied the plugging of nickel off-gas filters that may occur in the decladding step in which Zircaloy is reacted with a HCl–nitrogen stream in a fluid bed to form volatile $ZrCl_4$. The objectives of the bench-scale, simulated decladding runs were to determine the causes of plugging and to find ways of alleviating this problem. It was determined that a major source of plugging was $NiCl_2$ formed in the pores of the filters by reaction of HCl with filter material. Although it was found that filter plugging from this reaction is reduced by lowering the operating temperature of the filter to ~350°C, the minimum temperature is fixed by the need to volatilize all of the $ZrCl_4$ (sublimation temperature, 350°C). Another major source of plugging was deposition on the filter surface of fines formed when Zircaloy was hydrochlorinated. These fines were largely ZrO_2 and were produced by reaction with oxygen present in the Zircaloy or in trace amounts in the system. Deposition of alumina fines from the bed was a minor factor. Suggested as an alternative to nickel filters is a filter consisting of a packed bed of alumina.

At ORGDP, several filter materials were evaluated for their ability to remain permeable during repeated cycles of hydrochlorination with HCl, oxidation with oxygen, and fluorination with fluorine.[3,4] Temperatures differed for different runs, and charge compositions differed: either zirconium metal or Zircaloy, UO_2 present or absent, tabular alumina or prefluorinated magnesium fluoride. In one test, two in-series sintered-nickel-fiber filters at 315°C were exposed to off-gases from the reaction of hydrogen chloride with zirconium metal in an alumina bed to determine whether plugging increased or decreased in the absence of nonzirconium components of Zircaloy. Plugging developed more slowly in this 10-cycle test than in tests using a Zircaloy charge but reached essentially the same level of permeability by the end of the test series. In the next test a highly permeable filter fabricated of woven nickel wire and a sintered-nickel-fiber filter were installed in series, and filter temperatures were maintained at 315, 100, and 100°C during hydrochlorination, oxidation, and fluorination of the alumina–UO_2–Zircaloy charge. Excessive plugging within three cycles lent support to the possibility that plugging is of a chemical nature. Substitution of prefluorinated magnesium fluoride for alumina as the bed material, in a test similar to the preceding test, resulted in excessive plugging in the fifth cycle, indicating that this substitution would not solve the plugging problem. In another test an alumina–Zircaloy charge was exposed to decladding–oxidation–fluorination cycles, and the off-gases were passed through two filters fabricated of Inconel powder. Excessive plugging of these filters occurred in the sixth cycle, indicating that they are not suitable for the three-step operation.

Heat Generation by Radioactive Materials

Dunthorn at ORGDP[30] studied the effect of heatup of an irradiated fuel element (a square array of fuel rods) and of the bed itself in fluid-bed processing. Information was needed to establish the following: design philosophy for equipment, the actions to be taken in the event of equipment malfunction, limits on the radiation levels of the fuel elements to be processed, and the number of bed recycles possible before heat generation becomes a serious problem. For each of three cases, he calculated the heatup expected for two burnups: first, 130-day cooled, 10,000 Mwd/metric ton uranium fuel and, second, 30-day cooled, 25,000 Mwd/metric ton uranium fuel. For the first case, high-burnup fuel element in still air, the temperature is not expected to reach 500°C and is therefore not of serious concern. For either of two other cases, (1) a high-burnup fuel element immersed in a fluid bed and plugged with caked fluidizing medium and (2) a high-burnup fuel element covered with medium during a process shutdown, it is calculated that the maximum allowable temperature of 700°C could be exceeded in 40 min to 6 hr, depending on the temperature at which the decladding operation is performed and the level of fuel-element irradiation. A fourth case, a settled bed previously used to process irradiated fuel and generating 100 watts of heat per liter, would have to be cooled before being allowed to settle if it should be desired to reuse the bed for several fuel charges.

Safety Aspects and Environmental Contamination Control

Seven types of metallic micropore filters were evaluated at Mol[11] for removal of <15-μ U_3O_8 and 3- to 6-μ $UF_4-UO_2F_2$ dust from a gas stream. Such dusts will be elutriated in the off-gas from the Mol hot semiworks fluoride-volatility plant. On the basis of test results and economic factors, a 0.9-mm-thick Monel filter fabricated of rigid mesh with 2-μ pores was chosen for this application.

Also at Mol,[11] caustic liquid scrubbers were evaluated for washing the off-gases and ventilation air from the hot fluoride-volatility semiworks. Excellent removal of HF and fluorine from off-gases was achieved, and these gases and ClF_3 were removed efficiently from ventilation air.

Criticality calculations[31] were performed at Mol for volatility processing of irradiated UO_2-PuO_2 fuel from a fast 1000-Mw(e) reactor. The process is one of decladding with $HF-O_2$, fluorination of uranium with ClF_3, and fluorination of plutonium with fluorine, all in fluidized beds. The criticality problems are most severe at the finish of the decladding step and during fluorination of plutonium. Six situations that could occur during processing were assumed, and the following factors were varied: the presence of a water jacket, weight of alumina bed, number of irradiated fuel assemblies, thickness of alumina insulation, and density of bed mixture. The applicable multiplication factor, K_{eff}, was calculated for each situation. These data will be useful in determining the maximum number of irradiated fuel assemblies that can be processed simultaneously by fluorination.

Servais[32] has calculated doses that could be delivered from process vessels containing an amount of plutonium tetrafluoride (23.24 kg) or plutonium oxide (20.00 kg) equal to that contained on one fast reactor fuel assembly. From these data he calculated the biological shielding required to protect personnel working near such vessels.

Evaluation of Fluoride-Volatility Process

Allied Chemical plans to construct a fuel-reprocessing plant on the Savannah River near Aiken, S. C. It will have a capacity of 5 metric tons per day and will employ a modified aqueous process.[33]

A recent paper[34] by Allied Chemical mentions that a technical feasibility study of a conceptual fluoride-volatility process (employing aqueous processing for plutonium purification) for a Zircaloy-clad low-enrichment oxide fuel was made in 1967. The steps of the conceptual process were: (1) reaction of the Zircaloy cladding with HCl to form volatile $ZrCl_4$, (2) oxidation of the fuel with air to pulverize it, (3) selective fluorination of U_3O_8 with BrF_5 to form UF_6, (4) fluorination of PuF_4 with fluorine to form PuF_6, and (5) purification of plutonium by conversion to PuF_4 or $Pu(SO_4)_2$, dissolution in nitric acid, and treatment by ion-exchange methods. Extensive use of fluid-bed reactors was proposed, and the conceptual plant design provided for remote operation and maintenance and extensive shielding.

The advantages and disadvantages of the conceptual design and the relation between plutonium content of fuel and plant capacity are discussed.[34] The limiting conditions for the conceptual process are a 30-kg limit on the mass of plutonium in fluidization reactor due to criticality considerations, the low rate of fluorination of PuF_4, and the absence of simple, reliable chemical decladding operations for certain fuel-element materials. The advantages of a volatility process, in comparison to an aqueous process, were stated to be that it can handle fuels after shorter cooling times, that krypton and tritium containment are easier, that radiation-stable process reagents are used, and that conversion of fission products directly to stable solid compounds can ease waste disposal.

Fluorination of Uranium Compounds

REACTION OF URANIUM COMPOUNDS WITH BrF_5

The kinetics of the gas–solid reactions between BrF_5 and U_3O_8, UO_2, and UO_3 have been studied in the

temperature range 225 to 300°C and in the BrF_5 partial-pressure range 75 to 370 torrs.[35] All of the reactions probably proceed through the formation of UO_2F_2 as an intermediate compound. The final products of all three reactions are thought to be UF_6, O_2, and Br_2. In the reaction of U_3O_8 with BrF_5, UF_4 is formed, probably by the interaction of product UF_6 and U_3O_8. The following equations were derived to express the dependence of the rate constants on temperature and BrF_5 partial pressure for these reactions:

$U_3O_8 - BrF_5$:

$$\log k' = 0.90 \log P - 2000/T - 0.220$$

$UO_2 - BrF_5$:

$$\log k' = 0.84 \log P - 1630/T - 0.270$$

$UO_3 - BrF_5$:

$$\log k' = 1.05 \log P - 1680/T - 0.767$$

Values of the activation energy of 9.2, 7.5, and 7.7 kcal/mole were calculated for the reactions with U_3O_8, UO_2, and UO_3, respectively.

REACTION OF UO_2 WITH FLUORINE

Iwasaki[36] has studied the kinetics and mechanisms of the fluorination of UO_2 pellets to UF_6 with fluorine. Earlier[37] he observed that the reaction proceeds in two steps, the conversion of the oxide to UO_2F_2 and the conversion of UO_2F_2 to UF_6, with the first step the more rapid of the two. In new work[36] he postulates a three-step reaction: (1) the transformation of UO_2 pellets to partly fluorinated UO_2 powder (fluorine attacks the active sites at the grain boundaries), (2) the formation of an intermediate (identified as UO_2F_2 in two cases), and (3) the formation of UF_6. Below 400°C and with fluorine concentration up to 40%, the highest studied, a thick layer of intermediate, yellow at the surface and green at the UO_2–intermediate surface, is formed. Fluorination of this intermediate is the rate-limiting step of the three. Above 430°C (400 to 430°C is considered a boundary region) little intermediate is formed, and the conversion of UO_2 pellets to UO_2 powder is the rate-limiting step. With less than about 15% fluorine, the intermediate is black and has not been identified; with greater than 15% fluorine, the intermediate is white UO_2F_2.

REACTIONS OF ClF WITH URANIUM COMPOUNDS

A series of experiments was performed at Mol[8] to determine the effect of reaction temperature (20 to 300°C) on the nature of the gaseous products of the reactions between ClF and various uranium compounds. For the reaction between UO_2 and ClF at temperatures up to 100°C, the products are UF_6, Cl_2, ClO_2F_2, and O_2; above 100°C, UF_6, Cl_2, and O_2 are formed. When ClF is reacted with U_3O_8, the same products are formed as for UO_2, and ClO_2F is formed up to 300°C. Reaction of ClF with UO_2F_2 gives the same products as with U_3O_8, but ClO_2F is formed up to 400°C and perhaps at higher temperatures.

Reaction of Uranium Tetrafluoride with Water Vapor and Oxygen

At Mol[11] the reaction at 400 to 690°C of powdered UF_4 with water vapor and oxygen was studied by thermogravimetry and by chemical and X-ray diffraction analyses. The UF_4 can react with water to produce UO_2 which is oxidized to U_3O_8 or with water plus oxygen to produce UO_2F_2 which reacts with water to form UO_3. A mixture of U_3O_8 and UO_3, formed by the competitive reactions, is the product. The quantity of UO_3 in the product increases with partial pressure of oxygen and decreases with temperature.

Miscellaneous

Bibliographies and articles of general interest include the following:

1. A bibliography, compiled by the International Atomic Energy Agency, on nonaqueous processing of irradiated fuel[38] for the period 1955 to June 1966. Among the subjects covered are the fused-salt process, the chemistry of fluorination processes, the Nitrofluor process, the chemistry and physical chemistry of volatile fission-product fluorides, the chemistry and physical chemistry of uranium hexafluoride, the chemistry and physical chemistry of plutonium hexafluoride, decontamination and separation of uranium and plutonium hexafluorides, and corrosion in the fluoride-volatility process.

2. Cleveland[39] has presented the physical and chemical properties and method of preparation of many plutonium compounds, including the fluorides and oxides.

3. A recently published French book[40] on uranium presents the method of preparation, physical properties, and chemical properties of uranium compounds, including the fluorides and oxides.

4. Gutmann has compiled a book on halogen chemistry which includes the physical properties of the halogens, the inorganic chemistry of the halogens, and the physical and chemical properties of the halogen fluorides.[41] Physical, physicochemical, and spectral studies of fundamental halogen reactions are presented together with reviews of halogen-containing complexes, the electronic factors governing their formation, and the nature and properties of halogen bonds.

5. Thirty-eight papers[42] on the physical chemistry of protactinium were presented at an international conference at Orsay, July 2–8, 1965. Included

were papers concerning the complex halides of protactinium(V) (D. Brown), the preparation and properties of some alkali fluoride complexes of pentavalent protactinium (L. B. Asprey et al.), and the fluoride complexes of tetravalent protactinium (L. B. Asprey and R. A Penneman).

References

1. A. A. Jonke, M. Levenson, R. Steunenberg, and R. C. Vogel, Reprocessing of Reactor Fuels by Fluoride Volatility and Pyrochemical Techniques, in *Plutonium as a Reactor Fuel*, Symposium Proceedings, Brussels, 1967, pp. 537-546, International Atomic Energy Agency, Vienna, 1967 (STI/PUB/153).
2. A. A. Jonke, M. J. Steindler, and N. M. Levitz, Development of Fluoride Volatility Reprocessing Methods for Plutonium-Containing Fuels, *Chem. Eng. Progr., Symp. Ser.*, 63(80): 130-141 (1967).
3. J. H. Pashley, ORGDP Fuel Reprocessing Studies, Progress Report for Period Ending August 31, 1967, USAEC Report K-L-1780, Part 22, Oak Ridge Gaseous Diffusion Plant, Dec, 1, 1967.
4. J. H. Pashley, ORGDP Fuel Reprocessing Studies, Progress Report for Period Ending October 31, 1967, USAEC Report K-L-1780, Part 23, Oak Ridge Gaseous Diffusion Plant, Jan. 26, 1968.
5. M. E. Whatley, P. A. Haas, L. E. McNeese, A. D. Ryon, J. C. Suddath, and C. D. Watson, Unit Operations Section Quarterly Progress Report, October–December 1966, Chemical Technology Division, USAEC Report ORNL-4094, Oak Ridge National Laboratory, February 1968.
6. C. B. Bartlett, E. Wirsing, and L. P. Hatch, Process for Decladding Zirconium from Zirconium-Clad Nuclear Fuel Elements, U. S. Patent 3,294,492, Dec. 27, 1966.
7. L. J. Anastasia, P. G. Alfredson, and M. J. Steindler, Selective Decladding of Nuclear Fuel Elements, U. S. Patent 3,343,924, Sept. 26, 1967.
8. Centre d'Étude de l'Énergie Nucléaire, Reprocessing of Irradiated Fuels, Quarterly Report No. 27, October 1–December 31, 1966, USAEC Report EURAEC-1920, 1967.
9. Centre d'Étude de l'Énergie Nucléaire, Reprocessing of Irradiated Fuels, Quarterly Report No. 28, January 1–March 31, 1967, USAEC Report EURAEC-1868, 1967.
10. Centre d'Étude d l'Énergie Nucléaire, Reprocessing of Irradiated Fuels, Quarterly Report No. 29, April 1–June 30, 1967, USAEC Report EURAEC-1934, 1967.
11. J. Schmets, G. Camazzo, R. Heremans, G. Pierini, and Ph. Speeckaert, Reprocessing of Irradiated Fuels by Volatilization. Regeneration of Ceramic Fuels, Final Report, 1967, USAEC Report ANL-Trans-590 (EURAEC-1694), 1968.
12. L. J. Anastasia, P. G. Alfredson, and M. J. Steindler, Fluidized-Bed Fluorination of UO_2–PuO_2–Fission Product Fuel Pellets with Fluorine, *Nucl. Appl.*, 4: 320-329 (May 1968).
13. R. C. Vogel, E. R. Proud, and J. Royal, Chemical Engineering Division Semiannual Report, January–June 1967, USAEC Report ANL-7375, Argonne National Laboratory, October 1967.
14. *Reactor Fuel-Process. Technol.*, 11(3): 150 (Summer 1968).
15. C. L. Chernick and A. Glassner (Comps.), Reactor Development Program Progress Report, January 1968, USAEC Report ANL-7419, pp. 119-123, Argonne National Laboratory, Feb. 27, 1968.
16. C. L. Chernick and A. Glassner (Comps.), Reactor Development Program Progress Report, February 1968, USAEC Report ANL-7427, pp. 119-122, Argonne National Laboratory, Mar. 26, 1968.
17. R. C. Vogel, M. Levenson, E. R. Proud, and J. Royal, Chemical Engineering Division Semiannual Report, July–December 1966, USAEC Report ANL-7325, Argonne National Laboratory, April 1967.
18. G. Pierini, A. Francesconi, and J. Schmets, Process for the Reprocessing of Irradiated Compact Fuels by Fluorination, U. S. Patent 3,340,019, Sept. 5, 1967.
19. C. L. Chernick and A. Glassner (Comps.), Reactor Development Program Progress Report, March 1968, USAEC Report ANL-7438, pp. 107-112, Argonne National Laboratory, Apr. 26, 1968.
20. *Reactor Fuel-Process. Technol.*, 11(1): 56-58 (Winter 1967–1968).
21. S. H. Smiley, J. H. Pashley, H. L. Kaufman, M. J. Stephenson, and J. R. Merriman, Removal of Impurities from Uranium Hexafluoride by Selective Sorption Techniques, *Trans. Amer. Nucl. Soc.*, 10: 507 (November 1967).
22. J. M. Cleveland, Separation from Irradiated Uranium Hexafluoride, in *Plutonium Handbook*, O. J. Wick (Ed.), Vol. II, pp. 544-545, Gordon and Breach, Science Publishers, Inc., New York, 1967.
23. Semiannual Report of the Chemistry Department, June 1966–November 1966, Nuclear Research Center, Fontenay-aux-Roses, September 1967.
24. D. E. Ferguson et al., Chemical Technology Division Annual Progress Report for Period Ending May 31, 1967, USAEC Report ORNL-4145, pp. 78-81, Oak Ridge National Laboratory, October 1967.
25. S. Katz and G. I. Cathers, A Gas Sorption-Desorption Recovery Method for Plutonium Hexafluoride, USAEC Report ORNL-P-2731, Oak Ridge National Laboratory, (1966).
26. C. L. Chernick and A. Glassner (Comps.), Reactor Development Program Progress Report, November 1967, USAEC Report ANL-7399, pp. 130-131, Argonne National Laboratory, Dec. 28, 1967.
27. Ph. Speeckaert, Conversion of Fluorides into Chlorides, Bromides, or Iodides, *J. Inorg. Nucl. Chem.*, 29: 1542-1544 (1967).
28. E. L. Carls and N. M. Levitz, Blowback of Sintered Metal Filters: A Review of Tests and Operating Experience, USAEC Report ANL-7392, Argonne National Laboratory, January 1968.
29. P. D. Miller, E. F. Stephan, and W. K. Boyd, Studies of Off-Gas Filter Plugging in the Primary Reactor of the Fluidized-Bed Fluoride Volatility Process, USAEC Report BMI-X-490, Battelle Memorial Institute, Feb. 19, 1968.
30. D. I. Dunthorn, Removal of Radioactively Generated Heat in Fluoride Volatility Reprocessing Operations, USAEC Report K-L-1979, Oak Ridge Gaseous Diffusion Plant, Mar. 17, 1965.
31. F. Servais and P. De Myttenaere, Reprocessing of Irradiated Fuels: Criticality Calculations, USAEC Report EURAEC-1858, April 1967.
32. F. Servais, The Reprocessing of Irradiated Fuels. Gamma and Neutrons Protection Calculations, USAEC Report EURAEC-1938, October 1967.
33. Allied Chemical Corp., Press Release, Feb. 29, 1968.
34. A. Schneider, R. I. Newman, and M. Selman, The Impact of Plutonium Content of Spent Reactor Fuel in a Fluoride Volatility Reprocessing Plant, in *Plutonium as a Reactor Fuel*, Symposium Proceedings, Brussels, 1967, pp. 549-558, International Atomic Energy Agency, Vienna, 1967 (STI/PUB-153).
35. R. L. Jarry and M. J. Steindler, The Reaction of Gaseous Bromine Pentafluoride with Uranium Compounds, II. The Kinetics of the Reaction with U_3O_8, UO_2, and UO_3, *J. Inorg. Nucl. Chem.*, 30: 127-132 (January 1968).
36. M. Iwasaki, Kinetics of the Fluorination of Uranium Dioxide Pellets by Fluorine, *J. Nucl. Mater.*, 25(2): 216-226 (1968).

37. *Reactor Fuel Process.*, 8(3): 159 (Summer 1965).
38. *Nonaqueous Reprocessing of Irradiated Fuel*, Bibliographic Series, No. 26, International Atomic Energy Agency, Vienna, 1967 (STI/PUB/21/26).
39. J. M. Cleveland, Compounds of Plutonium, in *Plutonium Handbook*, O. J. Wick (Ed.), Vol. I, pp. 335-401, Gordon and Breach, Science Publishers, Inc., New York, 1967.
40. P. Pascal (Ed.), *Uranium, Nouveau Traité de Chimie in Minérale* (in French), Vol. XV, Part 4, Masson et Cie, Paris, 1967.
41. V. Gutmann, *Halogen Chemistry*, Academic Press Inc., New York, 1967.
42. Physical Chemistry of Protactinium. International Conference, Orsay, July 2–8, 1965, National Center of Scientific Research, Paris, 1966.

Compact Pyrochemical Processes

By W. E. Miller and R. K. Steunenberg

Pyrochemical processes are a class of high-temperature procedures for the recovery and purification of nuclear reactor fuels and for the production of materials of interest to the nuclear industry. The processes are characterized by the use of molten salts and metals as media in which reactions or separations are effected. Typical liquid metals employed in these processes are Mg, Zn, Cd, Bi, Cu, and alloys of these metals. The salts are usually mixtures of $MgCl_2$ with chlorides of alkali and alkaline-earth metals.

Much of the pyrochemical-processing development work is concerned with the processing of fast breeder reactor fuel. Pyrochemical processes are particularly suited for this purpose for several reasons: (1) short-cooled fuels can be handled since the high radiation doses from these fuels do not adversely affect process chemistry; (2) process volumes are low, and consequently compact equipment is used; (3) solid waste streams of low volume are produced; (4) direct decladding of fuel by immersion in molten metals offers a promising solution to the decladding problem; and (5) the processes are adaptable to on-site plants.

Salt-Transport Process for Fast Breeder Reactor Fuels

Pyrochemical research and development work at Argonne National Laboratory is primarily concerned with the salt-transport process. Process flow sheets for a batch process[1] and for a process incorporating continuous steps[2] were presented earlier in *Power Reactor Technology and Reactor Fuel Processing* and *Reactor and Fuel-Processing Technology*.

In the batch process, fuel elements are declad by dissolving the cladding in liquid zinc, which is subsequently removed from the UO_2-PuO_2 mixture. The oxide mixture is reduced by magnesium in a molten salt–liquid Cu–Mg system. The alkali, alkaline-earth, and rare-earth fission products are extracted into the salt phase, which is separated from the liquid metal. Uranium is essentially insoluble in the liquid metal, whereas plutonium is soluble. Plutonium is separated from the remaining fission products and the uranium by a salt-transport step in which the plutonium is removed from the Cu–Mg (donor) alloy and deposited in a Zn–Mg (acceptor) alloy. The metallic plutonium product is recovered by evaporating the Zn–Mg solvent metal.

It may be advantageous to incorporate continuous or semicontinuous steps in the process to provide potentially higher capacities and more efficient separations. In the flow sheet that incorporates continuous steps, the decladding and reduction steps are essentially the same as those in the batch process. However, the Cu–Mg–Pu metal phase from the reduction step is processed continuously to extract the rare-earth fission products into a salt phase; and, in the subsequent salt-transport step, plutonium is extracted continuously from the Cu–Mg (donor) alloy into a salt phase and is simultaneously deposited in a Cd–Mg (acceptor) alloy. The plutonium is recovered from the Cd–Mg by retorting as in the batch process. The objective of the present work at Argonne is to produce the technology necessary for the development of a plant-scale process. Work is being done on process chemistry, process development, corrosion, kinetics, and equipment design.

Zinc–magnesium alloys are used as plutonium acceptor alloys in the current pyrochemical flow sheet. More data on the solubility of plutonium in pure zinc and in Zn–Mg alloys were obtained.[3] The data are plotted in Fig. 1. The line for pure zinc is based on earlier experiments,[4] but the data points on the line are from the recent work.

As part of a program to investigate mass-transfer rates in liquid salt–metal systems, the distribution coefficient of cerium between Mg–Cd alloys and a 55 mole % $MgCl_2$–27 mole % NaCl–18 mole % KCl salt mixture was measured.[5] The measurements were made at 441, 500, 527, 578, and 636°C, with magnesium concentrations ranging from 10 to 60 at.%. The results are plotted in Fig. 2.

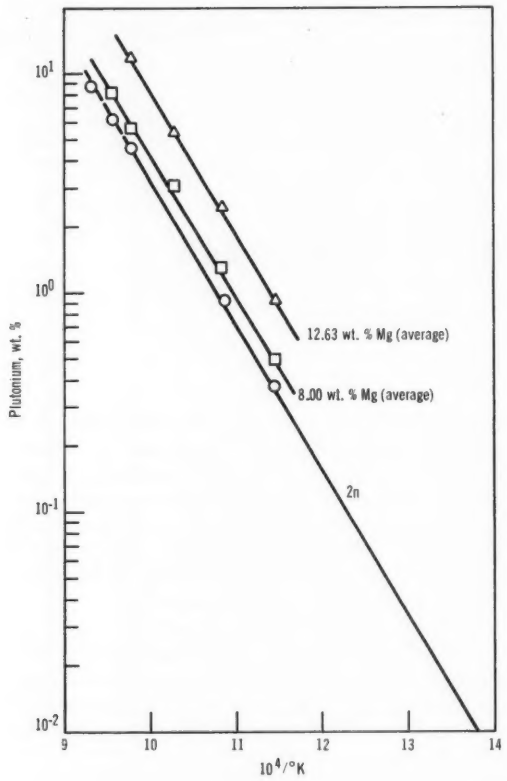

Fig. 1 Solubility of plutonium in zinc and Zn–Mg alloys.[3]

An alternative salt–metal system, namely, $CaCl_2$–CaF_2/Cu–Mg–Ca alloy, is being considered for the reduction step. The solubility of CaO in a $CaCl_2$–20 mole % CaF_2 salt mixture was measured[5] to determine the limits of oxide loading of this salt mixture. Two experiments were performed in which CaO in excess of the estimated solubility was mixed with purified $CaCl_2$–20 mole % CaF_2 in a baffled tantalum crucible at 900 to 950°C. Filtered samples were taken on both rising and falling temperature cycles after the salt had been equilibrated by stirring at each temperature for at least 2 hr. The solubility of CaO in the $CaCl_2$–20 mole % CaF_2 mixture was determined by analyses of the samples and is plotted as a function of temperature in Fig. 3. A break occurs in the curve at about 735°C, and a change in the ratio of fluoride to chloride in samples taken above and below the break indicates that a solid phase containing chloride precipitates below 735°C.

Another experiment[5] was performed to study the reduction of UO_2–PuO_2 solid solution in the $CaCl_2$–20 mole % CaF_2/Cu–Mg–Ca reduction system and to determine if plutonium would coprecipitate with uranium in the reduction. After the reduction the salt and supernatant Cu–Mg were poured away from the uranium precipitate, and the precipitate was dissolved in Zn–11 wt. % Mg alloy. Filtered samples were taken of both the Cu–Mg–Ca alloy during the reduction and the Zn–Mg alloy after the dissolution of the uranium precipitate. Analyses of the samples showed that the plutonium-to-copper ratio in the Zn–Mg alloy was the same as that in the Cu–Mg–Ca

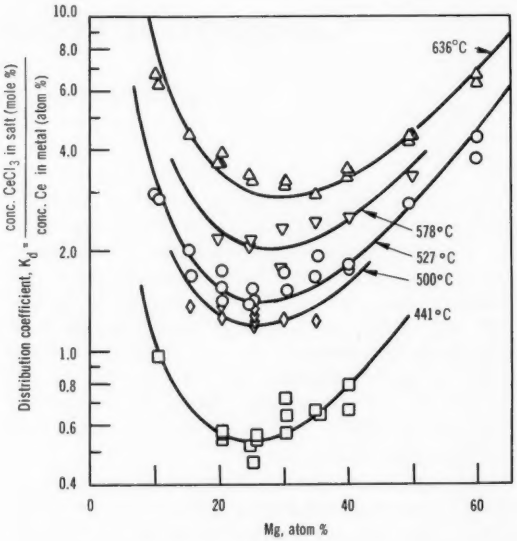

Fig. 2 Cerium distribution between Mg–Cd alloys and 55 mole % $MgCl_2$–27 mole % NaCl–18 mole % KCl salt.[5]

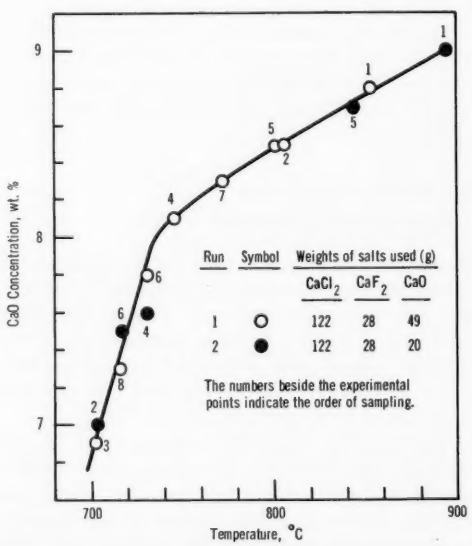

Fig. 3 Solubility of CaO in $CaCl_2$–20 mole % CaF_2 (Ref. 5).

reduction alloy. This result indicates that none of the plutonium coprecipitated with the uranium, since any coprecipitation of plutonium would have resulted in a higher plutonium-to-copper ratio in the Zn–Mg alloy. The analyses also indicated complete reduction of the UO_2-PuO_2.

Two decladding experiments were performed to study the removal of stainless-steel cladding from oxide fuels by dissolution of the cladding in molten zinc.[6] Simulated fuel subassemblies loaded with pellets and fines of UO_2 were immersed in molten zinc at 800°C. The subassemblies were constructed of 304 stainless steel and contained 13 tubes, which were $^3/_8$ in. in inside diameter and $12^1/_2$ in. long and had a wall thickness of 35 mils. The tubes were welded to three round plates 4 in. in diameter by $^1/_4$ in. thick. The subassemblies contained 2.68 kg of stainless steel and were loaded with 2.49 kg of UO_2.

Each subassembly was dissolved in 84.5 kg of molten zinc contained in a $9^3/_8$-in.-ID tungsten crucible. About 6 kg of $CaCl_2$–15 wt. % CaF_2 salt was added to the melt to retard vaporization of the zinc and to wet and collect UO_2 fines, which are reduced in the subsequent reduction step. After ~30 min immersion at 800°C, the stainless-steel tubing was completely dissolved, but the round plates were relatively unaffected. The subassembly was immersed for an additional 7 hr to ensure complete dissolution of the stainless steel. Filtered samples were taken during the course of the experiments and analyzed for iron to follow the progress of the dissolution. The results from one experiment are presented in Fig. 4. The results show that a period of approximately 4 hr was required to dissolve all of the stainless steel in the subassembly.

After the dissolution was complete, the molten zinc–stainless steel solution was transferred from the crucible. Subsequent inspection of the crucible showed that no undissolved stainless steel remained. The UO_2 pellets were distributed in a fairly uniform layer on the vessel's bottom and were partially covered with a zinc heel.

The zinc remaining in the crucible was removed by vacuum distillation. No major operational problems were experienced during the decladding and zinc-vaporization procedure in either experiment. The relatively zinc-free pellets remaining in the crucible after the decladding and zinc-removal procedures were suitable for the subsequent oxide-reduction step.

Processes for Molten-Salt Breeder Reactor Fuel

A number of recent reports describe the status of work directed toward the application of pyrochemical-processing techniques to molten-salt breeder reactor (MSBR) fuel. The molten-salt breeder reactor concept, which employs the Th–^{233}U fuel cycle, is being developed at Oak Ridge National Laboratory. Oak Ridge has built and operated a molten-salt reactor experiment (MSRE) fueled with ^{235}U, and

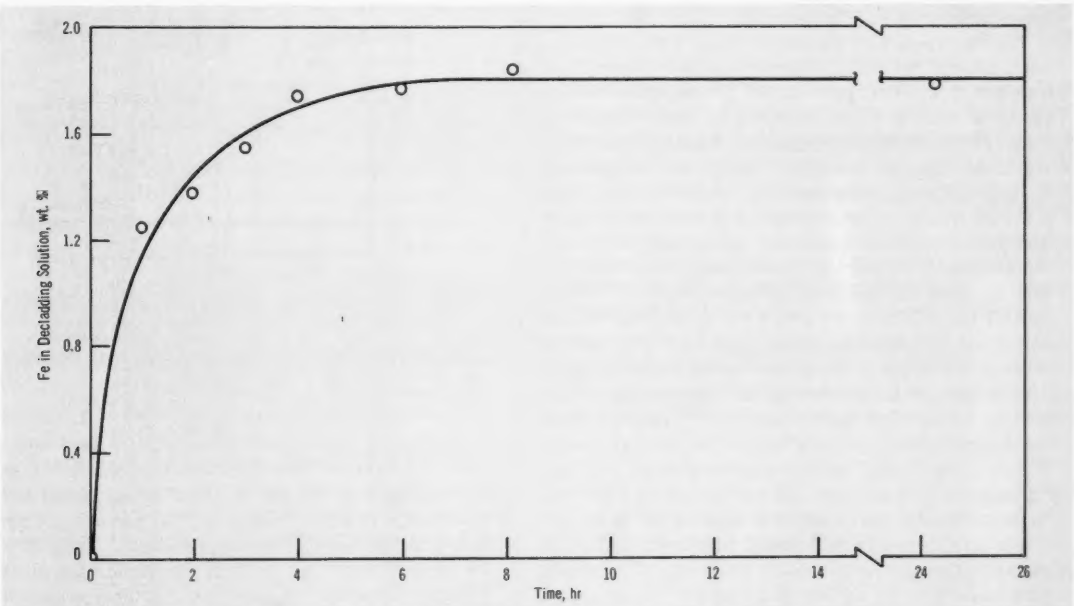

Fig. 4 Progress of decladding experiment.[6]

preparations are now being made to operate the experimental reactor with ^{233}U fuel.

Continuous processing concepts for treating molten-salt core and blanket fuel were discussed in a previous issue of *Reactor and Fuel-Processing Technology*.[7] In one processing concept, core fuel is contacted with fluorine to oxidize uranium from UF_4 to UF_6, which volatilizes. The barren carrier salt, $^7LiF-BeF_2$, is then vacuum distilled, and a highly concentrated solution of rare-earth salts in ^7LiF is left as a residue, which is discarded as a fission-product waste. The core fuel is reconstituted in a single operation in which UF_6 and H_2 are introduced into the purified salt and the UF_6 is reduced to UF_4. An alternative to the distillation process uses reductive extraction of the rare earths from the salt after the uranium has been removed from the salt by fluorination. One reductant that has been employed is lithium dissolved in bismuth.

Efficient breeding of ^{233}U requires that ^{233}Pa (bred from ^{232}Th) be removed from the neutron flux of the reactor to allow it to decay to ^{233}U. The problem of separating protactinium from molten fluorides is of utmost importance to the thermal breeder concept, and the problem is being investigated at Oak Ridge. Methods of removing protactinium from blanket salt were reviewed previously.[8]

In addition to research and development directly related to processing MSBR or MSRE fuels, supporting studies in molten-salt fuel chemistry are being carried out at ORNL. Some of these studies are concerned with solubility, vapor pressure, viscosity, thermodynamic, and electrical-conductivity measurements in molten-salt systems.

The distribution of fission products within the fuel-containment vessel of a molten-salt reactor is of interest to the fuel processor. Not all of the fission products remain in the molten salt. Some deposit on metal surfaces, some on graphite surfaces, and some volatilize into the gas phase within the containment vessel. Although the processor is dealing only with the salt phase, a knowledge of the fission-product distribution helps to determine which fission-product elements will be present in the salt. This information is being accumulated from two sources. Operation of the MSRE has yielded some information, and operation and postirradiation examination of in-pile thermal-convection loops have yielded additional data. The results of these studies are discussed in detail in two recent Oak Ridge reports.[9,10] Table 1 gives the distribution of some of the fission products in the MSRE.[9] The noble metals, molybdenum, tellurium, niobium, and ruthenium, did not behave as expected. Appreciable fractions of these fission products deposited on graphite and metal surfaces, and some entered the gas phase; only very small amounts circulated with the molten-salt stream.

The relative ease with which an element can be reductively extracted from $2LiF \cdot BeF_2$ into bismuth metal has been expressed in terms of extraction potentials.[9,10] The potentials that have been determined for certain fission products and other fuel constituents indicate the following ease of extraction:[9]

Li < Be < Ba < Eu < Th < Nd < Ce < Sm < Zr < La < U.

In a separate experiment it was shown that uranium could be quantitatively separated from cerium by the reductive extraction technique (see Fig. 5). It is possible that this procedure could be used as an alternative to fluorination for the removal of uranium from the salt prior to other fuel-reprocessing steps. A similar experiment with uranium and zirconium showed a somewhat less effective separation, but one that would still be adequate if two or more stages were used.

Table 1 APPROXIMATE FISSION-PRODUCT DISTRIBUTION[9] IN THE MSRE AFTER 32,000 Mw-hr

Isotope	Inventory in MSRE (dis/min)* $\times 10^{17}$	Percent in fuel	Percent on graphite	Percent on Hastelloy N	Cover gas,† %/day
^{99}Mo	7.91	0.94	10.9	40.5	77
^{132}Te	5.86	0.83	10.0	70.0	66
^{103}Ru	3.36	0.13	6.6	14.9	40
^{95}Nb	4.40	0.044	36.4	34.1	5.7
^{95}Zr	6.00	96.1	0.03	0.06	0.14
^{89}Sr	5.02	77.0		0.26	33
^{131}I	4.00	64.0		1.0	16

*This total inventory was calculated from the power history of the MSRE, assuming no losses to the cover-gas stream.

†These values represent the percentages of daily production rate lost to the cover gas per day.

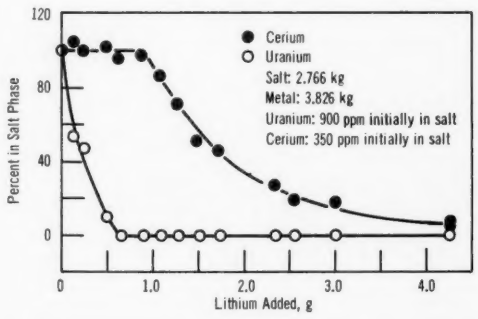

Fig. 5 Separation of uranium from cerium by reductive extraction with lithium from $LiF-BeF_2$ (67–33 mole %) into bismuth at 600°C (Ref. 9).

The status of the work on the extraction of protactinium from molten fluorides into molten metals is discussed in two recent Oak Ridge National Laboratory reports.[9,10] Studies of the removal of protactinium from solution in $LiF-BeF_2-ThF_4$ (73–2–25 mole %) salt by addition of thorium metal were reviewed earlier in *Reactor and Fuel-Processing Technology*.[8] Earlier experiments were performed with static systems in which simulated blanket salt

was in contact with bismuth and was contained in mild steel. These experiments substantiated the reduction of protactinium from the salt mixture but failed to demonstrate its quantitative dissolution in the metal phase. Since the extraction method utilizes the molten metal only as a transport medium, the apparently very low solubility of ^{233}Pa or its carrier in the molten metal is not necessarily detrimental to the process. A dynamic system was constructed and was operated by recirculating bismuth containing dissolved thorium through the simulated blanket salt mixture. Recovery of protactinium on a steel-wool column in the bismuth circuit accounted for about 43% of the ^{233}Pa initially in the salt phase. However, the recovery of ^{233}Pa was effected mainly by filtration rather than by adsorption. The filtered solids showed that the ^{233}Pa was associated with both iron and thorium.

More recent experiments[10] have been designed to demonstrate the reductive extraction of ^{233}Pa from the blanket salt mixture into a molten metal and its back extraction into a second salt mixture by hydrofluorination. The apparatus (shown schematically in Fig. 6) contained all of the liquid phases in graphite

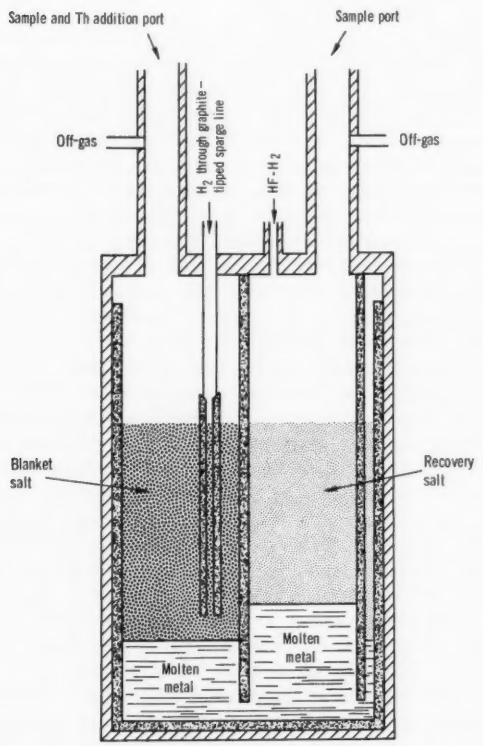

Fig. 6 Extraction vessel for ^{233}Pa removal from molten fluorides.[10] (All material in contact with salt and metal phases is graphite.)

to preclude the possible adsorption of ^{233}Pa on solid-metal surfaces. The initial experiment in this series demonstrated essentially complete removal of ^{233}Pa from the blanket salt, but only 65% of the ^{233}Pa was found in the recovery salt. Losses of ^{233}Pa that occurred in this experiment and in a later experiment were attributed to adsorption of the ^{233}Pa on metal particles formed by reduction of iron impurities in the blanket mixture.

Another experiment was conducted[10] in which tin was added to the metal phase to increase the iron solubility in the bismuth. In this experiment approximately 1.78 kg of the simulated $LiF-BeF_2-ThF_4$ (73–2–25 mole %) blanket salt and 1 mc of ^{233}Pa were in contact with 2.98 kg of bismuth that contained 0.41 kg of tin. Approximately 0.533 kg of $LiF-BeF_2$ (60–40 mole %) was also placed in contact with the molten-metal mixture to serve as a recovery salt. Figure 7 shows the transfer of ^{233}Pa during reduction

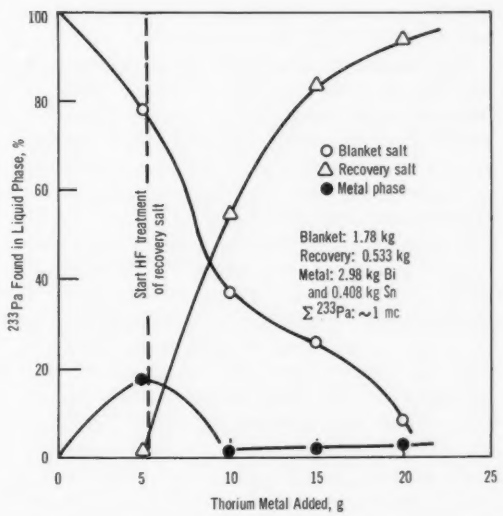

Fig. 7 Extraction of ^{233}Pa from $LiF-BeF_2-ThF_4$ (73–2–25 mole %) by reduction with thorium metal into $LiF-BeF_2$ (60–40 mole %) by hydrofluorination via molten Bi–Sn mixture at 650°C (Ref. 10).

by thorium-metal additions to the blanket salt and hydrofluorination of the recovery salt. Approximately 90% of the ^{233}Pa activity was found in the recovery-salt mixture, 2% was present in the molten-metal phase, and 8% remained in the blanket salt.

One of the proposed methods for processing the fuel stream of the MSBR includes a distillation step. In this step the $LiF-BeF_2$ carrier salt is distilled away from the less-volatile fission-product fluorides that must be removed from the reactor continuously. Current work is producing the information required for the design of distillation systems for MSBR

processing. Studies of the effect of a concentration gradient in a semicontinuous still, of factors limiting the vaporization rate, and of errors in measured relative volatilities are discussed in a recent ORNL report.[11]

Miscellaneous

Mullins and coworkers[12] have reported the distribution of ^{241}Am between liquid plutonium and a fused salt (NaCl–KCl) containing $PuCl_3$. Equilibrium measurements were made at 698, 730, and 775°C over a $PuCl_3$ mole-fraction range of 6×10^{-3} to 2×10^{-2}.

A recent report discusses the removal of americium from plutonium by electrorefining.[13] In 31 production runs, the plutonium metal containing an average of 267 ppm ^{241}Am was produced from a feed metal containing 960 ppm ^{241}Am. An average of 1% of the feed plutonium was retained in the salt as the chloride and an additional 11.2% was retained in the salt as finely divided plutonium metal.

Applications of molten-salt processing to plutonium recovery at Dow Chemical Company, Rocky Flats Division, were reported recently by Long.[14] Three areas of molten-salt processing were investigated, namely, electrorefining of plutonium, recovery of plutonium from electrorefining salts, and extraction of americium from plutonium.

Neptunium production at Rocky Flats was described in another Dow report.[15] Conversion of NpO_2 to NpF_4 with HF was followed by reduction of the NpF_4 to metal using calcium metal as the reductant in a bomb-type reduction. Iodine was added to the reduction charge to yield a more fluid slag. The average yield for eight reductions was 97.3%. The size of the NpO_2 batches charged was between 100 and 400 g of neptunium, and the impurities in the metal produced ranged from 179 to 1000 ppm.

A Japanese report discusses the reduction of ThO_2 by calcium.[16] The work was performed to determine the most favorable conditions for commercial preparation of the metal. Unlined stainless steel was the most suitable material for a reactor vessel; the yield deteriorated when a graphite reactor vessel was used. The optimum particle size of ThO_2 was about 150 μ. A high yield of metal could be obtained by using an amount of $CaCl_2$ flux equivalent to 20 to 40% of the weight of ThO_2 and about 25% more calcium metal than the amount theoretically required for the reduction. The reduction was most efficient when the system was heated for 4 hr at 950°C or for 3 hr at 1050°C. Under the above-mentioned conditions, the yield of thorium metal was about 90%, and the amount of residue that was insoluble in HCl was about 3 to 7%.

Another Japanese report[17] describes experiments in which UO_3 was reduced by calcium vapor. The resulting uranium powder was melted to determine the optimum conditions for preparing a uranium-metal powder that had good fusibility and high purity. Coarse uranium powder (gray-white) had better fusibility than fine uranium powder (black or brown-black). The optimum conditions for preparing coarse uranium powder were a reaction temperature of 1100°C, a Ca/UO_3 mole ratio of 9, and a reaction time of 2 to 3 hr (for this experimental scale). The yield percentage of coarse uranium powder was more than 90% under these conditions. Further experiments were conducted on the preparation of a small uranium-metal ingot from the uranium-powder product. The best procedure for making small uranium ingots was to place the metallic calcium outside of the crucible, but within the reaction vessel, and to heat the powder in 1 atm argon at a temperature greater than 1200°C. The purity of uranium ingots obtained under these conditions was greater than 99.9%.

A French report[18] describes a study of the electrorefining of beryllium in a molten $KCl-LiCl-BeCl_2$ bath at an average temperature of 475°C. The current production rate is 100 g of beryllium per 24 hr for a charge of 25 kg of electrolyte. The feasibility of obtaining a high-purity metal was demonstrated. The sum of the principal metallic impurities of commercial beryllium was lowered from a maximum of 4000 ppm to 35 ppm after electrorefining. However, there is a possibility of contaminating the fused salts with the materials constituting the cell, e.g., pyrex of silica. Prolonged contact of the baths with the cell materials caused contamination, principally by oxygen and sodium. Ion exchange between the lithium in the bath and the sodium in the pyrex occurred in the fused eutectic KCl–LiCl at 500°C. It was confirmed that the impurities concentrated in the immediate vicinity of the cathode. This phenomenon appeared to occur only with impurities that were more reducible than beryllium.

Corrosion tests from the Molten Salt Reactor Experiment are discussed in an ORNL report.[19] The first group of Hastelloy N surveillance specimens from the reactor core was removed after 7832 Mw-hr of reactor operation. During this period the specimens were held at 645 ± 10°C for 4800 hr, and they accumulated a thermal dose of 1.3×10^{20} neutrons/cm^2. The high-temperature ductility of these specimens, which were irradiated in a salt environment, was reduced, but the decrease was similar to that observed for Hastelloy N specimens irradiated in the Oak Ridge Research Reactor in a helium environment. The low-temperature ductility was also reduced, and this effect was attributed to the growth of intergranular precipitates. The specimens showed no evidence of corrosion. However, a carbon-rich layer, 1 to 2 mils in depth, was noted in areas where Hastelloy N and graphite were in contact. The mechanical properties of the Hastelloy N appear to be

adequate for the continued satisfactory operation of the MSRE. Test results are presented for the effects of several variables on the tensile ductility of irradiated and unirradiated Hastelloy N. These variables included test temperature, strain rate, and prestraining.

Pyrochemical preparation of U–3 wt.% Mo alloy powders was reported at a recent American Chemical Society meeting.[20] The alloy powder, which had a particle size of –200 mesh, was prepared for powder-metallurgy applications by bomb reduction of mixed uranium and molybdenum oxides with ground calcium. The oxygen content of the mixed oxides ranged from 12.1 to 15.3 wt.%. In some reductions, 0.1 to 1.0 mole of $CaCl_2$ per mole of uranium was used to reduce the average particle size of the alloy powder and to aid in dissolution of the slag. The particle-size distribution, molybdenum content, and purity of the alloy powders were compared with the oxygen content and purity of the oxide feeds. A higher oxygen content in the mixed oxides appeared to lead to a coarser metal alloy powder, other things being equal. In some cases the molybdenum content was higher in the larger-sized fractions but was lower when the larger particles consisted of filigree agglomerates of small particles. The metal alloy powders contained significantly less Na, Mg, Si, Mn, Cu, and Pb than the mixed-oxide feeds. The best yields of –200-mesh metal alloy powder, and the best-controlled molybdenum content, were obtained using a mixed-oxide feed with an oxygen content of 12 wt.%.

A French report[21] discusses an electrolytic method for the separation of uranium and plutonium fluorides in LiCl–KCl eutectic. The purpose of the work was to perfect the separation of the uranium and plutonium products of the fluoride-volatility reprocessing cycle and to obtain UO_2 of high purity which could be used directly in the refabrication of nuclear fuels. The first step of the procedure consists in dissolving a mixture of the two fluorides in the LiCl–KCl eutectic at 450°C. The solution is then oxidized to obtain the soluble uranium oxyhalogenide and to precipitate plutonium in the form of insoluble PuO_2. Uranium dioxide is deposited at the cathode by electrolysis. The residual PuO_2 is treated with hydrogen chloride (mixed with hydrogen if necessary), which renders it soluble in the form of $PuCl_3$. The plutonium metal can be recovered at another cathode by electrolysis at a higher potential. This new method has the advantage of using known experimental techniques. The separation tests carried out on uranium and cerium (a stand-in for plutonium) gave separation factors of 100.

Another French publication[22] reports the preparation of UO_2 crystals by electrolysis of a bath consisting of 20 wt.% UO_2F_2 dissolved in LiCl–KCl eutectic at 450°C. Of the UO_2 powder obtained, 80 to 90% was in good crystalline form.

References

1. *Power Reactor Technol. Reactor Fuel Process.*, 10(1): 80 (Winter 1966–1967).
2. *Reactor Fuel-Process. Technol.*, 11(3): 154 (Summer 1968).
3. C. L. Chernick and A. Glassner (Comps.), Reactor Development Program Progress Report, February 1968, USAEC Report ANL-7427, pp. 123-125, Argonne National Laboratory, Mar. 26, 1968.
4. I. Johnson and I. G. Dillon, The Solubility of Metals in Liquid Zinc, USAEC Report ANL-7083, Argonne National Laboratory, November 1965; I. Johnson and M. G. Chasanov, The Thermodynamics of the Plutonium–Zinc System, *J. Inorg. Nucl. Chem.*, 26: 2059 (1964).
5. C. C. Chernick and A. Glassner (Comps.), Reactor Development Program Progress Report, March 1968, USAEC Report ANL-7438, pp. 112-114, Argonne National Laboratory, Apr. 26, 1968.
6. L. B. Fosdick and A. Glassner (Comps.), Reactor Development Program Progress Report, April 1968, USAEC Report ANL-7445, pp. 119-122, Argonne National Laboratory, June 12, 1968.
7. *Reactor Fuel-Process. Technol.*, 11(1): 61-63 (Winter 1967–1968).
8. *Reactor Fuel-Process. Technol.*, 10(3): 235-236 (Summer 1967).
9. Oak Ridge National Laboratory, Reactor Chemistry Division Annual Progress Report for Period Ending Dec. 31, 1967, USAEC Report ORNL-4229, pp. 3-64, March 1968.
10. Oak Ridge National Laboratory, Molten Salt Reactor Program Semiannual Progress Report for Period Ending August 31, 1967, USAEC Report ORNL-4191, pp. 102-193, December 1967.
11. Oak Ridge National Laboratory, Chemical Technology Division, Unit Operations Section Quarterly Progress Report, January–March 1967, USAEC Report ORNL-4139, pp. 48-72, February 1968.
12. L. J. Mullins, A. J. Beaumont, and J. A. Leary, Distribution of Americium Between Liquid Plutonium and a Fused Salt. Evidence for Divalent Americium, *J. Inorg. Nucl. Chem.*, 30(1): 147-156 (1968).
13. James C. Brown, The Phase Distribution of Plutonium and Americium in Production Electrorefining, USAEC Report RFP-1065, Dow Chemical Company, Rocky Flats Division, Jan. 9, 1968.
14. Jack L. Long, Some Applications of Molten Salt Processing to Plutonium Purification and Recovery, paper presented at 155th American Chemical Society National Meeting, San Francisco, Apr. 1–5, 1968.
15. D. L. Baaso, W. V. Conner, and D. A. Burton, Production of Neptunium Metal on a 100–400 Gram Scale, USAEC Report RFP-1032, Dow Chemical Company, Rocky Flats Division, Dec. 5, 1967.
16. Sakae Takeuchi, Toshio Honma, Tsueno Satow, Susumer Sonoda, Hiroshi Kawai, and Keiji Koyama, Studies on the Reduction of Thoria by Calcium, *Nippon Kinzoku Gakkaishi*, 31: 42-48 (1967).
17. Takeo Oki and Jun Tanikawa, Preparation of Uranium by Means of Reduction of UO_3 by Calcium Vapor, *Nippon Kinzoku Gakkaishi*, 31: 1048-1052 (1967).
18. J. Bilard, G. Boisde, M. Bior, G. Chanvin, H. Corion, and J. Hardy, Production of High Purity Be by Electrorefining in Fused Salt Baths, *Metaux (Corros.-Ind.)*, 42: 259-269 (July–August 1967).
19. H. E. McCoy Jr., Evaluation of the Molten Salt Reac-

tor Experiment Hastelloy N Surveillance Specimens. First Group, USAEC Report ORNL-TM-1997, Oak Ridge National Laboratory, November 1967.

20. Marvin C. Trinkle, Preparation of U–3 Wt.% Mo Alloy Powders by Ca Reduction of Mixed Oxides, paper presented at 155th American Chemical Society National Meeting, San Francisco, Apr. 1–5, 1968.
21. Ph. Speeckaert, Considerations Theoriques sur la Separation Electrolytique de l'Uranium et du Plutonium en Sels Fondus, in *Thermodynamics of Nuclear Materials, 1967*, Symposium Proceedings, Vienna, 1967, pp. 195–201, International Atomic Energy Agency, Vienna, 1968 (STI/PUB/162).
22. Centre d'Études Nucléaires de Fontenay-aux-Roses Direction des Materiaux et Combustibles Nucléaires Department de Chimie, Rapport Semestriel du Departement de Chimie, Decembre 1966–Mai 1967, French Report CEA-N-856, December 1967.

Progress in Research and Development on Waste Disposal

By Phillip Fineman

Conversion of High-Level-Activity Wastes to Solids

FLUID-BED CALCINATION

In March 1968 the Idaho Chemical Processing Plant (ICPP) terminated on schedule its second waste-processing campaign[1] in which the aqueous fuel-reprocessing wastes that are produced there were treated by fluid-bed calcination in the Waste Calcining Facility (WCF) at the ICPP.[2]

During this campaign, which had been in continuous operation for nearly 2 years, 880,000 gal of aluminum nitrate-bearing wastes and 103,000 gal of fluoride-bearing zirconium wastes were processed through the WCF and converted to 12,200 cu ft of granular solids for an average overall volume reduction of 11. The calcined product is stored in underground bins. The process problems encountered in the campaign were minimal, and these were corrected by adjusting operating parameters.[3]

Since the completion of the campaign, the WCF has been placed on standby status, and preventative maintenance and minor repairs of WCF equipment are under way.[2]

POT CALCINATION PROCESS

A recent Pacific Northwest Laboratory (PNL) progress report[4] describes continuing developmental work on the pot calcination process[5] for the solidification of high-level-activity wastes. This process, which was originally developed at Oak Ridge National Laboratory (ORNL), is one of three solidification processes[6] that PNL is planning to demonstrate on an engineering scale with plant-level-activity wastes. Treatment of wastes by the ORNL process involves carrying out the calcination and solidification steps in the same vessel or pot. The pot also serves as the permanent storage container for the solidified waste product.

Two additional demonstration runs[4] (PC-4 and PC-5) were completed using simulated PW-1 wastes* prepared from Purex-process plant wastes. Arrangement of the equipment (designated as Mode C form of operation) for the two runs is shown in Fig. 1. In this arrangement the calciner pot is fed directly from the waste evaporator, and all of the pot condensate is continuously recycled directly to the evaporator. Thus a constituent that is volatilized from the pot will continue to increase in concentration in the feed stream until a steady-state concentration is attained. Waste solution is continuously supplied to the evaporator to replenish that fed to the calciner pot. In run PC-4, sodium hydroxide solution (4*M*) was fed to the top plate of the acid fractionator to determine if scrubbing of the fractionator off-gas would remove additional ruthenium.

In the two runs the recycling of the pot condensate resulted in decreased volatilization of ruthenium. Less than 5% and 3%, respectively, of the total ruthenium in the feed to the pot was volatilized in runs PC-4 and PC-5. In prior runs conducted with PW-2 waste,† 30% of the ruthenium volatilized. Although the reason for the low ruthenium volatility with PW-1 waste is not known, it is thought that the high iron content (~0.8*M*) of PW-1 wastes may be a key factor. The use of sodium hydroxide solution in run PC-4 to scrub the fractionator off-gas resulted in a ruthenium decontamination factor (across the fraction-

*PW-1 waste is a first-cycle Purex-process waste. It is high in nitric acid (~5*M*), free of sulfate ion, and contains added iron (~0.8*M*) from the dissolvable container used to transport chopped fuel. Because the plant wastes available for preparation of the PW-1 waste feeds for these two runs contained excessive amounts of sodium, sulfate was added to prevent the formation of volatile sodium and cesium oxides.

†PW-2 waste is a combined first- and second-cycle Purex-process waste. It is high in nitric acid (~5*M*) and contains iron (~0.4*M*) and sulfate (~0.8*M*) ions from the ferrous sulfamate reductant.

ator) that was 30 times greater than that for run PC-5, in which no sodium hydroxide solution was used.

Although operating difficulties (foaming and plugging) were encountered in the two runs, the runs were successfully completed. Early in run PC-4, foaming took place in the calciner pot and caused the expulsion of some of the feed solution to the safety-relief pot. To prevent further expulsion of feed, the solution level in the pot was lowered to allow more freeboard for foaming; however, no further foaming was observed during the remainder of the run. In run PC-5, sufficient freeboard for foaming was maintained.

Run PC-5. In this run an 8-in.-OD pot, also fabricated of 304L stainless steel, was used for the calcination of 520 liters of feed containing 1,200,000 curies of mixed-fission-product activity (including 18,000 curies of ruthenium). A calcine volume of 55 liters was produced for a volume reduction of about 9. This waste would be the equivalent of processing about 1.3 metric tons of 20,000-Mwd power-reactor fuel that had been allowed to cool for 1.5 years.

Internal heat generated (total of 4300 watts or 78 watts/liter) by the radioactivity in the pot was about 85% of the maximum thermal amount permitted for a pot containing solidified waste; at the maximum

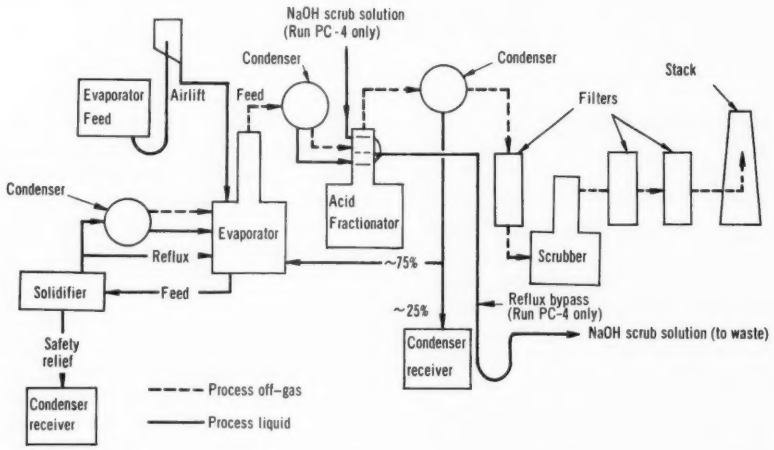

Fig. 1 Equipment arrangement (Mode C operation) for PNL pot solidification for runs PC-4 and 5 (Ref. 4).

Although foaming was evident, no feed was expelled. Plugging of the sparger and the specific-gravity dip tube in the waste evaporator occurred in both runs; the plugging condition was not corrected during the course of the runs. Additional details for each of the runs are presented below.

Run PC-4. A total of 1080 liters of feed containing 650,000 curies of mixed-fission-product activity (of which 47,000 curies was ruthenium and 30,000 curies was strontium) was processed in a 12-in.-OD pot fabricated of 304L stainless steel. The volume of calcine produced was 105 liters, which corresponds to a volume reduction (feed to calcine) of about 10. This waste would be the equivalent of processing about 3 metric tons of 20,000-Mwd power-reactor fuel that had been allowed to cool for 4.7 years.

The self-generating heat density of the calcine product was 25 watts/liter. At equilibrium (ambient air temperature of 38°C), the maximum centerline temperature of the pot was 477°C, and the temperature drop from the center line of the pot to its wall was 312°C.

value, upon which the design criteria for pot storage are based, the internal pot temperature of 900°C or the pot-wall temperature of 425°C would not be exceeded. At equilibrium the pot centerline temperature (ambient air at 38°C) was 725°C, and the temperature difference between pot center line and its wall was 495°C.

CONVERSION TO GLASS

The results of a design and cost study of a glass-fixation process developed at Harwell were presented at the 1967 American Institute of Chemical Engineers Symposium on Recent Advances in Reprocessing of Irradiated Fuel.[7] The process known as FINGAL (Fixation in Glass of Active Liquor)[8] incorporates highly radioactive nitric acid wastes for permanent storage in a chemically inert and highly insoluble glass. These wastes arise from the reprocessing of fuel from the U. K. nuclear power program. The FINGAL process, which has been under development at Harwell for some 10 years, is being considered as an alternative to the presently used system of liquid

storage.[7] A simplified flow sheet of the process is shown in Fig. 2. Processing of the nitric acid wastes, which have been previously concentrated by evaporation, is carried out on a batch-production basis and involves using three cylindrical vessels* of type 25/20 stainless steel connected in series. The concentrated wastes, to which are added silica and borax† (the glass formers), are fed to the first vessel maintained at 1050°C. Here the slurry mixture is dried and the solid residue fused into a glass. Process off-gas from the glassmaking vessel is passed successively through the other two vessels, each of which is equipped with a filter to remove volatilized ruthenium and other fission products, and then the off-gas is scrubbed with nitric acid and sodium hydroxide before discharge to the atmosphere. When the process cycle is complete, the vessel containing the solidified glass product is removed from the furnace and transferred to dry storage in a vault where the glass-filled vessel is cooled by an air stream.‡ For successive new process cycles, the other two vessels are progressively moved into the glassmaking position; the filter in this vessel is then dropped and incorporated in the glass melt. A new vessel with a new filter is installed in the processing train. (Design drawings showing details of the proposed glass vitrification plant and the storage vault are given in the original paper,[7] to which the reader is referred.)

The authors compared the costs of building the FINGAL process plant and operating it for a 20-year period with that of the existing method of storing concentrated acid wastes in stainless-steel tanks equipped with cooling coils. The capital and operating costs for the two schemes are based on the following assumptions:

1. The reprocessing of 1500 metric tons of Magnox fuel per year.

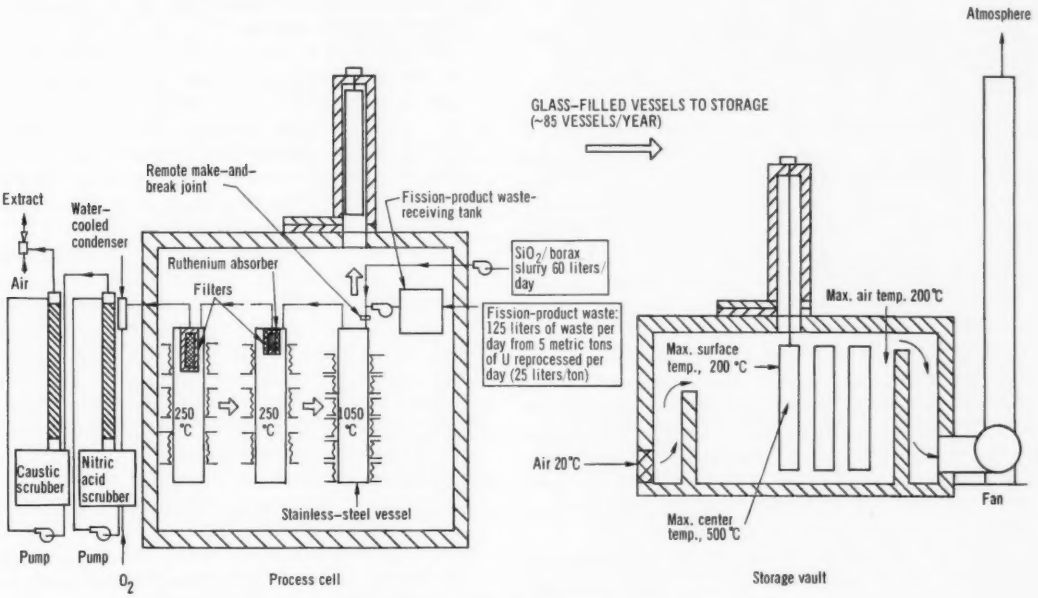

Fig. 2 Simplified flow sheet of Harwell FINGAL process.[7]

*The vessels are 1 ft in inside diameter by 8 ft high and will be filled to a glass depth of 6 ft. Each vessel will hold the waste arising from the processing of approximately 17 metric tons of Magnox fuel. A vessel of this size represents a compromise between obtaining the maximum amount of surface area available for heat transfer from the glass and reducing the number of cylinders which have to be produced from a large reprocessing program.

†Tests at Harwell have shown that up to 40 wt.% of waste oxide can be incorporated in a B–Si glass without adversely affecting its properties as a containment medium.[7]

‡The following thermal values were established for the storage of glass-filled vessels in dry vaults: (1) maximum centerline temperature of the filled vessel, 500°C; (2) maximum temperature at the surface of the vessel, 200°C; and (3) maximum cooling-air outlet temperature, 200°C. Sufficient cooling air (natural draft supplemented with fans) must be passed across the stored vessels of glass for a long period to maintain the temperatures below these values. The natural draft is furnished by a chimney 200 ft high by 10 ft in inside diameter, which can serve five storage vaults. Any one storage vault is capable of containing a total of 488 vessels stored in rows of 8 abreast with a maximum of 61 rows.

2. The tank storage of concentrated nitric acid waste (concentrate volume of 18 liters per metric ton of Magnox fuel).
3. The availability of one standby storage tank.
4. Present-day costs.
5. An operating period of 20 years.

	Cost, millions of pounds (British)	
	Concentrated liquid storage	FINGAL process and glass storage
Capital value of facilities	3.78	2.41
Operating costs	1.74	2.62
	5.52*	6.03†

*Equivalent to $12.5 million (U. S.).
†Equivalent to $16.9 million (U. S.).

The authors point out that, of the two schemes, liquid storage has a cost advantage, an advantage that would be very much greater if the liquid wastes were evaporated to higher concentration factors. However, some of the cost advantage would eventually be lost, once it became necessary to start replacing liquid-storage tanks. About 20% of the cost of operating the FINGAL process is attributed to the cost of the stainless-steel vessels; and, although no method of reducing this cost is apparent at present, this may be possible in the future. They also point out that this process has now been sufficiently developed in the United Kingdom so that there is enough information to utilize it directly on a substantial scale, and therefore no further extensive development is planned. However, the cost of introducing this process is not considered justifiable on safety grounds alone, and it is believed necessary to demonstrate that there are economic advantages to the system before it should be chosen to replace the already established liquid-storage system.

Selected Current Literature

Studies related to the storage of high-level-activity wastes in underground storage tanks are described in two reports, one issued by PNL[9] and the other by SRL (Savannah River Laboratory).[10] In the PNL report,[9] Willingham describes the use of a computer program developed for calculating steady-state temperatures in heat-generating and non-heat-generating systems. This program offers a reasonably accurate method of estimating temperatures expected in and around underground storage tanks containing radioactive wastes. These temperatures are important to know so that safety limits set by past experience are not exceeded. Programs with constant or temperature-dependent thermal conductivities, internal heat generation, and constant film or contact coefficients can be accommodated. The results are calculated by an iterative process, which the author describes in detail. In the SRL report,[10] Fenimore and Horton have examined the possible consequences of a release of waste due to tank leakage into the surrounding soil at SRL. (Tank design and operating controls minimize the possibility of this occurring at SRL.) In their laboratory experiments, they passed simulated wastes* containing radioactive cesium and strontium through small columns (2 in. in diameter by 6 in. long) of SRL soil, a sandy clay soil that surrounds the storage tanks. The rate of movement of cesium and strontium through the soil and the feasibility of recovering these radionuclides from the soil by leaching were studied. Their results indicated that, if radioactive waste leaked from a storage tank, the movement of strontium and cesium through the surrounding soil would be retarded because of reduced permeability† of the soil. The movement of strontium would accelerate as the waste became diluted with groundwater, but cesium would continue to move at a low rate. Strontium was readily leached from the waste-soil mixture by dilute solutions‡ of acid or salts, but cesium was not readily leached by any solution tested.

A series of articles devoted to the solvent extraction of useful fission products generated in the reprocessing of spent nuclear fuel is being presented in *Isotopes and Radiation Technology*, a Technical Progress Review published by the AEC.[11] The second[12] of these articles reviews the liquid–liquid extraction of cesium. Details are presented of specific extraction schemes as well as safety consideration of the organic solvents used.

Blomeke and Harrington,[13] ORNL, review the waste-management experience of several nuclear power-plant prototype stations (Dresden 1, Big Rock Point, Humboldt Bay, Elk River, Indian Point 1, and Yankee). The report discusses the sources and characteristics of wastes of these power stations and their waste-management systems. Descriptions of the systems and operational and cost experiences are presented.

Proceedings[14] have been published of the 1967 International Atomic Energy Agency symposium[15] on the disposal of radioactive wastes into the ground. English translations[16] of eight Russian papers presented at the symposium have become available.

ORNL has developed a computer (FORTRAN II) code for handling the vast amount of data obtained in its program[17] for the fixation of highly radioactive wastes into stable, solid media. This code was de-

*High-level-activity liquid wastes at SRL are essentially an alkaline solution of sodium salts, and consist, typically, of the following constituents: $NaNO_3$ (3.5*M*), Na_2CO_3 (0.3*M*), Na_2SO_4 (0.2*M*), NaOH (0.3*M*), and $NaAlO_2$ (0.6*M*). The wastes also contain such fission products as: ^{90}Sr, ^{95}Zr–^{95}Nb, ^{103}Ru, ^{106}Ru, ^{137}Cs, ^{141}Ce, and ^{144}Ce.

†Soil permeability was reduced due to dispersal of clay aggregates by sodium ions from the waste solution.

‡The solutions used for the leaching tests were untreated SRL groundwater and 0.1*N* solutions of KNO_3, HNO_3, and $Ca(NO_3)_2$.

signed to provide data storage, retrieval, and interpretation. Details of the computer code were presented in a previously issued ORNL report.[18] ORNL has recently issued a supplement[19] to this report in which is described an option for use with the computer code. The option was developed to permit arranging the data in order and comparing them with data collected either in the earlier part of the program or any data that may subsequently be stored in the program. The option can be used to select and compare solid compositions on the basis of their properties, the additives used in their formulation, and chemical equivalents (molecular weight of an element divided by the oxidation state of the element) of various ions in the solids.

The International Atomic Energy Agency has issued an annotated bibliography[20] on the recovery of fission products. The bibliography contains 720 references to the literature published during the period 1960 to 1966.

References

1. *Reactor Fuel-Process. Technol.*, 11(3): 159 (Summer 1968).
2. J. A. Buckham, Idaho Nuclear Corporation, Apr. 2, 1968, unpublished.
3. *Reactor Fuel-Process. Technol.*, 11(1): 65-66 (Winter 1967–1968).
4. A. M. Platt (Ed.), Fixation of Radioactive Residues, Quarterly Progress Report Research and Development Activities, July–October 1967, USAEC Report BNWL-677, pp. 2–9, Pacific Northwest Laboratory, March 1968.
5. *Reactor Fuel-Process. Technol.*, 10(4): 319-320 (Fall 1967).
6. *Reactor Fuel-Process. Technol.*, 11(2): 107 (Spring 1968).
7. D. W. Clelland, A. D. W. Corbet, and R. F. Coles, Design of a Plant for the Incorporation of Highly Active Wastes into Glass, a paper presented at the American Institute of Chemical Engineers Symposium on Recent Advances in Reprocessing of Irradiated Fuel, New York City, November 26–30, 1967, to be published.
8. *Power Reactor Technol. Reactor Fuel Process.*, 10(1): 90 (Winter 1966–1967).
9. W. E. Willingham, HOTANK—A Steady-State Heat Transfer Program for Use on the UNIVAC 1107/1108, USAEC Report BNWL-616, Pacific Northwest Laboratory, February 1968.
10. J. W. Fenimore and J. H. Horton, Jr., Influence of High Level Waste Salts on Movement of Strontium and Cesium in Savannah River Plant Soil, USAEC Report DP-1124, Savannah River Laboratory, January 1968.
11. *Reactor Fuel-Process. Technol.*, 10(4): 321 (Fall 1967).
12. *Isotop. Radiat. Technol.*, 5(2): 92 (Winter 1967–1968).
13. J. O. Blomeke and F. E. Harrington, Management of Radioactive Wastes at Nuclear Power Stations, USAEC Report ORNL-4070, Oak Ridge National Laboratory, January 1968.
14. *Disposal of Radioactive Wastes into the Ground*, Symposium Proceedings, Vienna, 1967, International Atomic Energy Agency, Vienna, 1967 (STI/PUB/156).
15. *Reactor Fuel-Process. Technol.*, 11(2): (Spring 1968).
16. Disposal of Radioactive Waste, Report JPRS-42565, U. S. Department of Commerce, Clearinghouse for Federal Scientific and Technical Information, Joint Publications Research Service, Washington, D. C. 20442.
17. *Reactor Fuel Process.*, 9(3): 172-173 (Summer 1966).
18. C. L. Fitzgerald, H. W. Godbee, M. H. Davis, and W. E. Clark, A Computer Code for Storing and Retrieving Data and Developing Improved Solids for Fixation of Highly Radioactive Wastes, USAEC Report ORNL-3824, Oak Ridge National Laboratory, March 1966.
19. USAEC Report ORNL-3824, Supplement 1, Oak Ridge National Laboratory, March 1968.
20. O. Vojtech (Comp.), *Recovery of Fission Products* (in English), Bibliographical Series, No. 25, International Atomic Energy Agency, Vienna, 1967 (STI/PUB/21/25).

Announcing the publication of

METEOROLOGY AND ATOMIC ENERGY—1968

This book is addressed to those who are concerned with the effects of atmospheric releases of radioactive materials from the various facilities of the nuclear energy industry. The book can be used as a handbook, a textbook, and a guide.

Contents

Introduction to the Meteorology—Atomic Energy Relation

Meteorological Fundamentals for Atmospheric Transport and Diffusion Studies

An Outline of Theories of Diffusion in the Lower Layers of the Atmosphere

Diffusion and Transport Equations

Processes Other Than Natural Turbulence Affecting Effluent Concentrations

Meteorological Instruments for Use in the Atomic Energy Industry

Radioactive Cloud-Dose Calculations

Environmental Safety Analysis

Available as TID-24190 from:

Clearinghouse for Federal Scientific and Technical Information
National Bureau of Standards, U. S. Department of Commerce
Springfield, Virginia 22151 $3.00

Index

Reactor and Fuel-Processing Technology

Volume 11

Note: The page range for each of the four issues of Vol. 11 is as follows:

No. 1, pages 1 to 68
No. 2, pages 69 to 116
No. 3, pages 117 to 166
No. 4, pages 167 to 231

A

Accidents
  analysis of nuclear in fast reactors, 1–3
  electrical cable fire in Peach Bottom Reactor during construction, 6
  superheating of liquid-metal coolants in fast reactors, 84–88
Actinide oxides
  electrolytic deposition from molten alkali-metal chlorides, 99–100
Allied Chemical Corporation
  plans for new fuel-processing plant, 205
Aluminum
  fast-neutron-induced bowing of ORR components, 18–20
Aluminum (SAP)
  dissolution, 49
Aluminum alloys (Al–Cd)
  fast-neutron-induced bowing of safety shim rods in ORR, 18–20
Aluminum alloys (Al–U)
  dissolution by HNO_3, effect of Si on, 201
Aluminum alloys (Al–U)(Al clad)
  fluoride-volatility processing of, 103–4
Aluminum fluoride (AlF_3)
  enthalpy of formation, 106
Americium
  distribution between liquid Pu and NaCl–KCl containing $PuCl_3$, 224
  preparation from AmO_2, 158
  recovery from Pu by electrorefining, 224
  recovery from Shippingport Reactor fuel, 202–3
  solvent extraction, 51
Aquafluor process
  processing of stainless-steel-clad UO_2 fuels, 54–56
  processing of zirconium-clad UO_2, 54–56
Aqueous processing
  Am recovery from Shippingport Reactor fuel, 202–3
  of BeO-based fuels, 144–45
  corrosion in processing Zr-type fuels with HF, 202
  Cm recovery from Shippingport Reactor fuel, 202–3
  decladding and dissolution of Shippingport blanket elements, 93–94
  decladding of SAP-clad UC and UO_2 fuels, 49
  design of delayed-neutron monitor for ^{235}U in leached hulls, 205–8
  design of modular pilot plant, 146–47
  design and operation of stacked-clone liquid–liquid contactors, 51–53
  dissolution of PuO_2, 91
  dissolution of pyrolytic carbon-coated $(Th,U)C_2$ and $(Th,U)O_2$ particles, 92–93
  dissolution of ThO_2, 91–92
  dissolution of U–Al alloys, effect of Si on, 201
  dissolution of UO_2 pellets containing Mo, 92
  dissolution of Zircaloy-clad ZrO_2–UO_2 fuel, 93
  of EBR-II fuel elements, 201–2
  Np recovery from Purex wastes, 203
  performance of centrifugal mixer–settler, 205
  Pu recovery from Purex wastes, 203
  process flowsheet for WAK fuel processing plant, 94–95
  solvent extraction of actinide elements, 50–51
  solvent extraction of ground graphite-base fuels, 94
  of stainless-steel-clad UO_2–PuO_2 fuels, 50
  symposium on, 146
Arsenic fluoride (AsF_5)
  structure, 105–6
Asphalt
  waste incorporation in, 67–68, 109
Attila cell
  design and operation, 103–4

B

Beryllium
  electrorefining, 224
Beryllium alloys (Be–Cd)
  fast-neutron-induced bowing of safety shim rods in ORR, 20
Beryllium fluoride systems (BeF_2–LiF–ThF$_4$)
  pyrochemical processing, 61–63, 99, 156–57, 221–24
Bibliographies
  on fission-product recovery from wastes, 231
  on nonaqueous processing of spent fuels, 216
Burnup
  prediction in thermal-reactor fuels, 69–71

C

Cadmium alloys (Al–Cd)
  fast-neutron-induced bowing of safety shim rods in ORR, 18–20
Cadmium alloys (Be–Cd)
  fast-neutron-induced bowing of safety shim rods in ORR, 20
Californium-252
  production estimate, 50
Cesium
  removal from liquid wastes by solvent extraction, 111–12, 230
Chalk River Nuclear Laboratories
  waste management, 164
Chlorine fluoride (ClF_5)
  preparation, 105
Conferences and meetings
  Disposal of Radioactive Wastes into the Ground, Vienna, 1967, 230
  International Conference on Fast Reactor Safety, Aix-en-Provence, France, Sept. 19–21, 1967, 1–3
  Nuclear Power Fuel Reprocessing: Technology and Economics, Augusta, Georgia, May 11–12, 1967, 152–53
  Recent Advances in Reprocessing of Irradiated Fuels, New York, Nov. 30, 1967, 146
Containment buildings
  electrical penetration systems, 5–12
Control rods
  fast-neutron-induced bowing in ORR, 18–20
Critical experiments
  analytical and experimental results of high conversion, 117–20
  review of DIMPLE, 121–22
Curium
  recovery from Shippingport Reactor fuel, 202–3
  solvent extraction by tributyl phosphine oxide, 51

D

Duranickel 301
  corrosion by Br_2, 152

E

Eurochemic Plant
  operating experience, 204–5

F

Filters
operation experience in fluid-bed reactors, 214
Fission products
recovery from wastes by solvent extraction, 111–12, 230
removal from PuF_6 and UF_6, 56–59
Fluoride-volatility process, 56–59, 101–6, 149–51, 209–16
Fluorine
production costs, properties, storage, and disposal, 152
Fuel blankets (UO_2)(Zircaloy clad)
aqueous processing, 93–94
Fuel elements
mechanical analysis of irradiated, problems in, 13–15
Fuels
burnup predictions in thermal reactors, 69–71
Fuels (Al–U)
aqueous processing, 201
Fuels (Al–U)(Al clad)
fluoride-volatility processing, 103–4
Fuels (BeO-base)
aqueous processing, 144–45
Fuels (graphite-base)
aqueous processing, 94
Fuels ($LiF–BeF_2–UF_4$)
pyrochemical processing, 61–63, 99, 156–57, 221–24
Fuels (PuO_2)
aqueous processing, 91
Fuels ($PuO_2–UO_2$)
fluorination with fluorine, 210–11
Fuels ($PuO_2–UO_2$)(stainless-steel clad)
aqueous processing, 50
salt-transport processing, 60–61, 96–99, 154–56, 219–21
Fuels (Pu–U)(Mg–Zr clad)
decladding by melting, 100
Fuels (ThO_2)
aqueous processing, 91–92
Fuels [(Th,U)C_2] (PyC coated)
aqueous processing, 92–93
Fuels [(Th,U)O_2] (PyC coated)
aqueous processing, 92–93
Fuels (U–fissium)
aqueous processing, 201–2
Fuels (U–Zr)(Zircaloy clad)
aqueous processing, 201–2
fluoride-volatility processing, 103–4, 209–10
Fuels (UC)
oxidation and hydrofluorination of, 213
Fuels (UC)(SAP clad)
decladding by aqueous process, 49
Fuels (UO_2)
purification, 158
Fuels (UO_2)(SAP clad)
decladding by aqueous process, 49
Fuels (UO_2)(stainless-steel clad)
aquafluor processing, 54–56
fluoride-volatility processing, 101–3
Fuels (UO_2)(304 stainless-steel clad)
critical experiments with 3 and 5 percent enriched, 117–20
Fuels (UO_2)(6061T-6 Al clad)
critical experiments with 5 percent enriched, 117–20
Fuels (UO_2) (Zircaloy clad)
fluoride-volatility processing, 101–3
Fuels (UO_2–Mo pellets)
aqueous processing, 92
Fuels ($UO_2–ZrO_2$)(Zircaloy clad)
aqueous processing, 93
Fused-salt process
bibliography on, 216

H

Halogens
physical and chemical properties of, 216
Heat exchangers
vibrations in HFBR, flow induced, 20–21
Huyck Felt metal
corrosion by Br_2, 152

I

Lanthanum
solvent extraction, 51
Liquid metals
impurity monitoring by plugging meters, 138–43
valve development for, 127–37
Lithium chloride systems (LiCl–KCl)
separation by zone melting and column crystallization, 63
Lithium fluoride systems ($BeF_2–LiF–ThF_4$)
pyrochemical processing, 61–63, 99, 156–57, 221–24

M

Magnesium alloys (Mg–Zr)
removal from Pu–U fuel elements by melting, 100
Meters (plugging)
use in monitoring impurity levels in liquid sodium, 134–43
Molybdenum alloys
preparation by pyrochemical process, 225
Molybdenum fluorides
physical and thermodynamic properties, 152
syntheses, 152
Molybdenum oxyfluorides
physical and thermodynamic properties, 152
syntheses, 152
Molybdenum systems ($Mo–UO_2$)
aqueous processing, 92
Monel
corrosion by Br_2, 152
Monel-400
corrosion by HF, 202

N

Neptunium
production from NpO_2, 224
recovery from Purex wastes, 203
Neptunium fluorides (NpF_6)
density, 152
long-wavelength, infrared-active fundamentals for, 152
removal from PuF_6 and UF_6 gas streams, 212–13
Neutron generators
design of pulsed, 72–74
Nickel 201
corrosion by Br_2, 152
Nitrofluor process
bibliography on, 216
processing of Zircaloy-clad UO_2 fuels, 54
Nonaqueous processing
Aquafluor process, 54–56
behavior of Np, 212–13
corrosion of construction materials by Br, 152
decomposition of PuF_6, 151
electrolytic processes, 99–100
filter studies, 214–15
fluoride-volatility processing of ceramic oxide fuels, 149–51, 209–12
fluorination of U compounds, 215–16
fluorine production costs, properties, 152
heat-generation problems, 215
Nitrofluor process, 54
oxidation and hydrofluorination of UC, 213
purification of PuF_6 and UF_6, 56–59, 151–52, 213–14
processes for molten-salt reactor fuels, 61–63, 99, 156–57, 221–24
properties of fluorides, 152
reaction of UF_4 with water vapor and O_2, 216
salt-transport processing of fast breeder reactor fuels, 60–61, 96–99, 154–56, 219–21
status report, 153
storage and disposal, 152

O

Oak Ridge National Laboratory
waste management, 164

P

Plant and equipment
Allied Chemical Corporation announcement of new fuel-reprocessing plant construction, 205
Attila cell for processing MTR-type fuel elements, 103–4
characteristics of air-pulsed systems, 147–48
design of delayed-neutron monitor for ^{235}U in leached hulls, 205–8
design of module for aqueous processing of irradiated fuels, 146–47
design and operation of stacked-clone liquid–liquid contactor, 51–53
design and operation of the WAK fuel-reprocessing plant, 94–95
Eurochemic Plant, operating experience, 204–5
performance of centrifugal mixer–settler, 205
Plugging meters
use in monitoring impurity levels in liquid sodium, 138–43
Plutonium
conversion to PuO_2 by burning, 91
electrorefining, 158, 224
production from PuO_2 by electrolysis, 99
purification by selective reduction in liquid BrF_3, 106
recovery from Purex wastes, 203
recovery from scrap by fluoride-volatility process, 151–52
Plutonium alloys (Pu–U)(Mg–Zr clad)
decladding by melting, 100
Plutonium fluorides (PuF_6)
bibliography on, 216
long-wavelength, infrared-active fundamentals for, 152
preparation of, 216
properties of, 216
purification of, 57–59, 213–14
radiation decomposition, 151

separation from UF_6, 214, 225
thermal decomposition, 151
Plutonium oxide (PuO_2)
conversion to Pu metal by electrolysis, 99
dissolution in aqueous processing, 91
preparation of, 216
properties of, 216
Plutonium oxide systems $(Pu,U)O_2$
fluorination with ClF and ClF_3, 211–12
Plutonium oxide systems (PuO_2–UO_2) (stainless-steel clad)
processing in the NFS Purex facility, 50
salt-transport processing, 60–61, 96–99, 154–56, 219–21
Polonium
volatilization from bismuth oxide, 158
Potassium chloride systems (LiCl–KCl)
separation by zone melting and column crystallization, 63
Potassium nitrate systems (KNO_3–$NaNO_3$)
separation by zone melting and column crystallization, 63
Protactinium
physical chemistry of, 216–17
solvent extraction, 51
Pumps
failure in Big Rock Point Reactor, 21–22
Purex process
evaluation for stainless-steel-clad UO_2–PuO_2 fuels, 50
Purex wastes
Np and Pu recovery from, 203
Pyrochemical processing (compact), 60–63, 96–100, 154–58, 219–25
(see also Nonaqueous processing)

R

Radioactive materials
handling and shipping, 68
heat-generation problems in fuel processing, 215
Reactor control
use of quasi-linear programming for, 123–26
Reactor coolants
ejection mechanisms in LMFBR, use in analyzing safety of, 180–85
liquid-metal impurity monitoring by plugging meters, 138–43
superheating of liquid metals in fast reactors, 84–88
Reactor dynamics
study, adiabatic method for, 174
study, direct method for, 176
study, modal method for, 174
study, nodal method for, 175
study, point-reactor kinetics method for, 173–74
Reactor safety
analysis of LMFBR, use of coolant ejection mechanisms in, 180–85
electrical penetrations in containment buildings, 7–12
fast reactors, conference on, 1–3
fast reactors, superheating of liquid-metal coolant in, 84–88
Reactor valves
design for use in LMFBR, 127–37
Reactors (Big Rock Point)
circulation-pump seal failure, 21–22
waste management, 230
Reactors (Briseis)
power-excursion experiments, 2
Reactors (BR-5)
operating experience, 3
Reactors (Cabri Swimming-Pool)
core-meltdown experiments, 2
Reactors (Calder Hall)
intrinsic reactivity-noise sources in, 169–70
Reactors (DFR)
intrinsic reactivity-noise sources in, 169–70
operating experience, 3
Reactors (DMTR)
intrinsic reactivity-noise sources in, 169–70
Reactors (Dresden 1)
waste management, 230
Reactors (Dresden 2)
containment, electrical penetrations, 7–12
intrinsic reactivity-noise sources in, 169–70
Reactors (EBR-II)
fuel processing by aqueous techniques, 201–2
fuel processing by pyrochemical techniques, 158
Reactors (Elk River)
intrinsic reactivity-noise sources in, 169–70
waste management, 230
Reactors (Enrico Fermi)
intrinsic reactivity-noise sources in, 169–70
Reactors (fast)
design of compact with heat pipes and direct converters, 187–200
safety, conference on, 1–3
Reactors (fast breeder)
coolant ejection mechanisms, use in analyzing safety of, 180–85
fuel processing by the salt-transport process, 60–61, 96–99, 154–56, 219–21
superheating of liquid-metal coolant, 84–88
Reactors (Fermi)
containment, electrical penetrations, 5–6
operating experience, 3
Reactors (Hanford Production)
hydriding of Zircaloy-2 process tubes, 17–18
Reactors (HFBR)
flow-induced vibrations in heat-exchanger tubes, 20–21
intrinsic reactivity-noise sources in, 169–70
Reactors (HFIR)
intrinsic reactivity-noise sources in, 169–70
transuranium-element production, 50
Reactors (HRE-2)
intrinsic reactivity-noise sources in, 169–70
Reactors (HTR)
intrinsic reactivity-noise sources in, 169–70
Reactors (Humboldt Bay)
waste management, 230
Reactors (Indian Point 1)
waste management, 230
Reactors (JRR-1)
intrinsic reactivity-noise sources in, 169–70
Reactors (JRR-2)
intrinsic reactivity-noise sources in, 169–70
Reactors (LMFBR)
coolant ejection mechanism, use in analyzing safety of, 180–85
large valves for, 127–37
superheating of Na coolant, 84–88
Reactors (molten-salt breeder)
corrosion tests, 224–25
fuel processing by pyrochemical techniques, 99, 156–57
Reactors (ML-1)
intrinsic reactivity-noise sources in, 169–70
Reactors (MSBR)
pyrochemical processing of fuels, 61–63
Reactors (MTR)
fuel processing, 103–4
Reactors (NRU)
replacement of Al vessel, plans for, 22–24
Reactors (ORR)
Al–Cd shim safety rods, fast-neutron-induced bowing in, 18–20
Be–Cd shim safety rods, fast-neutron-induced bowing in, 20
bowing of Al lattice components from fast-neutron damage, 18–20
intrinsic reactivity-noise sources in, 169–70
Reactors (Pathfinder)
intrinsic reactivity-noise sources in, 169–70
Reactors (Peach Bottom)
containment, electrical penetrations, 6–7
Reactors (power)
noise experiments, analysis and theory of, 167–71
Reactors (Rapsodie)
operating experience, 3
Reactors (Savannah)
intrinsic reactivity-noise sources in, 169–70
Reactors (Saxton)
intrinsic reactivity-noise sources in, 169–70
Reactors (Shippingport)
Am and Cm recovery from fuels of, 202–3
Reactors (SNAP-2)
intrinsic reactivity-noise sources in, 169–70
Reactors (sodium-cooled fast)
safety, conference on, 1–3
Reactors (Texas A and M Univ. Swimming Pool)
replacement of Al liner with stainless steel 304, 24–25
Reactors (thermal)
fuel-burnup predictions, panel proceedings on, 69–71
Reactors (TREAT)
core-meltdown studies, 2
Reactors (VBWR)
intrinsic reactivity-noise source in, 169–70
Reactors (Yankee)
waste management, 230
Reactors (Zero Power)
noise experiments, analysis and theory of, 167–71

S

Safety
(see Reactor safety)
Salt mines
storage of calcined wastes in, 110–11, 159–63
Salt-transport process, 60–61, 96–99, 154–56, 219–21
Seals
failure in Big Rock Point Reactor circulation pump, 21–22
Sodium (liquid)
behavior in reactor core accidents, 2

compressibility and sonic velocity, recommended values, 42–43
density, recommended values, 27–28
electrical resistivity, recommended values, 39–40
impurity monitoring by plugging meters, 138–43
saturation vapor pressure, recommended values, 28
superheating in fast reactors, 84–88
surface tension, recommended values, 40
thermal-expansion coefficient, 40–42
thermodynamic and P-V-T properties, recommended values, 28–35, 44–45
transport properties, recommended values, 32, 36–39
valve development for, 127–37
vaporization in reactor accidents, 2
Sodium nitrate systems (KNO_3–$NaNO_3$)
separation by zone melting and column crystallization, 63
Solvent extraction
of actinide elements, 50–51
air-pulsed systems for, characteristics of, 147–48
design and operation of centrifugal mixer–settler, 205
design and operation of stacked-clone liquid–liquid contactors, 51–53
deterioration of solvents under irradiation, 203–4
fission-product recovery from wastes by, 111–12
Space program
design of compact power generator featuring a fast reactor, heat pipes and direct converters, 187–200
Stainless steel (304)
performance in NaK at high temperatures, 67
Stainless steel (304L)
corrosion by HF, 202
Stainless steel (316)
performance in NaK at high temperatures, 67
Stainless steel (348)
performance in NaK at high temperatures, 67
Stainless steel (430)
corrosion by Pb–Bi eutectic, 158
Strontium
removal from liquid wastes by solvent extraction, 111–12
Symposia
(see Conferences and meetings)

T

Thermoelectric power generators
design of compact featuring a fast reactor, heat pipes and direct converters, 187–200
Thorium
solvent extraction by tributyl phosphine oxide, 51
Thorium carbide systems [$(Th,U)C_2$] (PyC coated)
dissolution in aqueous processing, 92–93
Thorium chloride ($ThCl_4$)
production, 100
Thorium fluoride systems (BeF_2–LiF–ThF_4)
pyrochemical processing, 61–63
Thorium oxide (ThO_2)
dissolution in aqueous processing, 91–92
reduction with Ca, 100, 224
Thorium oxide systems ($(Th,U)O_2$)
aqueous processing in BeO matrix, 144–45
Thorium oxide systems [$(Th,U)O_2$] (PyC coated)
dissolution in aqueous processing, 92–93
Transuranium elements
production in the HFIR, recovery in the TRU, 50
Transuranium Facility (TRU)
operation, 50

U

Uranium-233
solvent extraction, 51
Uranium-235
monitoring in leached hulls, design of instrument for, 205–8
Uranium alloys (Al–U)
dissolution by HNO_3, effect of Si on, 201
Uranium alloys (Al–U)(Al clad)
fluoride-volatility processing of, 103–4
Uranium alloys (Mo–U)
preparation by pyrochemical process, 225
Uranium alloys (Pu–U)(Mg–Zr clad)
decladding by melting, 100
Uranium alloys (U–Zr)(Zircaloy clad)
fluoride-volatility processing, 103–4
corrosion problems in processing with HF, 202
Uranium carbides (UC)
oxidation and hydrofluorination, 213
Uranium carbides (UC)(SAP clad)
decladding by chemical dissolution, 49
Uranium carbides (UC_2)
conversion to UF_6, 105
Uranium chlorides (UCl_4)
fission-product removal by zone melting, 63
Uranium fluoride systems (BeF_2–LiF–UF_4)
pyrochemical processing, 61–63
Uranium fluorides (UF_4)
conversion to UF_6, 105
preparation and properties, 216
reaction with water vapor and O_2, 216
Uranium fluorides (UF_6)
bibliography on, 216
conversion to UO_2, bibliography on, 152
density of liquid, 152
handling and container criteria, 104–5
long-wavelength, infrared-active fundamentals for, 152
preparation and properties, 216
preparation from UC_2 and $U_3O_8F_8$, 105
purification, 56–58, 213
purity specifications for enrichment by gaseous diffusion, 57
separation from PuF_6, 214, 225
structure, 105
Uranium oxide systems (Mo–UO_2)
aqueous processing, 92
Uranium oxide systems ($Pu,U)O_2$
fluorination with ClF and ClF_3, 211–12
Uranium oxide systems (PuO_2–UO_2)
fluorination with fluorine, 210–11
salt-transport processing, 96–99
Uranium oxide systems (PuO_2–UO_2) (stainless-steel clad)
processing in the NFS Purex facility, 50
salt-transport processing, 60–61, 96–99, 154–56, 219–21
Uranium oxide systems ($(Th,U)O_2$)
aqueous processing in BeO matrix, 144–45
Uranium oxide systems [$(Th,U)O_2$] (PyC coated)
dissolution in aqueous processing, 92–93
Uranium oxide systems (UO_2–ZrO_2) (Zircaloy clad)
dissolution in aqueous processing, 93
Uranium oxides (UO_2)
preparation, 216
preparation from UF_6, bibliography on, 152
preparation of crystals, 225
properties, 216
purification, 158
reaction with BrF_5, kinetics of, 215–16
reaction with F, kinetics of, 216
reaction with ClF, kinetics of, 216
Uranium oxides (UO_2)(304 stainless steel clad)
critical experiments with 3 and 5 percent enriched, 117–20
Uranium oxides (UO_2)(6061T-6 Al clad)
critical experiments with 5 percent enriched, 117–20
Uranium oxides (UO_2)(SAP clad)
decladding by chemical dissolution, 49
Uranium oxides (UO_2)(stainless-steel clad)
Aquafluor processing, 54–56
fluoride-volatility processing, 101–3
Uranium oxides (UO_2)(Zircaloy clad)
decladding and dissolution in aqueous processing, 93
fluoride-volatility processing, 101–3, 209–10
Nitrofluor processing, 54
Uranium oxides (UO_2)(Zr clad)
Aquafluor processing, 54–56
Uranium oxides (UO_3)
preparation and properties, 216
reaction with BrF_5, kinetics of, 215–16
Uranium oxides (U_3O_8)
preparation and properties of, 216
reaction with BrF_5, kinetics of, 215–16
reaction with ClF, 216
reduction by Ca vapor, 224
Uranium oxyfluoride (UO_2F_2)
conversion to UF_6, 105
Uranium oxyfluoride ($U_3O_5F_8$)
conversion to UF_6, 105

V

Valves
design for use in liquid-metal-cooled reactors, 127–37
Vibrations
flow-induced in HFBR heat exchangers, 20–21
Volatility processes, 54–59, 101–6, 149–53, 209–17
(see also Nonaqueous processing)

W

Waste disposal
categorization of wastes, 114–15
conversion of high-level-activity wastes to solids, 65–68, 159, 107–10, 159, 227–30, 231
final disposal methods, 159–64
fission-product recovery, bibliography on, 231
fission-product recovery by solvent extraction, 111–12
ground disposal, symposium on, 230
methods at CRNL, 164
methods at ORNL, 164
methods at various power reactors, 230

recovery of Cs by solvent extraction, 111–12, 230
research and development, 107–15
storage of calcined wastes in salt mines, 110–11, 159–64
storage of liquid wastes in geologic formations, 163–64
storage of liquid wastes in tanks, 112, 230

Y

Yttrium
production by fused-salt electrorefining, 99

Z

Zinc-65
extraction from pure Zn and Zn–Pb alloys, 157–58
Zircaloy-2
hydriding of process tubes in Hanford Production Reactors, 17–18
Zirconium alloys (Mg–Zr)
removal from Pu–U fuel elements by melting, 100
Zirconium alloys (U–Zr)(Zircaloy clad)
fluoride-volatility processing, 103–4
Zirconium oxide systems (UO_2–ZrO_2) (Zircaloy clad)
dissolution in aqueous processing, 93

LEGAL NOTICE

This journal was prepared under the sponsorship of the U. S. Atomic Energy Commission. Neither the United States, nor the Commission, nor any person acting on behalf of the Commission:

A. Makes any warranty or representation, expressed or implied, with respect to the accuracy, completeness, or usefulness of the information contained in this journal, or that the use of any information, apparatus, method, or process disclosed in this journal may not infringe privately owned rights; or

B. Assumes any liabilities with respect to the use of, or for damages resulting from the use of any information, apparatus, method, or process disclosed in this journal.

As used in the above, "person acting on behalf of the Commission" includes any employee or contractor of the Commission, or employee of such contractor, to the extent that such employee or contractor of the Commission, or employee of such contractor prepares, disseminates, or provides access to, any information pursuant to his employment or contract with the Commission, or his employment with such contractor.

AEC SYMPOSIUM SERIES

Available for $3.00 each from the Clearinghouse for Federal Scientific and Technical Information, National Bureau of Standards, U. S. Department of Commerce, Springfield, Virginia 22151

1 **Progress in Medical Radioisotope Scanning (TID-7673),**
Oak Ridge Institute of Nuclear Studies, 1962

2 **Reactor Kinetics and Control (TID-7662),**
The University of Arizona, 1963

3 **Dynamic Clinical Studies with Radioisotopes (TID-7678),**
Oak Ridge Institute of Nuclear Studies, 1963

4 **Noise Analysis in Nuclear Systems (TID-7679),**
University of Florida, 1963

5 **Radioactive Fallout from Nuclear Weapons Tests (CONF-765),**
U. S. Atomic Energy Commission, 1964

6 **Radioactive Pharmaceuticals (CONF-651111),**
Oak Ridge Institute of Nuclear Studies, 1965

7 **Neutron Dynamics and Control (CONF-650413),**
The University of Arizona, 1965

8 **Luminescence Dosimetry (CONF-650637),**
Stanford University, 1965

9 **Neutron Noise, Waves, and Pulse Propagation (CONF-660206),**
University of Florida, 1966

10 **Use of Computers in Analysis of Experimental Data and the Control of Nuclear Facilities (CONF-660527),**
Argonne National Laboratory, 1966

11 **Compartments, Pools, and Spaces in Medical Physiology (CONF-661010),**
Oak Ridge Associated Universities, 1967

12 **Thorium Fuel Cycle (CONF-660524),**
Oak Ridge National Laboratory, 1968

13 **Radioisotopes in Medicine: In Vitro Studies (CONF-671111),**
Oak Ridge Associated Universities, 1968

Nuclear Science Abstracts

The U. S. Atomic Energy Commission, Division of Technical Information, publishes *Nuclear Science Abstracts (NSA)*, a semimonthly journal containing abstracts of the literature of nuclear science and engineering.

NSA covers (1) research reports of the U. S. Atomic Energy Commission and its contractors; (2) research reports of government agencies, universities, and industrial research organizations on a worldwide basis; and (3) translations, patents, books, and articles appearing in technical and scientific journals.

Complete indexes covering subject, author, source, and report number are included in each issue. These indexes are cumulated and sold separately.

Availability of NSA

SALE *NSA* is available on subscription from the Superintendent of Documents, U. S. Government Printing Office, Washington, D. C. 20402, at $42.00 per year for the semimonthly abstract issues and $38.00 per year for the cumulated-index issues. Subscriptions are postpaid within the United States, Canada, Mexico, and all Central and South American countries, except Argentina, Brazil, Guyana, French Guiana, Surinam, and British Honduras. Subscribers in these Central and South American countries, and in all other countries throughout the world, should remit $52.50 per year for subscriptions to semimonthly abstract issues and $47.50 per year for the cumulated-index issues. The single-copy price for the abstract issues is $1.75 postpaid, with this exception: Add one-fourth of $1.75 for mailing to the countries to which the $52.50 subscription rate applies.

EXCHANGE *NSA* is also available on an exchange basis to universities, research institutions, industrial firms, and publishers of scientific information. Inquiries should be directed to the Division of Technical Information Extension, U. S. Atomic Energy Commission, P. O. Box 62, Oak Ridge, Tennessee 37830.

TECHNICAL PROGRESS REVIEWS may be purchased from Superintendent of Documents, U. S. Government Printing Office, Washington, D. C. 20402. *Nuclear Safety* at $3.50 per year (six issues) for each subscription or $0.60 per issue; each of the other journals at $2.50 per year (four issues) or $0.70 per issue. The use of the order form below will facilitate the handling of your order.

POSTAGE AND REMITTANCE: Postpaid within the United States, Canada, Mexico, and all Central and South American countries except Argentina, Brazil, Guyana, French Guiana, Surinam, and British Honduras. For these Central and South American countries and all other countries: add, for each annual subscription, $1.00 for *Nuclear Safety* and $0.75 for each of the other journals; for single issues, add one-fourth of the single-issue price. Payment should be by check, money order, or document coupons, and MUST accompany order. Remittances from foreign countries should be made by international money order or draft on an American bank payable to the Superintendent of Documents or by UNESCO book coupons.

order form

SUPERINTENDENT OF DOCUMENTS
U. S. GOVERNMENT PRINTING OFFICE
WASHINGTON, D. C. 20402

Please send — 1, 2, or 3 years

- ☐ Isotopes and Radiation Technology ____
- ☐ Nuclear Safety ____
- ☐ Reactor and Fuel-Processing Technology ____
- ☐ Reactor Materials ____

Enclosed: document coupons ☐ check ☐ money order ☐

Charge: Superintendent of Documents No._____

SUPERINTENDENT OF DOCUMENTS
U. S. GOVERNMENT PRINTING OFFICE
WASHINGTON, D. C. 20402

(Print clearly)

_____
Name

_____
Street

_____
City, State, ZIP Code